



Design and synthesis of polymer and organic functionalized porous silica gels extracted from diatomaceous earth and their application in the treatment of oil impacted water.

Oisaemi Uduagele Izevbekhai (17023788)

Promoter: Prof. WM Gitari (University of Venda)

Co-Promoter: Dr. NT Tavengwa (University of Venda)

A thesis submitted to the department of Ecology and Resource Management, School of Environmental Sciences, University of Venda in fulfilment of the requirements for the award of the degree of Doctor of Philosophy.

September 2020

Declaration

I, Oisaemi Uduagele Izevbekhai (17023788), hereby declare that this work “**Design and synthesis of polymer and organic functionalized porous silica gels and their application in the treatment of oil impacted water**” submitted for a PhD in Environmental Sciences (Ecology and Resource Management) at the University of Venda is my own work in design and execution and has not been previously submitted for any degree or examination at this or any other institution. All reference materials contained therein have been fully acknowledged.

Signature..........

Date.....18/02/21.....

Acknowledgements

- My supervisor Prof MW Gitari, thanks for the training, exposure, financial support and otherwise.
- My co-supervisor, Dr NT Tavengwa, thanks for reading my numerous write-ups and abstracts repeatedly.
- My wife, Elohor Izevbekhai (nee Udoro), words can't express how grateful I am for your love and support.
- My mum, Eunice Izevbekhai (nee Enu), you are exceptional. Thank you for your prayers, support and encouragement.
- My siblings and their husbands, Ayodele and Daniel Ifon, Ideleli and Texmond Nwabuebo, Aina and Loveday Asemota, your prayers and support will never be forgotten.
- My parents, brothers and sisters in – law, thanks for your prayers.
- My colleagues, Enviren Research Group members and Dr Tavengwa's postgraduate students, working with you was fun. I look forward to future collaborations.
- The pastorate, leaders and members of Christ Tabernacle church, especially Dr Joshua Edokpayi, thank you for the support, prayers and encouragement.
- The Research and Publication Committee of the University of Venda, thank you for the financial support.

Dedication

To Michelle and Ivana, my daughters, your strength knows no bounds. I went through this to make sure you have a better life than I did.

To my beautiful wife, for being my support.

Abstract

This study aims to synthesize silica gel-based adsorbents for organic contaminated wastewater treatment using diatomaceous earth as the silica precursor. First, the extraction of silica from diatomaceous earth was optimized with the help of response surface methodology (RSM) and then the extracted silica was used to produce the silica gels using non – templated methods. The synthesized porous gels then were surface grafted with selected organic materials such as polypyrrole, acetyl groups and a novel benzimidazolone based polymer. The grafted gels were characterized using techniques such as scanning electron microscopy, Fourier Transform – Infra Red (FT – IR), X – ray powder diffraction (XRD) and ^1H and ^{13}C NMR to ascertain the physicochemical properties and morphological arrangement of the synthesized gels. The gels were then tested for the treatment of synthetic oily wastewaters.

The first part of the work presented the optimization of silica from diatomaceous earth (DE) using response surface methodology. Three methods were used in the optimization namely conventional solvent extraction (CSE), ultrasound assisted extraction using alkali (Alkali UAE) and ultrasound assisted extraction using acids (Acid UAE). The CSE and alkali UAE methods produced silica of 87% and 79% purity and 13% and 16% yield respectively which was less than the amount of silica in DE while the acid UAE method produced silica of 95% purity and 82% yield with optimum parameters: 1.99 h for sonication time, 2.82 M for concentration of HCl, 220 mL for volume, 0.524 for cycle and 72.6% amplitude.

In the second part, the successful solvent free synthesis and characterization of benzimidazolone and analogues is reported as well as their functionalization on silica. The benzimidazolone functionalized silica were then applied in the removal of oil from laboratory simulated oily wastewater as well as the optimization of oil removal using response surface methodology. The results show a percentage oil adsorption of 98% using 0.004 g of adsorbent, 6650 mg/L oil concentration, and a contact time of 16 h.

Part three reports the synthesis and characterization of acetylated silica and the application of this in the removal of oil from synthetic oily wastewater (SOWW) and the optimization of oil removal using response surface methodology. The optimum conditions for oil removal were as follows

9250 mg/L oil concentration, with adsorbent dosage of 0.003 g and a duration of 16 h. The percentage oil adsorption was found to be 99.3%.

The final section looks at the behaviour of synthesized polypyrrole-silica complex in the removal of oil from SOWW as well as the optimization of oil removal from SOWW using response surface methodology with and without shaking. The adsorbent showed excellent oil uptake when compared with similar materials with optimum conditions being 7250 mg/L oil concentration, 0.003 g adsorbent dosage and contact time of 38.2 h in experiments without shaking giving a percentage oil adsorption of 99.3%.

The study successfully created an optimized method for the extraction of silica from diatomaceous earth and created new polymer and organic functionalized porous silica gels for the removal of oil from synthetic oily wastewater. Also, the physicochemical and morphological properties of diatomaceous earth, extracted silica and all synthesized gels were studied. A relatively cheap and conservative method for the recycling of organic wastewaters and oily wastewater has thus been found and this is expected to help ease the water stress in South Africa and other countries. For the first time, three silica-based adsorbents have been synthesized with all three having over 98% oil removal. Future work will entail further characterization of the adsorbents and regeneration studies.

Academic outputs

Published proceedings

- **O Izevbekhai, W Gitari and N Tavengwa, 2018. Diatomaceous earth: the future of ultra-pure silica - a review.** Proceedings of the First International Conference in Sustainable Management of Natural Resources. 15th -17th October 2018, Bolivia Lodge, Polokwane, South Africa.
- **L Mulaudzi, WM Gitari and O Izevbekhai, 2018. Harnessing waste plant material, rice husk ash, for the production of high-quality silica.** Proceedings of the First International Conference in Sustainable Management of Natural Resources. 15th -17th October 2018, Bolivia Lodge, Polokwane, South Africa.

Published manuscripts

- **Izevbekhai, O.U, Gitari, W. M, Tavengwa, N. T, Ayinde, W.B and Mudzielwana, R. (2020) Application of synthesized acetylated silica in the remediation of oily wastewater.** Journal of Taibah University for Science. 14(1), 1033-1041.
- **Izevbekhai, O.U, Gitari, W. M, Tavengwa, N. T, Ayinde, W.B and Mudzielwana, R. (2020) Response surface optimization of oil removal using synthesized polypyrrole-silica.** Molecules. 25(20), 4628-4644. 10.3390/molecules25204628.

Submitted manuscripts

- **Izevbekhai, O.U, Gitari, W. M, Tavengwa, N. T, Ayinde, W.B and Mudzielwana, R. (2021) Synthesis and evaluation of the oil removal potential of 3-bromo-benzimidazolone polymer grafted silica gel.** RSC Advances. Status: *Under review*.
- **Izevbekhai, O.U, Gitari, W. M, Tavengwa, N. T (2020) Optimization of silica extraction from diatomaceous earth using the central composite design of response surface methodology.** South African Journal of Chemistry. Status: *Accepted*.

Conferences presentations

- **Izevbekhai, O.U, Gitari, W. M, Tavengwa, N. T., 2018. Diatomaceous earth: the future of ultra-pure silica - a review.** First International Conference in Sustainable Management of Natural Resources. 15th -17th October 2018, Bolivia Lodge, Polokwane, South Africa.
- **Izevbekhai, O.U, Gitari, W. M, Tavengwa, N. T., 2019. Optimization of silica extraction from diatomaceous earth using response surface methodology.** Oral presentation at the 20th WaterNet/WARFSA/GWPSA Symposium at the Indaba Hotel, Spa & Conference Centre Fourways, Johannesburg, South Africa from 30th October – 1st November 2019.

Table of contents

Declaration	i
Acknowledgements	ii
Dedication	iii
Abstract	iv
Academic outputs	vi
Table of contents	vii
List of figures	xi
List of tables	xiii
Chapter One: Introduction	1
1.1. Background	1
1.2. Problem statement	2
1.3. Research objectives	4
1.4. Motivation	4
1.5 Thesis layout	5
1.6. References	6
Chapter Two: Literature review	9
2.1. Oil in wastewater	9
2.2. Impact of oily wastewater	11
2.3. Porous silica hydrogels	13
2.4. Synthesis of porous silica gels	15
2.5. Diatomaceous Earth	17
2.6. References	19
Chapter Three: Optimization of silica extraction from diatomaceous earth using the central composite design of response surface methodology	24
Abstract	24
3.1. Introduction	25
3.2. Materials and Methods	27
3.2.1. Chemicals and reagents	27
	vii

3.2.2. Alkali ultrasound – assisted extraction (Alkali UAE method)	27
3.3. Conventional solvent extraction (CSE)	28
3.4. Acid ultrasound – assisted extraction (Acid UAE method)	28
3.5. Characterization of diatomaceous earth and extracted silica	29
3.6. Results and discussion	29
3.6.1. Design of experiment	29
3.7. Response surface model	33
3.8. Response surface optimization	39
3.8.1. Alkali UAE	39
3.8.2. Acid UAE	46
3.8.3. Conventional solvent extraction (CSE)	57
3.9. Characterization of diatomaceous earth and extracted silica	59
3.9.1. Raw DE	59
3.9.2. Alkali UAE	59
3.9.3. Acid UAE	60
3.9.4. Conventional solvent extraction (CSE)	61
3.9.5. XRD plots for Alkali UAE, Acid UAE and CSE	62
3.10. Conclusions	63
3.11. References	64
Chapter Four: Synthesis and Evaluation of the Oil Removal Potential of 3-Bromo-Benzimidazolone Polymer Grafted Silica Gel	67
Abstract	67
4.1. Introduction	68
4.2. Materials and methods	69
4.2.1. Chemicals and reagents	69
4.2.2. Synthesis of benzimidazolone	70
4.2.3. Polymerization of 3-bromo benzimidazolone	70
4.2.4. Response surface optimization of oil removal	71
4.2.5. Experimental design	71
4.3. Results and discussion	72
4.3.1. Functional group analysis	72

4.3.2. Structure elucidation of 3-bromo benzimidazolone polymer	75
4.3.3. Morphological studies	77
4.3.4. Response surface experiments and model fitting	77
4.3.4.1. Regression model and analysis of variance (ANOVA)	80
4.3.4.2. Effect of oil concentration and sorbent dosage	81
4.3.4.3. Effect of oil concentration and time	82
4.3.4.4. Effect of adsorbent dosage and time	83
4.4. Conclusion	84
4.5. References	86
Chapter Five: Application of Synthesized Acetylated Silica in the Remediation of Oily Wastewater	91
Abstract	91
5.1. Introduction	91
5.2. Materials and Methods	93
5.2.1. Chemicals and reagents	93
5.2.2. Acetylation of silica	93
5.2.3. Characterization	93
5.2.4. Preparation of synthetic oily wastewater	93
5.2.4.1. Response surface optimization of oil removal	94
5.2.5. Experimental design	94
5.3. Results and Discussion	95
5.3.1. Characterization of synthesized adsorbent	95
5.3.2. RSM experiments and model fitting	98
5.3.3. Regression model and analysis of variance (ANOVA)	102
5.3.4. Effect of oil concentration and sorbent dosage	103
5.3.5. Effect of oil concentration and time	104
5.3.6. Effect of adsorbent dosage and time	105
5.4. Conclusion	106
5.5. References	107
Chapter Six: Response Surface Optimization of Oil Removal Using Synthesized Polypyrrole-Silica Polymer Composite	112

Abstract	112
6.1. Introduction	112
6.2. Materials and Methods	114
6.2.1 Materials	114
6.2.2. Preparation of polypyrrole modified silica	114
6.2.3. Characterization of synthesized silica composite	115
6.2.4. Preparation of synthetic oily wastewater	115
6.2.5. Response surface optimization of oil removal	115
6.2.6. Experimental design	116
6.3. Results	116
6.3.1. Characterization of polypyrrole - silica composite	116
6.3.2. Optimization of oil removal	119
6.3.2.1. RSM Experiments and model fitting	119
6.3.2.2. Regression Model and Analysis of Variance (ANOVA)	124
6.3.2.3. Effect of oil concentration and sorbent dosage	124
6.3.2.4. Effect of oil concentration and time	127
6.3.2.5. Effect of adsorbent dosage and time	129
6.3.3. Comparison to other adsorbents	131
6.3.4. Effect of empty tea bags	131
6.4. Conclusions	132
6.5. References	133
Chapter Seven: Conclusions, recommendations, and future work	138
7.1. Conclusions and recommendations	138
7.2. Future Work	139

List of figures

Figure 2. 1. Classification of oils in wastewater (Yang, 2011).....	9
Figure 3. 1. Comparison between values predicted by response surface methodology (RSM) model and experimentally determined.	35
Figure 3. 2. Response surface plots for alkali UAE.....	45
Figure 3. 3. Response Surface plots for acid UAE.	56
Figure 3. 4. Response surface plots for CSE.....	58
Figure 3. 5. (a) SEM and (b) EDS for raw DE.....	59
Figure 3. 6. (a) SEM (b) EDS and (c) TEM for alkali UAE.....	60
Figure 3. 7. (a) SEM (with higher magnification inset) (b) EDS (c) TEM for acid UAE.	61
Figure 3. 8. (a) SEM (b) EDS and (c) TEM for CSE.....	62
Figure 3. 9. XRD plots for acid UAE, alkali UAE and CSE.	63
Figure 4. 1. (a) sealed empty tea bag (b) sealed tea bag containing adsorbents.	71
Figure 4. 2. FTIR spectra for Urea, 3- bromo-1,2-phenylenediamine, 3- bromobenzimidazolone and 3-bromobenzimidazolone polymer.	74
Figure 4. 3. (a) ¹ H, (b) ¹³ C and (c) DEPT NMR of 3- bromo-benzimidazolone.	76
Figure 4. 4. TEM, SEM and EDX of (a) unmodified silica (b) 3- bromo-benzimidazolone modified silica.....	77
Figure 4. 5. Pictures of adsorbent treated synthetic oily wastewater (Experimental conditions are as presented in Table 2).	78
Figure 4. 6. Comparison between values predicted by response surface methodology (RSM) model and experimentally determined values.	80
Figure 4. 7. Response surface plot for the effect of initial oil concentration and adsorbent dosage on percentage adsorption.	82
Figure 4. 8. Response surface plot for the effect of initial oil concentration and time on percentage adsorption.	83
Figure 4.9. Response surface plot for the effect of contact time and adsorbent dosage on percentage adsorption.	84
Figure 5. 1. (a) sealed empty tea bag (b) sealed tea bag containing adsorbents.	94
Figure 5. 2. FT-IR spectra of raw silica and acetylated silica.....	96
Figure 5. 3. XRD plots of raw and acetylated silica.	97
Figure 5. 4. TEM, SEM and EDX micrographs of (a) raw silica (b) acetylated silica.	98

Figure 5. 5. Pictures of adsorbent treated synthetic oily wastewater (Experimental conditions are as presented in Table 2).	100
Figure 5. 6. Comparison between values predicted by response surface methodology (RSM) model and experimentally determined values.	102
Figure 5. 7. Response surface plots for the effect of changes in oil concentration and adsorbent dosage on percentage adsorption.	104
Figure 5. 8. Response surface plots for the effect of changes in initial oil concentration and contact time on percentage adsorption.	105
Figure 5. 9. Response surface plots for the effect of changes in contact time and adsorbent dosage on percentage adsorption.	106
Figure 6. 1. (a) sealed empty tea bag (b) sealed tea bag containing adsorbents.	115
Figure 6. 2. FTIR plots of pyrrole, silica and polypyrrole-silica composite.	118
Figure 6. 3. (a), (c) SEM of unmodified and polypyrrole-silica composite respectively and (b), (d) the corresponding EDX.	119
Figure 6. 4. Pictures of adsorbent treated synthetic oily wastewater (Experimental conditions are as presented in columns 1 to 3 of Table 6.3).	121
Figure 6. 5. Comparison between values predicted by response surface methodology (RSM) model and experimentally determined values for (a) percentage adsorption and (b) TOC.	123
Figure 6. 6. Response surface plots for 'effect of oil concentration and adsorbent dose.	126
Figure 6. 7. Response surface plots for effect of oil concentration and time.	128
Figure 6. 8. Response surface plots for effect of contact time and adsorbent dosage.	130
Figure 6. 9. (a) Adsorbent treated SOWW (b) Empty tea bag treated SOWW (Initial oil concentration – 6650mg/L; duration – 16 h.	132

List of tables

Table 2. 1. Composition of produced water (Pearce and Whyte, 2005).	10
Table 2. 2. Composition of refining wastewater (Pearce and Whyte, 2005).	11
Table 2. 3. Conventional treatment methods of oily wastewater (Pearce and Whyte, 2005).	12
Table 2. 4. Adsorbents reported for oil sorption.	13
Table 3. 1. Range of parameters optimized in the extraction of silica in the conventional extraction and alkali UAE method.	28
Table 3. 2. Central composite experimental design for Ultrasound assisted extraction and conventional solvent extraction.	30
Table 3. 3. Analysis of variance of all model terms.....	38
Table 4. 1. Range of optimized parameters.....	72
Table 4. 2. RSM design and the actual values of responses.....	79
Table 4. 3. ANOVA for model and model terms.	81
Table 5. 1. Range of optimized parameters.....	95
Table 5. 2. RSM design and the actual values of responses.....	101
Table 5. 3. ANOVA for model and model terms.	103
Table 6. 1. Range of optimized parameters.....	116
Table 6. 2. RSM Design and the actual values of responses.....	120
Table 6. 3. ANOVA for applied model and model terms.	124
Table 6. 4. Comparison of adsorption capacity for different adsorbents.	131

Chapter One: Introduction

1.1. Background

According to the United Nations, about 2.2 billion people worldwide do not have access to safe drinking water (WHO/UNICEF, 2019) and 500 million people around the world live where demand for water more than doubles local supply (WWAP, 2017). Water scarcity, which could lead to economic crises, displacement of families, death of children and ultimately wars, as was seen in Syria and Somalia (WWAP, 2017; WWF-SA, 2017a), places fourth on the global risk rankings (WEF, 2019). A 2016 study observed that about four billion people worldwide experience water scarcity for at least 30 days in a year (Mekonnen and Hoekstra, 2016). According to a UNICEF report, about 319 million people in sub – Saharan Africa and 3.64 million people in South Africa did not have access to safe drinking water in 2015 (UNICEF and WHO Joint Monitoring Programme, 2015).

South Africa is dangerously close to scarcity as only 2% of useable water remains for future allocation with most of its rivers threatened or endangered especially by the Witswatersrand goldfields, the Mpumalanga coal fields (WWF-SA, 2017a) and petrochemical industries in the Mpumalanga and Witswatersrand areas and will grow worse once full scale gas exploration commences in the country (Enqvist and Ziervogel, 2019).

Rainfall in South Africa is generally about half the global average with some regions having way less (Hedden and Cilliers, 2014; WWF-SA, 2017a) and this amount has further dropped in recent years (Le Maitre et al., 2018) leading to a low amount of surface and ground water supply and creating a shortage in pipe borne water (Le Maitre et al., 2018). According to the World Bank (2016), South Africa, whose economy is directly linked to water resources, is among the regions expected to experience a decline in gross domestic product (GDP) as a result of water shortages if nothing is done to save the situation.

Water availability in a nation is as good as its water management laws and institutions (Ivey et al., 2004). The South African government has always been committed to water management. The Public Health Act of the Union of South Africa, 1919 (Phillips, 1990) in order to protect the water bodies, stated among other things, that sewage and other wastes must be disposed on land. As the South African economy moved from a mainly agrarian one to a partly industrial one, and as it was becoming clear that water demand was rapidly growing, the Water Act of 1956 (Tempelhoff, 2017) was promulgated which required all effluent waters to be returned to

the water bodies where they emanated. In 1984, this act was amended (DEA, 2018) to incorporate uniform effluent standards. The South African constitution of 1996 states that South Africans have a right to water and a protected environment and listed these as human rights. In 1998, the current Water Act (Maphela and Cloete, 2019) was passed and the minister for Water and Forestry was charged with the duties of protection, regulation of use, development, conservation and management of water for all. Water management in South Africa was decentralized after the apartheid regime to better cater for the water needs, and this worked well for a time (Lévite et al., 2003). South Africa generally, has strong water governance that has resulted in almost half the population of the country having water sources in their homes (WWF-SA, 2017b), but a lot still needs to be done especially before 2025 when the country is expected to approach physical water scarcity and plunge into a 17% deficit by 2030 (WWF-SA, 2017b). Everyone, including consumers, must be committed to the proper management of the limited water resources. These efforts must include appropriate disposal of wastewaters, especially in industrial areas like Mpumalanga Highveld coal fields and other mining areas.

1.2. Problem statement

There is a severe water problem globally, that will keep getting worse if nothing is done. This, according to the World Bank, will lead to a drop in GDP in many nations including South Africa, whose rainfall is below the global average and the amount is expected to drop further in the next five years thereby worsening the already growing problem of pipe borne water shortage (WWAP, 2015). This will worsen the already growing problem of poverty in Africa and other continents. South Africa is expected to be one of the worst hit because its economy is directly linked to the highest water consuming sector, agriculture, which uses 63% of available water in the country. This Figure is expected to rise by 1% annually (WWF-SA, 2017a).

Pollution of the marine ecosystem by wastewaters from industries helps to further deplete the amount of useful water. Every year, about 450 billion kg of wastes is generated in South Africa mainly from mining (DEA, 2018; Heath et al., 2009) and a large portion of this and sewage wastes are discharged untreated into the water ways (Oberholster and Ashton, 2008). This renders most of South African fresh waters unfit for consumption. For example, according to Musingafi (2014) industrial (especially mining) and agricultural activities have adversely affected water quality in Limpopo Province. They found that the Luvuvhu River and Nandoni

Dam water quality has been affected by these activities and by toxic levels of DDT which has been used to control malaria in the area annually for almost a century (Bornman et al., 2017). Johnson and Hallberg (2005) reported that the acid mine drainage in Gauteng is a major pollutant of surface and ground water in the province and Maree et al. (2004) reported that significant amounts of acid mine water and decant (DWAF, 2004) are being discharged from closed mines into the Olifants River daily. In Witswatersrand, most of the fountains have been blocked because of acid mine discharged from gold mines (Musingafi, 2014) and in Johannesburg, the ground water and streams have been contaminated and acidified because of oxidized pyrite in mine tailings dumped in and around mines and the discharge of the ground water into streams (Naicker et al., 2003).

Pollution of water bodies is also a common occurrence in oil rich regions. Oil spills occur regularly both as a result of accidents and the nefarious activities of vandals (Jernelöv, 2010). This makes it difficult for people in those regions to get clean water to meet their daily needs. Aquatic life is also affected, leaving the people in that region without food and without a means of livelihood. South Africa is located on one of the busiest sea routes with over 4000 ships, transporting oil from the Middle East to Europe and from North and West Africa to China, going through the Cape of Good Hope yearly (Wang and Lu, 2015). This places the country at the receiving end of accidental spills which could have devastating effect on marine animals and on the water body itself. There has been some major oils spills in South Africa. Examples are the accidental sinking of the ‘MV Treasure’ oil bunker in 2000 which threatened the population of African Penguins and more recently, a spill in Durban in 2015 (Teagle, 2015).

South Africa is expected to start large scale drilling of its about 390 trillion cubic feet of shale gas resources in the near future (Chapman et al., 2016). This exploration, just like all fossil fuel extraction, requires a lot of water. Millions of gallons of water (per well) is introduced into shale formations to make them more permeable (Wilson and VanBriesen, 2012). A portion of this water flows back to the surface immediately as flowback (Pichtel, 2016) and the remaining either pervade the formation or return to the surface all through the life of the well as ‘produced water’ (Wilson and VanBriesen, 2012). Both flowback and produced water are very rich in organics (Wilson and VanBriesen, 2012) and is therefore expected to put a further strain on South Africa’s water resources (Mueller, 2015).

As a result of these, this research is motivated by the large amounts of organic wastewaters discharged into the environment by industries especially petrochemical industries and even

larger amounts that will be discharged from gas exploration once it commences fully. It is also motivated by the severe shortage of water that these activities will immediately bring and therefore seeks an affordable way to recycle these wastewaters.

1.3. Research objectives

The main objective of this work is to synthesize substituted benzimidazolone, polypyrrole, acetyl and cations modified silica gels using pore formers, and non – templated methods for the treatment of organic wastewater.

The specific objectives of this work are to:

1. Evaluate the physico-chemical and morphological properties of diatomaceous earth, optimize the extraction of silica from diatomaceous earth using response surface methodology (RSM) and characterize the extracted silica
2. Synthesize substituted benzimidazolone derivatives of porous gels and evaluate the physico-chemical and morphological properties of the gel.
3. Synthesize acetyl and polypyrrole modified porous silica gels using non – templated methods and evaluate the physico-chemical and morphological properties of the gel.
4. Evaluate the synthesized gels for the treatment of organic and oil contaminated wastewaters as well as optimize adsorption parameters such as initial oil concentration, adsorbent dose and adsorption time.

1.4. Motivation

South Africa has a growing water problem with the whole country getting a yearly average rainfall (the main source of water) which is less than half of the yearly global average and with 21% of the population getting a yearly average of almost one – quarter the yearly global average (WWF-SA, 2017b). The water situation is being compounded by the high yearly average rate of evaporation which is placed at 1800 mm (three times the yearly average rainfall) (WWF-SA, 2017b) resulting in a negative net rainfall.

Petrochemical industries use large amounts of water for their daily operations and oily wastewaters generated from these industries and others like it as well as oil spills which occur every now and then, contaminate most of the fresh water supplies in the country. Also, South Africa is expected to begin exploration of its large shale gas reserves soon. This operation is

expected to use large amounts of water and generate large volumes of wastewaters rich in oil and dissolved organic compounds. These operations create increasingly complex problems for water planners and managers and further depletes the amount of useable water.

With the water shortages currently facing the country and especially with the not so good prediction of physical water scarcity by 2025 (WWF-SA, 2017b), water demand deficit by 2030 (WWF-SA, 2017b) and the impending economic meltdown as a result of this (World Bank, 2016), a lot of effort must be made to make more water available using methods that will not put any further strain on the economy. A number of researchers have reported the use of surface modified diatomaceous earth, which is very rich in silica (between 86 and 94% silicon dioxide (SiO₂) (Izuagie et al., 2016; Tsai et al., 2004) and the use of porous silica gels in the purification of water but very few studies report the use of porous silica gels in the treatment of organic wastewaters and even fewer studies have reported the use of these gels in the treatment of oil and gas produced water. Even though diatomaceous earth is silica rich, it has never been used as a source of silica in the production of porous silica gels. The study is motivated by the water shortages in the country and the lack of cheap and efficient water recycling technologies in the country.

1.5 Thesis layout

This section presents the layout of the chapters:

Chapter 1: Introduction

Chapter 2: Literature review

Chapter 3: Optimization of silica extraction from diatomaceous earth using the central composite design of response surface methodology

Chapter 4: Synthesis and evaluation of the oil removal potential of 3-bromo-benzimidazolone polymer grafted silica gel

Chapter 5: Application of synthesized acetylated silica in the remediation of oily wastewater

Chapter 6: Response surface optimization of oil removal using synthesized polypyrrole-silica polymer composite

Chapter 7: Conclusions, recommendations, and future work

1.6. References

Bornman, M.S., Aneck-Hahn, N.H., de Jager, C., Wagenaar, G.M., Bouwman, H., Barnhoorn, I.E.J., Patrick, S.M., Vandenberg, L.N., Kortenkamp, A., Blumberg, B., Kimmins, S., Jegou, B., Auger, J., DiGangi, J. & Heindel, J.J., 2017 Endocrine disruptors and health effects in africa: A call for action. *Environmental health perspectives*, 125, pp.085005-085005.

Chapman, G., Wait, R. & Kleynhans, E., 2016 The governance of shale gas production in south africa. *South African Journal of International Affairs*, 23, pp.69-88.

DEA, D.o.E.A., Republic of South Africa, 2018 *South african water quality guidelines for coastal marine waters -natural environment and mariculture use*. CapeTown.

DWAF, D.o.W.A.a.F., South Africa, 2004 *Olifants water management area: Internal strategic perspective*. Pretoria.

Enqvist, J.P. & Ziervogel, G., 2019 Water governance and justice in cape town: An overview. *WIREs Water*, 6, pp.e1354.

Heath, R., Zyl, H.v., Schutte, C. & Schoeman, J., 2009 *First order assessment of the quantity and quality of non-point sources of pollution associated with industrial, mining and power generation* Pretoria.

Hedden, S. & Cilliers, J., 2014 Parched prospects: The emerging water crisis in south africa. Institute for security studies (iss). *African Futures Paper*, 11, pp.1-16.

Ivey, J.L., Smithers, J., de Loe, R.C. & Kreutzwiser, R.D., 2004 Community capacity for adaptation to climate-induced water shortages: Linking institutional complexity and local actors. *Environ Manage*, 33, pp.36-47.

Izuagie, A.A., Gitari, W.M. & Gumbo, J.R., 2016 Defluoridation of groundwater using diatomaceous earth: Optimization of adsorption conditions, kinetics and leached metals risk assessment. *Desalination and Water Treatment*, 57, pp.16745-16757.

Jernelöv, A., 2010 The threats from oil spills: Now, then, and in the future. *Ambio*, 39, pp.353-366.

Johnson, D.B. & Hallberg, K.B., 2005 Acid mine drainage remediation options: A review. *Science of The Total Environment*, 338, pp.3-14.

Le Maitre, D.C., Seyler, H., Holland, M., Smith-Adao, L., Nel, J.L., Maherry, A. & Witthüser, K., 2018 *Identification, delineation and importance of the strategic water source areas of south africa, lesotho and swaziland for surface water and groundwater*. Pretoria.

Lévite, H., Sally, H. & Cour, J., 2003 Testing water demand management scenarios in a water-stressed basin in south africa: Application of the weap model. *Physics and Chemistry of the Earth, Parts A/B/C*, 28, pp.779-786.

Maphela, B. & Cloete, F., 2019 Johannesburg's implementation of the national water act, 1998 in soweto, south africa. *Development Southern Africa*, 10.1080/0376835X.2019.1647834, pp.1-18.

Maree, J.P., Hlabela, P., Nengovhela, R., Geldenhuys, A., Mbhele, N., Nevhulaudzi, T. & Waanders, F., 2004 Treatment of mine water for sulphate and metal removal using barium sulphide. *Mine Water and the Environment*, 23, pp.195-203.

Mekonnen, M.M. & Hoekstra, A.Y., 2016 Four billion people facing severe water scarcity. *Science Advances*, 2, pp.e1500323.

Mueller, D., 2015 *Recycling wastewater from oil and gas wells pose challenges*.

Musingafi, M., 2014 Fresh water sources pollution: A human related threat to fresh water security in south africa. *Journal of Public policy and Governance*, 1, pp.72-81.

Naicker, K., Cukrowska, E. & McCarthy, T.S., 2003 Acid mine drainage arising from gold mining activity in johannesburg, south africa and environs. *Environ Pollut*, 122, pp.29-40.

Oberholster, P. & Ashton, P., 2008 An overview of the current status of water quality and eutrophication in south african rivers and reservoirs. *CSIR/NRE/WR/IR/2008/0075/C*.

Phillips, H., 1990 The origin of the public health act of 1919. *S Afr Med J*, 77, pp.531-532.

Pichtel, J., 2016 Oil and gas production wastewater: Soil contamination and pollution prevention. *Applied and Environmental Soil Science*, 2016, pp.1-24.

Teagle, A. 2015 No drop to waste: Tackling south africa's water crisis. *Daily Maverick*, [Online] Available from: <https://www.dailymaverick.co.za/article/2015-11-06-no-drop-to-waste-tackling-south-africas-water-crisis/#.WKN3h4VOLmI>.

Tempelhoff, J., 2017 The water act, no. 54 of 1956 and the first phase of apartheid in south africa (1948–1960). *Water History*, 10.1007/s12685-016-0181-y.

Tsai, W.T., Hsien, K.J. & Yang, J.M., 2004 Silica adsorbent prepared from spent diatomaceous earth and its application to removal of dye from aqueous solution. *J Colloid Interface Sci*, 275, pp.428-433.

UNICEF and WHO Joint Monitoring Programme, 2015 *25 years progress on sanitation and drinking water: 2015 update and mdg assessment*. Switzerland: WHO Press.

Wang, Y. & Lu, J., 2015 Optimization of china crude oil transportation network with genetic ant colony algorithm. *Information*, 6, pp.467-480.

WEF, W.E.F., 2019 *The global risks report 2019 (14th edition)*. Geneva: Forum, W.E.

WHO/UNICEF, U.N.C.s.F.U.a.W.H.O., 2019 *Progress on household drinking water, sanitation and hygiene 2000-2017. Special focus on inequalities*. New York.

Wilson, J.M. & VanBriesen, J.M., 2012 Research articles: Oil and gas produced water management and surface drinking water sources in pennsylvania. *Environmental Practice*, 14, pp.288-300.

World Bank, 2016 *High and dry: Climate change, water, and the economy*. Washington, DC.

WWAP, U.N.W.W.A.P., 2015 *The united nations world water development report 2015: Water for a sustainable world*. Paris.

WWAP, U.N.W.W.A.P., 2017 *The united nations world water development report 2017: Wastewater, the untapped resource*. UNESCO, Paris.

WWF-SA, 2017a *Wwf south africa integrated annual report* Cape Town.

WWF-SA, 2017b *Scenarios for the future of water in south africa*.

Chapter Two: Literature review

2.1. Oil in wastewater

For many nations, petroleum is a major source of energy. Its daily consumption globally is expected to increase to about 106.6 million barrells in 2030. South Africa has a modest amount of oil but has the 8th largest shale gas reserves with about 390 trillion cubic feet of technically recoverable shale gas reserves. Large scale exploration of this resources is expected to begin in the near future (Pichtel, 2016). This exploration, just like all fosil fuel extraction, requires a lot of water. Millions of gallons of water (per well) is introduced into shale formations to make them more permeable (Wilson and VanBriesen, 2012). A portion of this water flows back to the surface immediately as flowback (Pichtel, 2016) and the remaining either pervade the formation or return to the surface all through the life of the well as ‘produced water’ (Wilson and VanBriesen, 2012). Both flowback and produced water are very rich in oils (Wilson and VanBriesen, 2012). Generally, oils in wastewater are classified as either dissolved or dispersed (Figure 2.1).

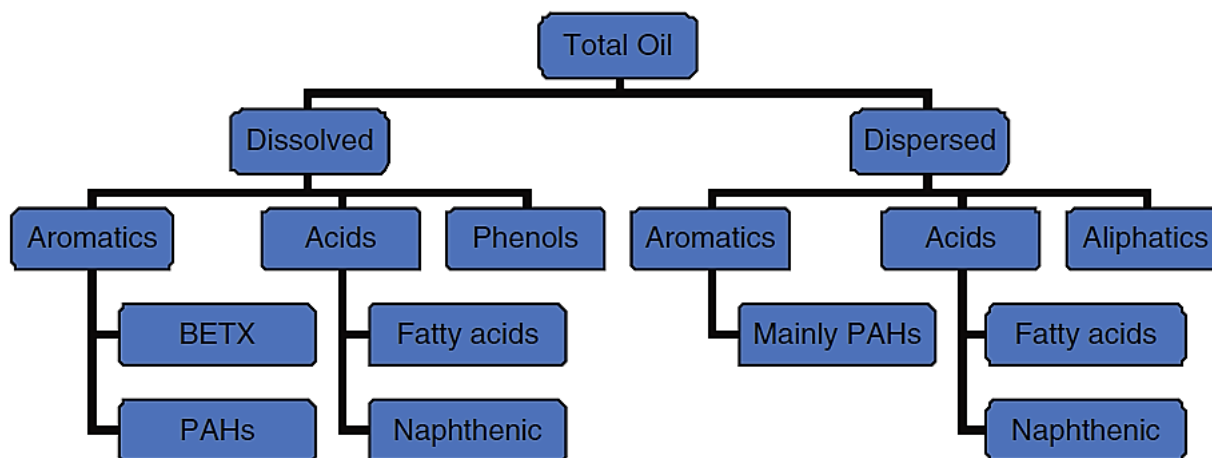


Figure 2. 1. Classification of oils in wastewater (Yang, 2011).

The major constituents of produced water (Table 2.1) are oil, salts, suspended solids, metals and organics like hydrocarbon compounds. Oil and gas exploration is said to produce about 80% of wastewater which increases to about 95% in aging wells and about 40% of this is discharged into the environment (Pichtel, 2016). This additional amount of water use as well as the associated

wastewater generated is expected to put a further strain on South Africa's water resources (Mueller, 2015).

Table 2. 1. Composition of produced water (Pearce and Whyte, 2005).

Parameter	Values
Density (kg/m ³)	1014 – 1140
Surface tension (dynes/cm)	43 – 78
TOC (mg/L)	0 – 1500
COD (mg/L)	1220
TSS (mg/L)	1.2 – 1000
pH	4.3 – 10
Total oil (IR: mg/L)	2 – 565
Volatile (BTX: mg/L)	0.39 – 35
Total non-volatile oil & grease by GC/MS (g/L)	275
Total polar (mg/L)	9.7 – 600
Higher acids (mg/L)	<1 – 63
Phenols (mg/L)	0.0009 – 23
Volatile fatty acids (mg/L)	2 – 4900

Also, wastewater from synthetic fuel facilities is said to have high amount of oil and other dissolved organics. Table 2.2 gives a composition of wastewater from a typical synthetic fuel refinery.

Table 2. 2. Composition of refining wastewater (Pearce and Whyte, 2005).

Contaminant	Minimum monthly average concentration (mg/L)	Maximum allowable limit (mg/L)
Oil	3.6	2.5
Sulphide	0.1	Not reported
Phenol	3	Not reported
COD	179	75
Ammonia	1.2	6
pH	7.2	9.5

2.2. Impact of oily wastewater

Oily wastewater is a growing environmental problem in the world today. Its negative effect is felt on both terrestrial and marine environments (Ismail, 2015). Attention is however focused mainly on marine ecosystem as a result of the devastating economic effect it can have on this ecosystem as well as on those who exploit it (Ismail, 2015).

The impact of oil on marine organisms depends on the fate of oil in the ecosystem. For example, dispersed oil harms marine organisms like larvae, fish and plankton, which is food for many animals. This will ultimately lead to the death of the larger marine organisms which depend on them for food and will eventually have a negative effect on the the economy of the people living in that area (Ismail, 2015).

To ease water stress in South Africa and other parts of the world, one of the most obvious steps that could be taken is to reuse and recycle water. This requires appropriate treatment of wastewater as well as the immediate and proper clean-up of oil spills when they occur.

In oil fields currently, to reduce the effect of pollution from produced water, first the wells are protected with cement and other materials to prevent or minimize the amount of water that flows out, the water is reused by injecting it back to its formation or used in other formations or reused in drilling but this method pollutes ground water in the long term. The water is also applied in irrigation, wildlife consumption or discharged as long as it meets onshore/ offshore requirements

but the water discharged is usually not free of pollutants especially dissolved organic contaminants, heavy metals and dissolved oil and hydrocarbons (Igunnu and Chen, 2012).

Methods that have been previously used in the removal of organic pollutants from water and in the treatment of produced water (Table 2.3) are coagulation, filtration with coagulation, precipitation, ozonation, adsorption, ion exchange, reverse osmosis, biological methods and advanced oxidation processes. All these methods, with the exception of adsorption, are expensive to run, cannot be used without proper training and in the case of biological methods, takes up too much time (Rashed, 2013).

Table 2. 3. Conventional treatment methods of oily wastewater (Pearce and Whyte, 2005).

Conventional methods	Disadvantages
Flotation	Long time, high energy, device manufacturing and repairing problems
Coagulation	Selected coagulants can't make theoretical predictions. Lots of experiments to screen
Biological treatment	Long time
Membrane separation	Contamination of film, thermal stability, small volume. Generally used with other techniques

Adsorption has some advantages over the other listed methods which makes it successful in the removal of trace and organic pollutants as well as toxic metals. These advantages are high removal efficiency, low energy demand, less chemical investment and reuseability (Dinker and Kulkarni, 2015). Over the years, several adsorbents like activated carbon, zeolites, clays, nanomagnetic particles have been used. Moazed and Viraraghavan (2005) used bentonite clay to remove oil from water and it was shown to be able to adsorb 70% of its weight in oil and had an oil removal capacity of 100% but they were not successful in the removal of organic compounds. Other adsorbents were found to have relatively low adsorption capacities (Dinker and Kulkarni, 2015). This created the need to find other adsorbents with high porosity, large surface area and high functionality, all of which were lacking in the aforementioned adsorbents. Silica gels have been found to have all these

characteristics (Dinker and Kulkarni, 2015). Table 2.4 shows some other adsorbents that have been tested for oil sorption studies. Many natural adsorbents have been used with great success recording sorption capacities of as high as 5560 mg/g for natural wool fibre (Rajakovic et al., 2007). Silica gels have relatively high sorption capacity and can be extracted from diatomaceous earth in high yield using readily available materials and do not have as many competing uses as other adsorbents with comparable sorption capacities.

Table 2. 4. Adsorbents reported for oil sorption.

Adsorbent	Oil studied	Sorption capacity (mg/g)	Reference
Bentonite	Crude oil	493	Okiel et al. (2011)
Natural wool fibre	Oily wastewater	5560	Rajakovic et al. (2007)
Crab-shell-derived biochar	Diesel oil	93.9	Cai et al. (2019)
Textile fibres	Crude oil	4200	Sulyman et al. (2018)
Banana peel	Crude oil/gas oil	6630	Alaa El-Din et al. (2018)
Polystyrene organogel	Chlorophenols	345	Ghobashy et al. (2018)
Magnetic carbon nanotubes	Crude oil	990	Zhang et al. (2020)
Mullite-Zeolite-Activated carbon	Synthetic oily wastewater	999	Jafari et al. (2020)
Acetylated corncobs	Oily water	2500	Nwadiogbu et al. (2016)
Silica aerogels	Dibutylphthalate	3500	Filipovic et al. (2010)

2.3. Porous silica hydrogels

The characteristics of these materials are dependent on the size, shape, arrangement, constituent materials, and porosity of their pores. Ordered porous materials can be synthesized using porogens (templates) or pore forming agents while disordered / amorphous porous materials are usually synthesized without the use of templates or pore forming agents (Chevalier et al., 2008). Templates

can be made of a combustible material (mostly organic in nature) which can be burnt off when heated, to leave ordered pores (Chevalier et al., 2008). They could also be made of soluble additives, which are dissolved in appropriate solvents to give ordered pores (Chevalier et al., 2008). Several materials have been used as templates/ pore formers over the years in the synthesis of various porous materials. The most popular template in the synthesis of porous silica gels, which is the focus of this study, is cetyl trimethyl ammonium bromide (CTAB). One major drawback in the use of this template though, is the application of very high temperatures to ‘burn them off’. Hydrogels are gels that have water as its liquid component (Ahmed, 2015). They are basically polymers that can swell and retain water within its cross-linked structure without it dissolving (Ahmed, 2015).

Mesoporous materials are materials that lie between micro-porous and macro-porous materials and have pore sizes between 2 and 50 nm (Haber, 1991). Since a patent for the production of low – bulk density silica was approved in 1969 and published in 1971 (Chiola et al., 1969), and since a patent was filed for the use of the gels in the clarification of apple juice in 1986 (Harville et al., 1986), porous silica gels have become the ‘go – to’ technology in water purification. Especially since 1997 when the process was reproduced (Di Renzo et al., 1997), it has found application in the removal of such pollutants as heavy metal ions, inorganic anions, metalloids, pesticides and polyaromatic hydrocarbons (Nasreen and Rafique, 2012; Bruzzoniti et al., 2016; Nasreen et al., 2016; Hossain et al., 2020).

Porous silica particles have found application in many areas such as drug delivery (Numpilai et al., 2017; Ghosh, 2019; Ruan et al., 2019; Gisbert-Garzarán et al., 2020) and water purification (Sun et al., 2017; Albertini et al., 2018; Jeelani et al., 2019), among others. They have been used in chromatography, waste removal and many other applications. They have certain characteristics which make them highly desirable. These characteristics include high surface area, high porosity, they are not cytotoxic and they have highly ordered pores (Torres et al., 2015). These materials have been researched widely in recent times for use in environmental remediation and many new porous gels have been synthesized (Nasreen et al., 2016; Vazquez et al., 2017; Vlasenkova et al., 2019) with a number of them using tetraethyl orthosilicate as silica precursor. This makes production of these gels expensive. There is still therefore, the need to find cost effective, novel

silica-based compounds using cheap feedstock. It is necessary to first take a look at some of the methods that have been employed in the synthesis of these materials.

2.4. Synthesis of porous silica gels

Various methods have been used in the production of porous silica hydrogels, the most popular being the Stöber process, first reported by Stöber et al. (1968). It is a sol - gel method that uses the precursor, tetraethyl orthosilicate (TEOS) whose acid hydrolysis in alcohol was catalysed by ammonia to give ethoxysilanols which were hydrolysed further and condensed to produce silica of uniform pore sizes (Stöber et al., 1968). This method was however not reproducible and bulk densities were too high and not controllable. A year after this method was published, a patent for the preparation of low – density silica gels, an improvement on the process for preparing silica, was filed but was only approved in 1971 (Chiola et al., 1969). The method controlled the hydrolysis of tetra alkyl silicates by employing ammoniacal hydrolysis of the silicates to give silica of lower and controlled bulk densities. This created further interest in the synthesis of these materials, but they were not truly appreciated until the 1980s when several patents describing various applications of the materials surfaced. Dewolf II and Glemza (1981) described a method for producing hydrogels and incorporating them into dentifrice compositions. They reacted sodium silicate with sulphuric acid, delivering both reactants into a high-speed mixer at room temperature to form hydrosol, allowed the sol to set into a gel and washed with aqueous acid to remove unreacted sodium sulphate. In 1986, a patent describing the use of hydrogels, prepared in much the same way as that of DeWolf, in the clarification of Apple juice was filed and approved (Harville et al., 1986).

Hilonga et al. (2009) prepared silica alcogels by first diluting TEOS with methanol, ethanol, butanol or isopropanol and then mixing this with 0.01 M oxalic acid with constant stirring for 30 min. After 24 h, 0.1 M base catalyst, ammonium hydroxide was added dropwise into the acid catalysed sol. Mole ratio of TEOS : Alcohol : Water (acidic) : Water (basic) was 1 : 6.9 : 3.5 : 2.2. Hilonga et al. (2009) modified their alcogels via one step solvent exchange surface modification process. Aged alcogels were immersed in a solution mixture of alcohol / trimethylchlorosilane / perfluorohexane for 2 h at room temperature. The gels were then washed with perfluorohexane and dried at 50°C for 12 h, 80°C for 2 h and 200°C for 1 h. Hilonga's work was time saving and very practical in that it produced gels with low density and very high surface area and even though

the gels formed were not of uniform size, they had large pore volume. Mesoporous silica particles have also been synthesized and used for controlled release of anticancer drugs by mixing TEOS, AHO 647 – conjugated 3 – aminopropyltrimethoxysilane (APTS), CTAB and a base catalyst, ammoniumhydroxide. The surfactant, CTAB was then removed by extracting with an ammonium nitrate / alcohol solution and the gels were grafted with trimethylammonium groups and further complexed with hydrazone (Lee et al., 2010). Instead of using high temperatures to remove the template, extraction was employed thereby saving energy. About the same time, Teng et al. (2010) stirred 0.5 mL TEOS, 40.5 mL of different ratios of water/ethanol mix, 0.08 g CTAB and 0.5 mL 25 wt% ammonia solution at 25°C for 3 h after which they collected the resulting products after centrifugation and calcined them in air at 200°C for 6 h and 600°C for 6 h. Unlike Lee et al. (2010) though, they used high temperatures to remove the template and calcine leading to energy wastage.

Using polystyrene homopolymers as porogen, Wang et al. (2016) synthesized silica hydrogels. First, using α – bromo terminated polystyrene intermediate, synthesized via atom transfer radical polymerization, they synthesized polystyrene hydroxide and stirred this solution with 3 – isocyanatopropyltriethoxysilane (IPTES) (to make the polystyrene hydroxide more reactive), dibutyltin dilaurate as catalyst and anhydrous THF. The solution was then cooled to room temperature and poured into a polyethylene beaker and TEOS and THF was added and the solution stirred. Then HCl was added and the solution stirred vigorously. The beaker was sealed and left to stand at room temperature for 4 weeks to allow the solution to gel. In this process Wang et al. (2016) used polystyrene homopolymers as porogen instead of the regular surfactants giving rise to organic – inorganic hydrogels without macroscopic phase separation and removal of the organic phase led to the creation of gels with well ordered pores. To make the polystyrene polymers as reactive as TEOS however, they had to react them with IPTES using dibutyltin dilaurate as catalyst to give them terminal triethoxysilane moieties. Commonly organic surfactants for example cetyl trimethyl ammonium bromide (CTAB) (Pan et al., 2009) and organic moieties for example polystyrene latex are used as templates. Polystyrene latex has proven to be better templates in that no aspherical pores are formed (Velev et al., 1997). This is possibly the justification for the use of porogens by Wang et al. (2016) Exploring green synthesis of gels further, Alves et al. (2017) prepared gels by adding acetic acid dropwise to sodium silicate from sugarcane waste ash with stirring till neutral pH. The gels they obtained were then aged at room temperature for 20 h, washed with distilled water, filtered and dried at 80°C for 24 h.

As is seen in almost all the reported literature Numpilai et al. (2017), in order to give silica hydrogels specific properties, their surfaces have been grafted with certain materials over time. After preparation of their gels, Numpilai et al. (2017) grafted their silica with aldehyde by mixing silica, toluene and triethoxysilylbutyraldehyde with stirring and collecting the solid products after centrifugation. These were dried in vacuum at 40°C. Izuagie et al. (2016) reported grafting of silica with Al^{3+} , Fe^{3+} and Al/Fe oxide by shaking diatomaceous earth with Al^{3+} and Fe^{3+} separately and then with NaOH. They grafted silica with Al/Fe oxide, Al^{3+} and Fe^{3+} were mixed together, diatomaceous earth was added. The mixture was shaken and NaOH was added, shaken and centrifuged. The solid was left exposed, washed and dried in the oven and used in ground water defluoridation. Sun et al. (2017) reported the use of Al/Fe composite to clean up oil from water.

There is continued interest to find new and efficient ways to synthesize mesoporous silica gels (Wang et al., 2016). There has been several attempts to synthesize organic – modified mesoporous gels through one - pot synthesis and post synthesis grafting giving rise to products that are efficient in the removal of heavy metals from wastewater (Feng et al., 2000). There are however, very few reports on the synthesis of polymer – modified mesoporous hybrid materials despite the successful synthesis of these materials by Feng et al. (2000). The application of these hybrid materials have also not been explored. This study explores the synthesis of polymer – modified gels (containing hydrazino substituted benzimidazole rings) and compares their applicability to gels grafted with similar materials. Also, one major drawback of most of the reported syntheses is the use of high energy conventional heating especially in the removal of templates.

In almost all the reviewed literature, TEOS was used as silica source in the synthesis of porous gels. Some other studies made use of sorghum bargasse, sugarcane leaves, sugarcane bargasse and sugarbeet bargasse and most studies, with the exception of Hilonga et al. (2009) and a few others, used one form of template / porogen or the other. This study aims to use a cheaper and more readily available source of silica, diatomaceous earth.

2.5. Diatomaceous Earth

Diatomaceous earth (DE) also known as diatomite, tripolite or kieselgur is a white powder occurring naturally as a soft sedimentary rock containing about 80 to 90% silica (Antonides, 1998;

Izuagie et al., 2016). It is sometimes called infusorial earth or mountain meal (MohamedBakr, 2010). It is formed naturally due to the accumulation of the silica cell walls of dead, microscopic, single celled, aquatic algae called diatoms. There are many species of diatoms some of which produce the nerve poison, domoic acid which can cause rapid death if ingested (Antonides, 1998).

Diatomaceous earth has been used in a variety of areas over the years in building (Antonides, 1998); as stabilizer of nitro-glycerine in dynamite (Antonides, 1998); as filter aid for water, sugar, sweetener liquors, oils, fats, alcoholic beverages, chemicals, and pharmaceuticals. It can be used in this way because it is highly porous, has low density and high surface area (MohamedBakr, 2010). This accounts for half the worldwide use of diatomite (MohamedBakr, 2010). It has also been used as filler in paints, plastics, Portland cement, as catalysts and as absorptive carrier in pesticides (Mazidi et al., 2017). Furthermore, it has been used as absorbent for industrial spills (oils and toxic liquids), as abrasive in polishes, in insulation material (Antonides, 1998), in grain preservation (Subramanyam et al., 1994), as a natural insecticide (Tsai et al., 2005), as an anticaking agent (Antonides, 1998; Tsai et al., 2004), and in chemical analysis, it is used in chromatographic columns (Tsai et al., 2005).

In all reviewed literature, it is seen that the most common silica source is tetraethyl orthosilicate (TEOS) which is relatively expensive especially for industrial production of silica. Also, most of the studies make use of porogens such as cetyl trimethyl ammonium bromide (CTAB) which further increases the cost of silica production. There is therefore need for cheap and readily available silica sources as well as the use of non-templated methods in the production of silica. Also, it has been established in literature that surface modification of silica makes it applicable in specific areas such as water purification and others because of the introduction of additional functional groups. Polymers and organic moieties introduce several organic moieties to silica but there is a paucity of reported studies on the modification of silica with these.

2.6. References

Ahmed, E.M., 2015 Hydrogel: Preparation, characterization, and applications: A review. *J Adv Res*, 6, pp.105-121.

Alaa El-Din, G., Amer, A.A., Malsh, G. & Hussein, M., 2018 Study on the use of banana peels for oil spill removal. *Alexandria Engineering Journal*, 57, pp.2061-2068.

Albertini, F., Ribeiro, T., Alves, S., Baleizão, C. & Farinha, J.P., 2018 Boron-chelating membranes based in hybrid mesoporous silica nanoparticles for water purification. *Materials & Design*, 141.

Alves, R.H., Reis, T.V.d.S., Rovani, S. & Fungaro, D.A., 2017 Green synthesis and characterization of biosilica produced from sugarcane waste ash. *Journal of Chemistry*, 2017, pp.1-9.

Antonides, L.E., 1998 Diatomite. *U.S. Geological Survey Mineral Commodity Summaries*, pp.56-57.

Bruzzoniti, M.C., De Carlo, R.M., Rivoira, L., Del Bubba, M., Pavani, M., Riatti, M. & Onida, B., 2016 Adsorption of bentazone herbicide onto mesoporous silica: Application to environmental water purification. *Environ Sci Pollut Res Int*, 23, pp.5399-5409.

Cai, L., Zhang, Y., Zhou, Y., Zhang, X., Ji, L., Song, W., Zhang, H. & Liu, J., 2019 Effective adsorption of diesel oil by crab-shell-derived biochar nanomaterials. *Materials*, 12, pp.236.

Chevalier, E., Chulia, D., Pouget, C. & Viana, M., 2008 Fabrication of porous substrates: A review of processes using pore forming agents in the biomaterial field. *J Pharm Sci*, 97, pp.1135-1154.

Chiola, V., Ritsko, J.E. & Vanderpool, C.D. 1969 *Process for producing low-bulk density silica*.

Dewolf II, R.B. & Glemza, R. 1981 *Hydrous silica gel containing dentifrice*.

Di Renzo, F., Cambon, H. & Dutartre, R., 1997 A 28-year-old synthesis of micelle-templated mesoporous silica. *Microporous Materials*, 10, pp.283-286.

Dinker, M.K. & Kulkarni, P.S., 2015 Recent advances in silica-based materials for the removal of hexavalent chromium: A review. *Journal of Chemical and Engineering Data*, 60, pp.2521-2540.

Feng, Q., Xu, J., Dong, H., Li, S. & Wei, Y., 2000 Synthesis of polystyrene-silica hybrid mesoporous materials the nonsurfactant-templated sol-gel process. *Journal of Materials Chemistry*, 10, pp.2490-2494.

Filipovic, R., Lazić, D., Perusic, M. & Stijepović, I., 2010 Oil absorption in mesoporous silica particles. *Processing and Application of Ceramics*, 4.

Ghobashy, M.M., Younis, S.A., Elhady, M.A. & Serp, P., 2018 Radiation induced in-situ cationic polymerization of polystyrene organogel for selective absorption of chlorophenols from petrochemical wastewater. *Journal of Environmental Management*, 210, pp.307-315.

Ghosh, S., 2019 Chapter 9 - mesoporous silica-based nano drug-delivery system synthesis, characterization, and applications. In: Mohapatra, S.S., Ranjan, S., Dasgupta, N., Mishra, R.K. & Thomas, S. (eds.). *Nanocarriers for drug delivery*: Elsevier.

Gisbert-Garzarán, M., Manzano, M. & Vallet-Regí, M., 2020 Mesoporous silica nanoparticles for the treatment of complex bone diseases: Bone cancer, bone infection and osteoporosis. *Pharmaceutics*, 12, pp.83.

Haber, J., 1991 Manual on catalyst characterization. *Pure & Applied Chemistry*, 63, pp.1227-1246.

Harville, C.L., Burnie, G. & Williams, T.E. 1986 *Apple juice clarification by using silica hydrogels*. H000089.

Hilonga, A., Kim, J.-K., Sarawade, P.B. & Kim, H.T., 2009 Low-density teos-based silica aerogels prepared at ambient pressure using isopropanol as the preparative solvent. *Journal of Alloys and Compounds*, 487, pp.744-750.

Hossain, N., Bhuiyan, M.A., Pramanik, B.K., Nizamuddin, S. & Griffin, G., 2020 Waste materials for wastewater treatment and waste adsorbents for biofuel and cement supplement applications: A critical review. *Journal of Cleaner Production*, 255, pp.120261.

Igunnu, E.T. & Chen, G.Z., 2012 Produced water treatment technologies. *International Journal of Low-Carbon Technologies*, 9, pp.157-177.

Ismail M.K., 2015 Impact of oil spills on marine life. In: Larramendy M.L and Soloneski S. (ed.) *Emerging Pollutants in the Environment - Current and Further Implications*. Rijeka, Croatia: InTech Publisher.

Izuagie, A.A., Gitari, W.M. & Gumbo, J.R., 2016 Defluoridation of groundwater using diatomaceous earth: Optimization of adsorption conditions, kinetics and leached metals risk assessment. *Desalination and Water Treatment*, 57, pp.16745-16757.

Jafari, B., Abbasi, M. & Hashemifard, S.A., 2020 Development of new tubular ceramic microfiltration membranes by employing activated carbon in the structure of membranes for treatment of oily wastewater. *Journal of Cleaner Production*, 244, pp.118720.

Jeelani, P.G., Mulay, P., Venkat, R. & Ramalingam, C., 2019 Multifaceted application of silica nanoparticles. A review. *Silicon*, 10.1007/s12633-019-00229-y.

Lee, C.H., Cheng, S.H., Huang, I.P., Souris, J.S., Yang, C.S., Mou, C.Y. & Lo, L.W., 2010 Intracellular ph-responsive mesoporous silica nanoparticles for the controlled release of anticancer chemotherapeutics. *Angew Chem Int Ed Engl*, 49, pp.8214-8219.

Mazidi, M., Mosayebi Behbahani, R. & Fazeli, A., 2017 Screening of treated diatomaceous earth to apply as v2o5 catalyst support. *Materials Research Innovations*, 21, pp.269-278.

Moazed, H. & Viraraghavan, T., 2005 Use of organo-clay/anthracite mixture in the separation of oil from oily waters. *Energy Sources*, 27, pp.101-112.

MohamedBakr, H.E.G.M., 2010 Diatomite: Its characterization, modifications and applications. *Asian J. Mater. Sci.*, 2 pp.121-136.

Mueller, D., 2015 *Recycling wastewater from oil and gas wells pose challenges*.

Nasreen, S. & Rafique, U., 2012 Synthesis, characterization and application of novel nano-adsorbents for the treatment of nitrates and phenols in wastewater. *International Journal of Chemical and Environmental Engineering*, 3, pp.355-361.

Nasreen, S., Urooj, A., Rafique, U. & Ehrman, S., 2016 Functionalized mesoporous silica: Absorbents for water purification. *Desalination and Water Treatment*, 57, pp.29352-29362.

Numpilai, T., Witoon, T., Chareonpanich, M. & Limtrakul, J., 2017 Impact of physicochemical properties of porous silica materials conjugated with dexamethasone via ph-responsive hydrazone bond on drug loading and release behavior. *Applied Surface Science*, 396, pp.504-514.

Nwadiogbu, J.O., Ajiwe, V.I.E. & Okoye, P.A.C., 2016 Removal of crude oil from aqueous medium by sorption on hydrophobic corncobs: Equilibrium and kinetic studies. *Journal of Taibah University for Science*, 10, pp.56-63.

Okiel, K., El-Sayed, M. & El-Kady, M.Y., 2011 Treatment of oil–water emulsions by adsorption onto activated carbon, bentonite and deposited carbon. *Egyptian Journal of Petroleum*, 20, pp.9-15.

Pan, W., Ye, J., Ning, G., Lin, Y. & Wang, J., 2009 A novel synthesis of micrometer silica hollow sphere. *Materials Research Bulletin*, 44, pp.280-283.

Pearce, K. & Whyte, D., 2005 *Water and wastewater management in the oil refining and re-refining industry*. Pretoria.

Pichtel, J., 2016 Oil and gas production wastewater: Soil contamination and pollution prevention. *Applied and Environmental Soil Science*, 2016, pp.1-24.

Rajakovic, V., Aleksic, G., Radetic, M. & Rajakovic, L., 2007 Efficiency of oil removal from real wastewater with different sorbent materials. *J Hazard Mater*, 143, pp.494-499.

Rashed, M.N., 2013 Adsorption technique for the removal of organic pollutants from water and wastewater. In: Rashed, M.N. (ed.). *Organic pollutants-monitoring, risk and treatment*. Rijeka, Croatia: InTech Publisher.

Ruan, L., Chen, W., Wang, R., Lu, J. & Zink, J.I., 2019 Magnetically stimulated drug release using nanoparticles capped by self-assembling peptides. *ACS Applied Materials & Interfaces*, 11, pp.43835-43842.

Stöber, W., Fink, A. & Bohn, E., 1968 Controlled growth of monodisperse silica spheres in the micron size range. *Journal of Colloid and Interface Science*, 26, pp.62-69.

Subramanyam, B.H., Swanson, O.L., Madamanchi, N. & Norwood, S., 1994 Effectiveness of insecto, a new diatomaceous earth formulation, in supporting several stored-grain insect species. Canberra:650-659.

Sulyman, M., Sienkiewicz, M., Haponiuk, J. & Zalewski, S., 2018 New approach for adsorptive removal of oil in wastewater using textile fibers as alternative adsorbent. *Acta Scientific Agriculture*, 2, pp.32-37.

Sun, Y.J., Zhu, C.Y., Zheng, H.L., Sun, W.Q., Xu, Y.H., Xiao, X.F., You, Z.Y. & Liu, C.Y., 2017 Characterization and coagulation behavior of polymeric aluminum ferric silicate for high-concentration oily wastewater treatment. *Chemical Engineering Research & Design*, 119, pp.23-32.

Teng, Z., Han, Y., Li, J., Yan, F. & Yang, W., 2010 Preparation of hollow mesoporous silica spheres by a sol-gel/emulsion approach. *Microporous and Mesoporous Materials*, 127, pp.67-72.

Torres, C.C., Urbano, B.F., Campos, C.H., Rivas, B.L. & Reyes, P., 2015 Composite hydrogel based on surface modified mesoporous silica and poly[(2-acryloyloxy)ethyl trimethylammonium chloride]. *Materials Chemistry and Physics*, 152, pp.69-76.

Tsai, W.T., Hsien, K.J. & Yang, J.M., 2004 Silica adsorbent prepared from spent diatomaceous earth and its application to removal of dye from aqueous solution. *J Colloid Interface Sci*, 275, pp.428-433.

Tsai, W.T., Hsien, K.J., Chang, Y.M. & Lo, C.C., 2005 Removal of herbicide paraquat from an aqueous solution by adsorption onto spent and treated diatomaceous earth. *Bioresour Technol*, 96, pp.657-663.

Vazquez, N.I., Gonzalez, Z., Ferrari, B. & Castro, Y., 2017 Synthesis of mesoporous silica nanoparticles by sol-gel as nanocontainer for future drug delivery applications. *Boletín de la Sociedad Española de Cerámica y Vidrio*, 56, pp.139-145.

Velev, O.D., Jede, T.A., Lobo, R.F. & Lenhoff, A.M., 1997 Porous silica via colloidal crystallization. *Nature*, 389, pp.447-448.

Vlasenkova, M.I., Dolinina, E.S. & Parfenyuk, E.V., 2019 Preparation of mesoporous silica microparticles by sol-gel/emulsion route for protein release. *Pharmaceutical Development and Technology*, 24, pp.243-252.

Wang, C.Y., Li, L. & Zheng, S.X., 2016 Synthesis and characterization of mesoporous silica monoliths with polystyrene homopolymers as porogens. *RSC Advances*, 6, pp.105840-105853.

Wilson, J.M. & VanBriesen, J.M., 2012 Research articles: Oil and gas produced water management and surface drinking water sources in pennsylvania. *Environmental Practice*, 14, pp.288-300.

Yang, M., 2011 Measurement of oil in produced water. *Produced water*

Zhang, B., Huang, K., Wang, Q., Li, G., Wu, T. & Li, Y., 2020 Highly efficient treatment of oily wastewater using magnetic carbon nanotubes/layered double hydroxides composites. *Colloids and Surfaces A: Physicochemical and Engineering Aspects*, 586, pp.124187.

Chapter Three: Optimization of silica extraction from diatomaceous earth using the central composite design of response surface methodology

Abstract

Silicon (IV) oxide (silica) is the second most abundant element of the earth's crust. It is one of the valuable basic raw materials widely used in the production of semiconductors, ceramics and polymers. It can be found in various forms including in gel, crystalline and amorphous forms. Common uses of silica, such as water purification, require high purity silica which can be extracted from sand and other quartz containing minerals. In nature, silica is extensively found as a major mineral in most igneous, sedimentary (e.g sand and sand stones) and metamorphic rocks (quartzite) but the amount of silica that can be obtained from these ores is not enough to meet the vast and varied uses the oxide can be put to. In addition, extraction of silica from these minerals is based on mechanical, physical and energy intensive thermal operations at high temperatures using large amounts of reactants and generating high volumes of effluents. This is so because the ores contain high amounts of impurities which are difficult to dissolve. Diatomaceous earth (DE) contains about 80 to 90% silica and has been shown to have few impurities and is therefore easy to purify. Also, DE is cheap and readily available unlike alternative sources of silica which are not readily available and therefore expensive. This work used response surface methodology (RSM) to optimize the extraction of silica from DE. Conventional solvent extraction (CSE) and ultrasound assisted extraction (UAE) using NaOH and HCl to extract silica from DE were used. Statistical models of each method were used to get the best percentage yield and percentage extracted silica using response surface methodology (RSM). Stirring time and concentration of NaOH were optimized in the CSE method. Sonication time, concentration of NaOH/HCl, cycle and amplitude were optimized in the UAE methods. The data from percentage yield and percentage purity from all methods were analyzed using ANOVA and regression analysis. The fitness of the obtained models was good and the coefficient of determination R^2 of the models was relatively high, hence the models obtained were adequate. The overall yield and purity were very low with the alkali UAE and CSE methods but were high with the acid UAE method making this the most effective method for silica extraction. The Acid

UAE method was shown to be feasible for the extraction of silica from diatomaceous earth and optimum parameters were 1.99 h for sonication time, 2.82 M for concentration of HCl, 220 mL for volume, 0.524 for cycle and 72.6% amplitude with a desirability of 1.00 giving silica of 95% purity and 82% yield. This research confirms that application of heat in the extraction of silica is very important. It also, for the first time, shows that ultrasonic acid pre-treatment is an important step in silica extraction.

Keywords: Diatomaceous earth, silica, response surface methodology, ultrasound assisted extraction, conventional solvent extraction.

3.1. Introduction

Response surface methodology (RSM) is a statistical approach of experimental design that can be used to optimize the extraction of silica and other analytes. It investigates the variables (extraction conditions) and interactions of the variables simultaneously (Zhao et al., 2011). In contrast, the classical approach of experimental planning looks at one factor at a time while keeping all others constant. This classical method takes up a lot of effort, time and fails to consider interactions between factors (Zhao et al., 2011).

RSM, introduced in 1951 by Box and Wilson Box et al. (2005), is an experimental statistical approach used for combined regression analysis using data from well-planned experiments to solve multivariate equations simultaneously. Graphs obtained from these equations are used to tell the effect of the test factors and their possible interactions on the responses. RSM takes complicated responses and replaces them with a simpler approximate function by looking at the relative significance of the effects of the factors on the responses. It has the ability to effectively choose few points to represent all possible points in the design space thereby reducing the number of runs required to study the significance of different factors that may affect the response of interest (Box et al., 2005).

Diatomaceous earth (DE), also known as diatomite, tripolite or kieselgur is a white powder occurring naturally ubiquitously as a soft sedimentary rock containing about 80 to 90% silica (Antonides, 1998; Izuagie et al., 2016a). It has been used in its raw form in building (Antonides, 1998); as stabilizer of nitro – glycerine in dynamite (Antonides, 1998); as filter aid for water, sugar,

sweetener liquors, oils, fats, alcoholic beverages, chemicals, and pharmaceuticals (MohamedBakr, 2010). It can be used in this way because it is highly porous, has low density and high surface area (MohamedBakr, 2010). It has also been used as a filler in paints, plastics, cement, as catalysts and as absorptive carrier in pesticides (Mazidi et al., 2017). It has been used as absorbent for industrial spills (oils and toxic liquids), as abrasive in polishes, in insulation material (Antonides, 1998), in grain preservation (Subramanyam et al., 1994), as a natural insecticide (Tsai et al., 2005) and in analysis, it is used in chromatographic columns (Tsai et al., 2005).

Silica, which is contained in high amounts in DE, can be mined from natural ores, but the supply that can be obtained from these ores is limited and not sufficient when compared to the vast amount of uses the oxide and elemental silicon can be put to (Bessho et al., 2009). There is therefore the need to consider other sources of silica. Silica has been extracted by several researchers from a variety of sources, mainly of agricultural origin; rice husk (Rafiee et al., 2012; Carmona et al., 2013; Fernandes et al., 2017; Todkar et al., 2016), sugarcane bagasse (Adebisi et al., 2017; Harish et al., 2015), palm ash (Pa et al., 2016) and corn cob (Ogunfowokan et al., 2011; Okoronkwo et al., 2016), and others. Most of the extraction methods used by these authors involved either acid pretreatment or hydrothermal treatment or a combination of both. Treatment with very high temperatures resulted in particles with very high particle size but acid pretreatment before thermal treatment gave particles with much lower particle size. The purest silica (about 99.9%), however, came from samples that were treated hydrothermally in addition to one other treatment method. Even though some authors did not give information about the particle size of silica extracted, it is evident from literature that the extraction method influences the particle size with thermal treatment giving the highest particle size.

DE can be used as natural source of silica because it contains high amount of silica, which is the main component of roads, is used as filler for paints, rubber and in water filtration and agriculture (Vatalis et al., 2015). It is also used as precursor for silica gels, ferrosilicon and elemental silicon which is used in modern day technology in optical data transmission fibers and precision casting and in solar – hydrogen energy systems (Vatalis et al., 2015). Basically, most of the uses of DE are as a result of its high silica content. Despite the large amount of silica contained in DE there is still a paucity of literature on the extraction of silica from it. The few publications available have not optimized the extraction. Since silica occurs naturally in DE in combination with other

elements and oxides, there is the need for cheap and innovative ways to purify it. This work employs the use of RSM, which has reported advantages, to optimize the extraction of silica from DE as opposed to the classical approach of optimization. It compares three different methods employed in silica extraction with a view to finding the best in terms of yield and purity.

3.2. Materials and Methods

3.2.1. Chemicals and reagents

Diatomaceous earth was obtained from Eco – Earth (Midrand, South Africa) and used in its natural state. Sodium hydroxide and hydrochloric acid were of analytical grade and obtained from Rochelle Chemicals (Johannesburg, South Africa) and Milli-Q water from Millipore S.A.S (Molsheim, France) (18.2 MV cm at 25°C) was also used in all dilutions. Ultrasonic processor (UP 4005) Hielscher ultrasound technology, with amplitude of 20 to 100% and cycle of 0.1 – 1 (Berlin, Germany), pH meter from Accsen Instrumental S.L.L. (Barcelona, Spain) and Bruker handheld S1 Titan XRF (Cramerview, South Africa) were used in the study.

3.2.2. Alkali ultrasound – assisted extraction (Alkali UAE method)

The extraction of silica from diatomaceous earth was carried out by modifying the method reported by Bessho et al(year) and optimized with the help of the central composite design (CCD) in the design expert program version 11 as shown in Table 3.1.

To about 20 g of DE in a 250 mL beaker, 100 mL of varying concentrations of NaOH (1 - 4 M) were added and sonicated for varying amount of time (1 - 4 h), cycle (0.1 – 1.0) and amplitude (20% – 100%). Thereafter, the solutions were filtered, and the pH of the filtrate adjusted to 10.5, filtered again and the pH adjusted to 9, filtered and the residue washed with milli-Q water and dried in the oven at 50°C for 12 h. The percentage purity of silica extracted was measured using an XRF and the percentage yield was calculated using Eq. 3.1.

$$\text{Percentage yield} = \left(\frac{\text{weight of silica}}{\text{weight of DE}} \right) * 100 \quad (3.1)$$

Table 3. 1. Range of parameters optimized in the extraction of silica in the conventional extraction and alkali UAE method.

Extraction method	Parameter	Low	High
CSE	Stirring time (h)	6.00	56.7
	NaOH concentration (M)	0.38	4.60
Alkali UAE	Sonication time (h)	1.00	4.00
	NaOH concentration (M)	1.00	4.00
	Cycle	0.10	1.00
	Amplitude (%)	20.0	100
Acid UAE	Sonication time (h)	1.50	2.50
	HCl concentration (M)	2.50	3.50
	Cycle	0.50	0.60
	Amplitude	60.0	80.0
	HCl volume	150	250

3.3. Conventional solvent extraction (CSE)

To 20 g of DE in a 250 mL beaker, 100 mL of varying concentrations of NaOH (0.38 – 4.6 M) was added and the mixture was stirred using a magnetic stirrer for between 6.0 and 56.7 h. The resulting mixture was filtered, and silica was recovered in same way as in the alkali UAE method. The percentage silica extracted was measured using an XRF, and percentage yield were calculated using Eq. 3.1 as in section 3.2.

3.4. Acid ultrasound – assisted extraction (Acid UAE method)

To about 20 g of DE in a 250 mL beaker, 150 - 250 mL of varying concentrations of HCl (2.5 to 3.5 M) was added and sonicated for varying amount of time (1.5 to 2.5 h) while varying cycle (0.5 – 0.6) and amplitude (60% - 80%). After this, the solution was filtered and washed with milli-Q water and dried in the oven at 50°C for 12 h. The percentage silica extracted was measured using

an XRF, and the percentage yield was calculated using Eq. 3.1. The pH of the filtrate was then adjusted to 10.5 and then to 9 and the residue was further purified by stirring a portion in 1M HCl for about 33 h, filtered and the pH of the filtrate adjusted to about 10 and processed in the same way as in the alkali UAE method.

3.5. Characterization of diatomaceous earth and extracted silica

Silica samples with the highest percentage silica (from XRF analysis) extracted using the alkali UAE and CSE methods and samples with the three highest percentage silica from the acid UAE method were characterized. The chemical and mineralogical composition of raw DE and extracted silica from the alkali UAE, acid UAE and CSE methods were determined using X-ray fluorescence (XRF) from ThermosFisher ARL Perform'X Sequential instrument (Basel, Switzerland) and X-ray diffraction (XRD) from Bruker(Bremen, Germany), respectively. XRD analysis was done using a PANalytical X'Pert Pro powder diffractometer in θ - θ configuration with an X'Celerator detector, variable divergence, and fixed receiving slits with Fe-filtered Co-K α radiation ($\lambda = 1.789 \text{ \AA}$). Scanning electron microscope and energy dispersion X-ray spectroscope (EDX), FEI Nova NanoSEM 230 with field emission gun (Eindhoven, Netherlands) was used to examine the morphology and elemental composition of raw DE and the extracted silica samples and a FEI T20 transmission electron microscope (TEM with a CCD camera embedded (2048X2048) was used for further morphological evaluation.

3.6. Results and discussion

3.6.1. Design of experiment

Two main parameters were selected in the CSE method, four in the alkali UAE method and five in the acid UAE method for the optimization of the extraction of silica to avoid overfitting, which occurs in complex models which have too many parameters (Zhao et al., 2011). The range of parameters optimized in both methods are shown in Table 3.1 and their experimental design together with the corresponding responses are shown in Table 3.2.

Table 3. 2. Central composite experimental design for Ultrasound assisted extraction and conventional solvent extraction.

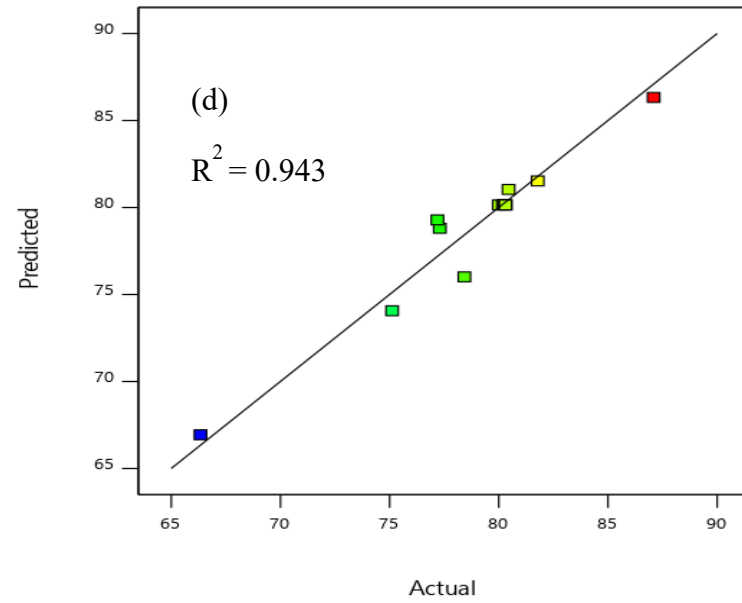
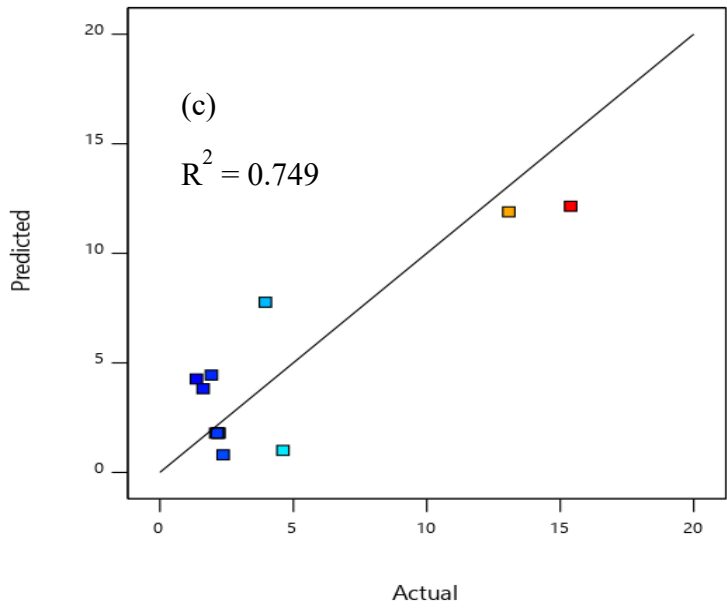
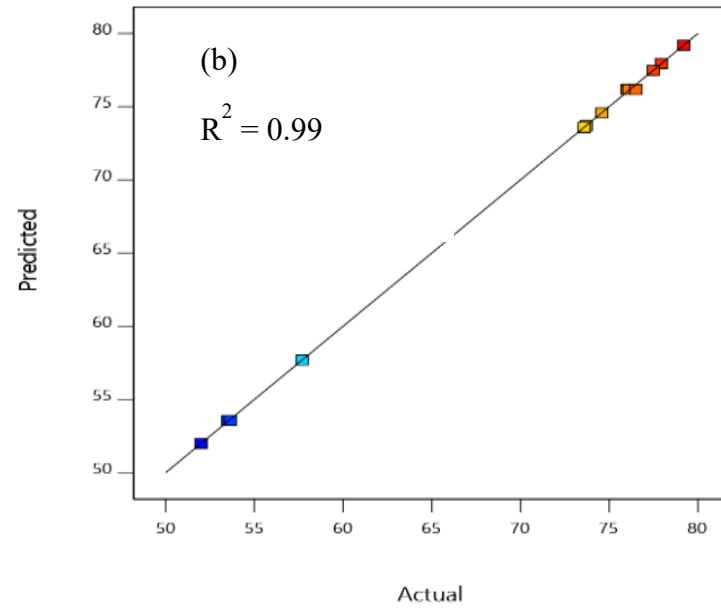
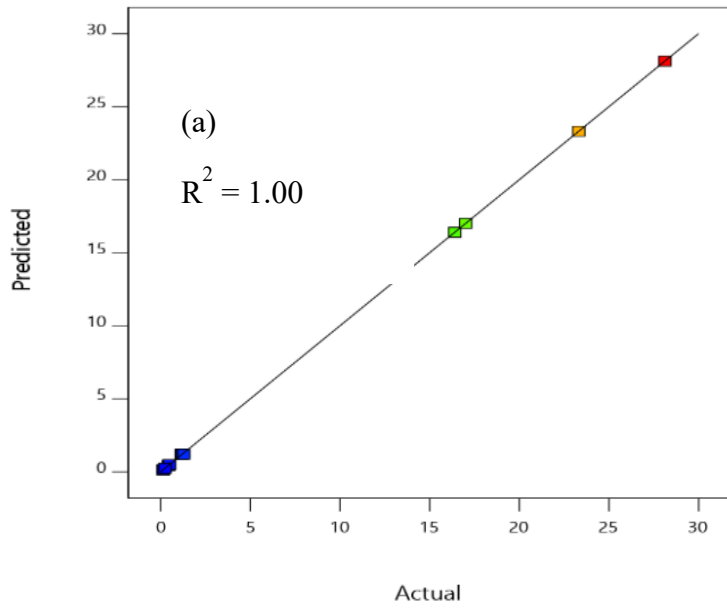
	Run	Sonication/ stirring time (h)	NaOH/HCl Concentration (M)	Cycle	Amplitude (%)	Volume of acid (mL)	% Yield	Amount of silica extracted (%)
Alkali UAE	1	2.5	2.5	0.6	60	-	1.15	76.1
	2	1.0	4.0	0.1	100	-	0.15	53.7
	3	4.0	1.0	0.1	100	-	0.50	52.0
	4	2.5	2.5	0.6	60	-	1.20	76.1
	5	1.0	1.0	1.0	100	-	23.3	77.9
	6	2.5	2.5	0.6	60	-	1.17	76.0
	7	4.0	1.0	1.0	20	-	17.0	74.6
	8	4.0	4.0	1.0	100	-	0.45	73.7
	9	1.0	1.0	0.5	70	-	16.4	79.2
	10	2.5	2.5	0.6	60	-	1.30	76.5
	11	4.0	4.0	0.1	20	-	0.45	73.6
	12	4.0	2.5	0.5	70	-	28.1	77.8
	13	1.0	1.0	0.1	20	-	0.25	57.7
CSE	1	27	2.5	-	-	-	2.15	80.3
	2	48	1.0	-	-	-	13.1	87.1
	3	27	2.5	-	-	-	2.20	80.8
	4	27	4.6	-	-	-	4.61	77.2
	5	6.0	4.0	-	-	-	1.93	75.1
	6	27	2.5	-	-	-	2.20	80.0
	7	48	4.0	-	-	-	1.37	78.4
	8	6.0	1.0	-	-	-	2.37	66.3
	9	57	2.5	-	-	-	15.4	77.3
	10	27	0.4	-	-	-	1.62	81.8
	11	27	2.5	-	-	-	2.19	80.3
	12	27	2.5	-	-	-	2.09	80.2
	13	48	2.5	-	-	-	3.95	80.5
Acid UAE	1	2.5	3.0	0.55	60	200	60.7	90.5
	2	2.0	2.5	0.60	70	200	77.0	88.2
	3	1.5	3.0	0.55	80	200	76.7	93.1
	4	2.5	3.0	0.55	70	250	70.3	85.3

5	2.0	3.0	0.55	60	150	80.3	89.1
6	2.5	2.5	0.55	70	200	74.6	86.7
7	2.0	3.0	0.50	80	200	73.0	94.3
8	2.0	2.5	0.55	70	150	72.6	86.1
9	2.0	2.5	0.55	80	200	75.2	89.7
10	2.0	3.0	0.50	70	190	74.3	92.3
11	2.0	3.5	0.55	80	200	81.4	88.5
12	2.5	3.0	0.60	70	200	73.5	93.6
13	1.5	3.5	0.55	70	200	81.6	88.1
14	2.0	3.0	0.55	70	200	84.4	87.2
15	2.0	3.0	0.55	80	250	82.4	88.6
16	2.0	3.0	0.60	70	250	84.3	92.1
17	1.5	3.0	0.50	70	200	86.2	87.9
18	2.0	3.0	0.55	80	150	84.4	85.8
19	2.0	3.0	0.60	60	200	74.7	93.2
20	2.5	3.0	0.50	70	200	84.7	90.4
21	2.0	2.5	0.50	70	200	83.3	94.0
22	2.0	3.5	0.55	60	200	83.5	95.1
23	2.0	3.5	0.55	70	150	79.2	87.8
24	1.5	3.0	0.55	60	200	82.5	87.2
25	2.5	3.0	0.55	80	200	82.3	95.1
26	2.5	3.5	0.55	70	250	81.1	87.1
27	2.0	3.5	0.55	70	200	77.9	89.5
28	2.0	3.0	0.55	70	200	84.8	88.7
29	1.5	3.0	0.55	70	150	80.2	88.1
30	2.0	3.0	0.50	70	150	82.9	94.0
31	2.0	3.0	0.55	70	200	81.8	87.2
32	2.0	3.5	0.50	70	200	70.5	94.9
33	2.0	3.0	0.50	60	200	86.1	90.6
34	2.0	3.0	0.55	60	250	81.1	83.0
35	2.5	2.5	0.55	70	200	74.6	85.8
36	2.0	3.00	0.50	70	250	84.0	86.6
37	2.0	2.5	0.55	70	250	77.9	89.8

38	1.5	2.5	0.55	70	200	84.1	87.9
39	2.0	3.0	0.60	80	200	84.8	89.4
40	1.5	3.0	0.60	70	200	82.2	91.5
41	2.0	3.0	0.55	70	200	82.8	87.0
42	1.5	3.0	0.55	70	250	83.9	88.1
43	2.0	3.0	0.55	70	200	85.6	90.3
44	2.0	2.5	0.55	60	200	83.6	86.3
45	2.5	3.0	0.55	70	150	70.7	88.2
46	2.0	3.0	0.55	70	200	81.2	91.9
47	2.0	3.0	0.60	70	150	77.9	93.6

3.7. Response surface model

The model chosen for the experimental design of the CSE, acid UAE and alkali UAE methods was a quadratic model of the CCD based on the number of factors to be optimized. The model predictions for amount of silica and percentage yield of extracted silica were compared with the experimental data and were plotted in Figure 3.1 to provide the coefficient of determination for each of them. The coefficient of determination obtained indicated that the predicted and actual values for all the methods employed are in good agreement (Adebisi et al., 2017; Olawale et al., 2012) especially for alkali UAE method where the R^2 is 1 for percentage yield and 0.99 for amount of silica extracted.



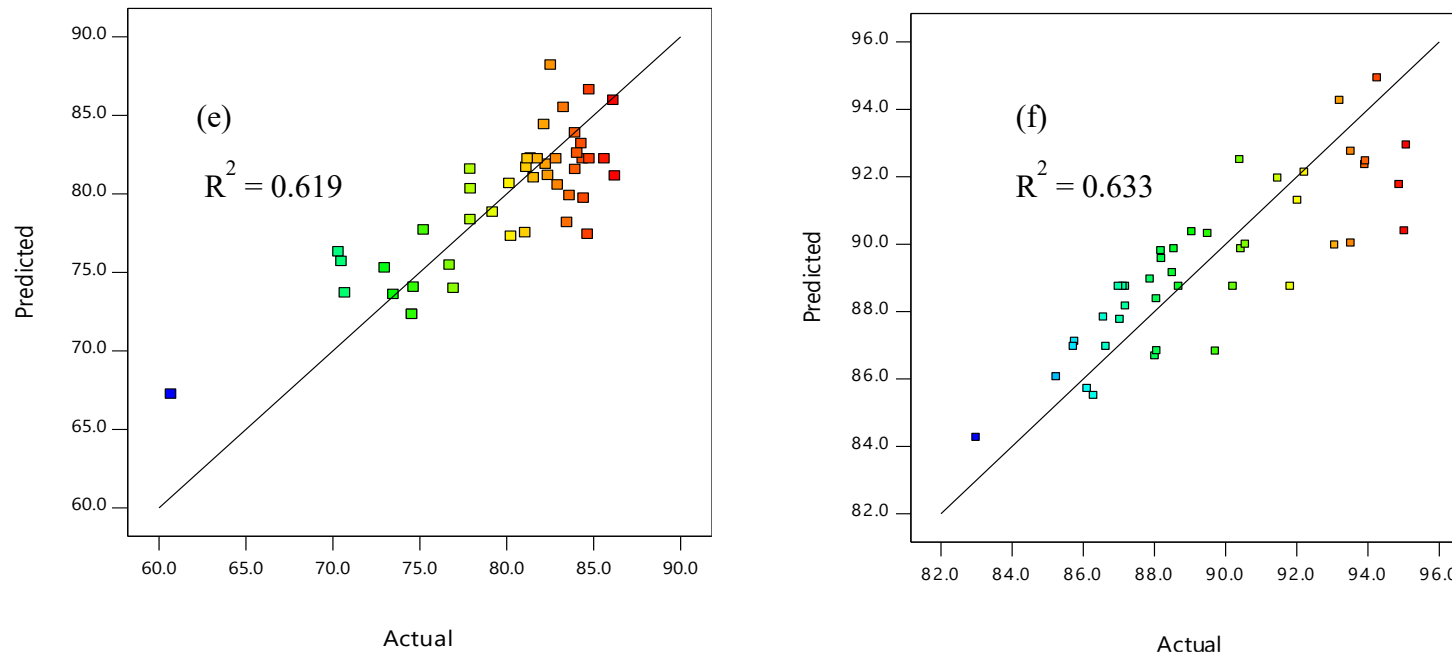


Figure 3. 1. Comparison between values predicted by response surface methodology (RSM) model and experimentally determined.

Analysis of variance (ANOVA) was used to indicate which terms were statistically significant in each of the quadratic models, and the values are presented in Table 3.3. In this Table, the p – values for all the models were less than 0.05 which usually indicates that the model terms are significant (Box et al., 2005) meaning that the quadratic model of the CCD chosen, was sufficient to represent the extraction of silica. This is in agreement with what was found by Adebisi et al. (2017); Matlob et al. (2011); Olawale et al. (2012); Qisti et al. (2017). However, p -values for many of the terms in the CSE and acid UAE methods were found to be greater than 0.05 which means that those terms are not significant model terms implying that they do not have a direct impact on the percentage yield or the amount of silica extracted. For example, all model terms have a direct impact on the percentage yield and amount of silica extracted in the alkali UAE method since change Na^+ ions, time and transient temperature will have an effect on the amount of sodium silicates produced. This is in line with the findings from the study by Matlob et al. (2011) who found that a change in NaOH concentration, exposure time and microwave power level had a significant effect on the concentration of Si in coal fly ash extracts. On the other hand, neither concentration of alkali nor stirring time nor the interaction of both nor their quadratic functions had any effect on percentage yield in the CSE method. The assumption here is that the yield depends on the skill of the operator in recovering all the silica formed but this could not be verified as most authors considered only the purity of silica (amount of silica extracted). The amount of silica extracted is however influenced by stirring time, the interaction between stirring time and concentration of alkali and the quadratic function of stirring time because there is more time for the silica in DE to interact with NaOH to form silicates. This is in agreement with findings in literature (Matlob et al., 2011). In the acid UAE method, sonication time and concentration of HCl as well as the interaction between sonication time and amplitude, concentration and cycle, concentration and amplitude as well as cycle and amplitude are factors that affect percentage yield while only changes in concentration of HCl affects the amount of silica extracted as a change in the amount of Cl^- and time of contact between the ion and DE means a change in the number of ions and the time available to chloridize elements that form impurities and hence a change in purity and yield of silica formed (Kuwahara et al., 2010).

Generally, the higher the Fischer's (F-test) value and the lower the probability (p – value) for a particular model term, the more significant, statistically, the model term is and the greater role these factors play in achieving a higher percentage yield and a larger amount of extracted silica. The CSE method has significant lack of fit as a result of the low p – values which means

that the model doesn't fit and is not adequate to represent the relationship between the responses and the independent variables (Pilkington et al., 2014).

Table 3. 3. Analysis of variance of all model terms.

Responses	Model terms	F-value	p-value
Percentage yield (Alkali UAE)	Model	43278.17	< 0.0001
	A-Sonication time	1.213E+05	< 0.0001
	B-Concentration	2.044E+05	< 0.0001
	C-Cycle	482.42	< 0.0001
	D-Amplitude	15339.39	< 0.0001
	AB	14461.52	< 0.0001
	AC	92595.77	< 0.0001
	AD	1.100E+05	< 0.0001
	BC	1.274E+05	< 0.0001
	BD	85655.43	< 0.0001
Amount of silica extracted (Alkali UAE)	Model	3889.16	< 0.0001
	A-Sonication time	4366.42	< 0.0001
	B-Concentration	2273.32	< 0.0001
	C-Cycle	15140.1	< 0.0001
	D-Amplitude	7411.63	< 0.0001
	AB	1459.62	< 0.0001
	AC	5769.73	< 0.0001
	AD	4961.79	< 0.0001
	BC	4697.07	< 0.0001
	BD	6318.06	< 0.0001
Percentage yield (CSE)	Model	4.19	0.0443
	A-Stirring time	4.25	0.0783
	B-Concentration	0.8900	0.3769
	AB	3.57	0.1007
	A ²	5.04	0.0597
	B ²	0.0710	0.7975
	Residual lack of fit	9756.64	< 0.0001
	Model	23.21	0.0003
Amount of silica extracted (CSE)	A-Stirring time	67.14	< 0.0001
	B-Concentration	2.35	0.1695
	AB	35.40	0.0006
	A ²	38.97	0.0004
	B ²	0.0508	0.8282
	Residual lack of fit	290.15	< 0.0001
	Model	2.11	0.0370
Percentage yield (Acid UAE)	A-Sonication time	10.9	0.00285
	B-Concentration	0.384	0.541
	C-Cycle	0.0152	0.903
	D-Amplitude	0.186	0.670
	E-Volume of acid	1.69	0.205
	AB	0.479	0.495
	AC	0.648	0.428
	AD	9.63	0.00458
	AE	0.00513	0.943
	BC	4.33	0.0475
	BD	0.509	0.482
	BE	0.0248	0.876

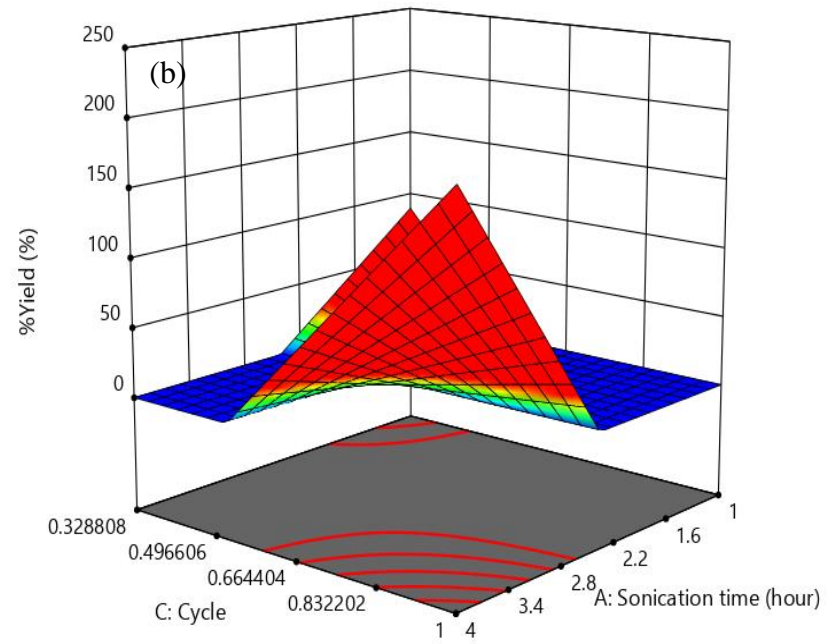
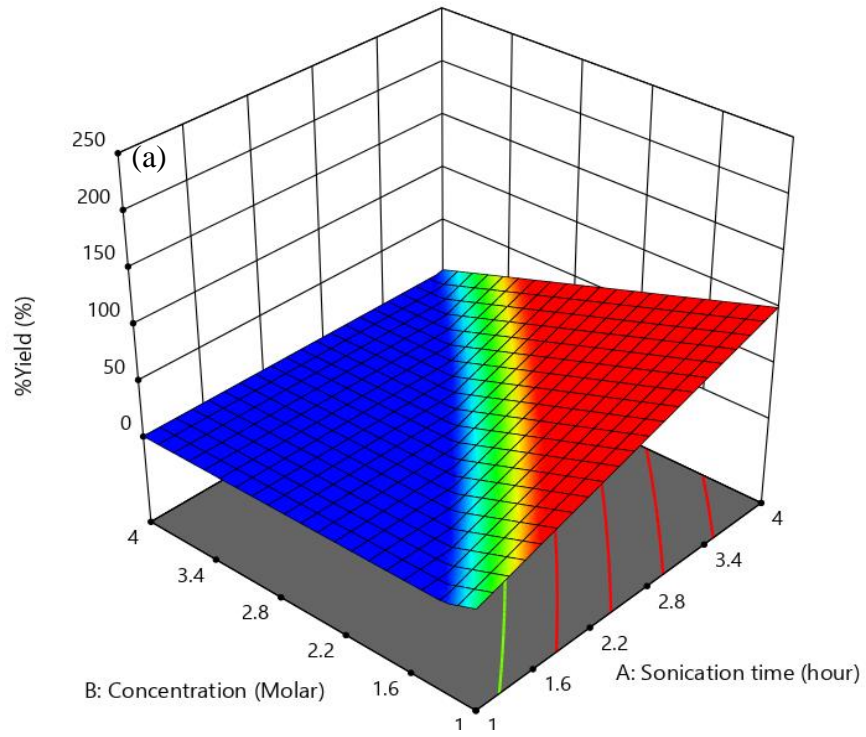
	CD	6.95	0.0140
	CE	0.193	0.664
	DE	0.111	0.742
Amount of silica extracted (Acid UAE)	Model	2.24	0.0273
	A-Sonication time	0.767	0.389
	B-Concentration	3.81	0.0619
	C-Cycle	0.167	0.686
	D-Amplitude	0.941	0.341
	E-Volume of acid	1.86	0.184
	AB	1.65	0.211
	AC	0.0119	0.914
	AD	0.0706	0.793
	AE	0.621	0.438
	BC	1.06	0.312
	BD	4.20	0.0506
	BE	1.16	0.292
	CD	2.42	0.132
	CE	1.50	0.232
DE	3.35	0.0788	

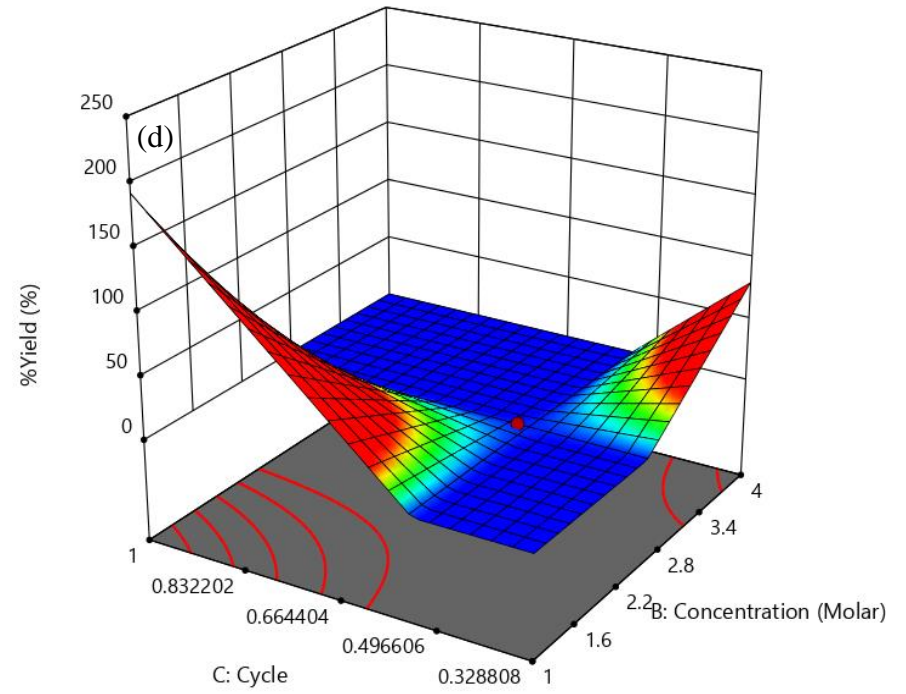
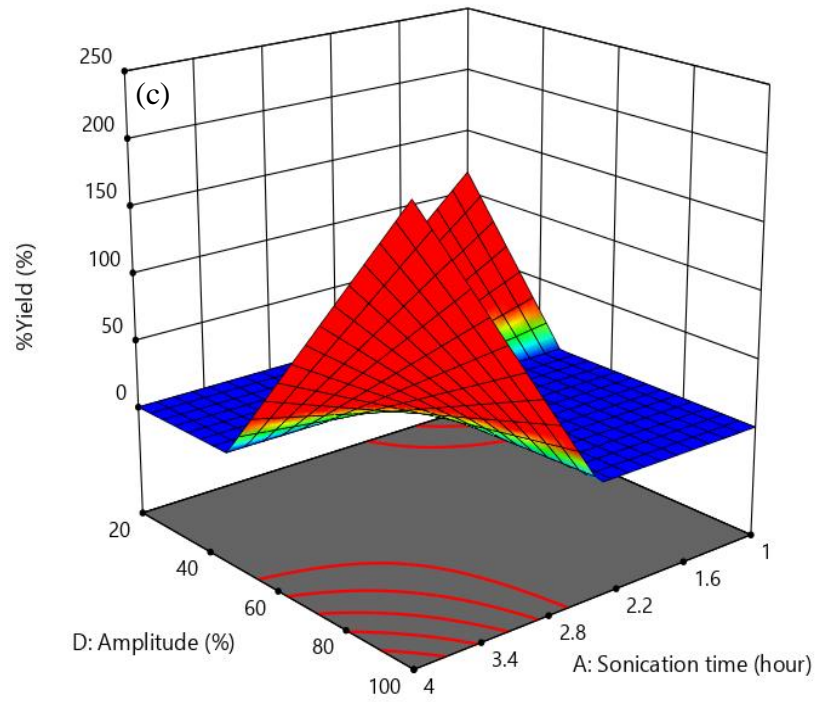
3.8. Response surface optimization

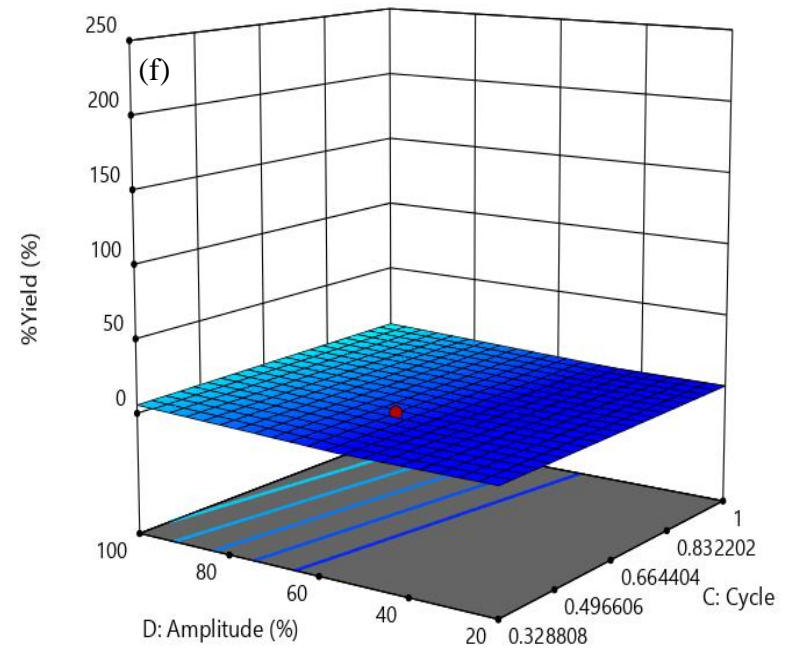
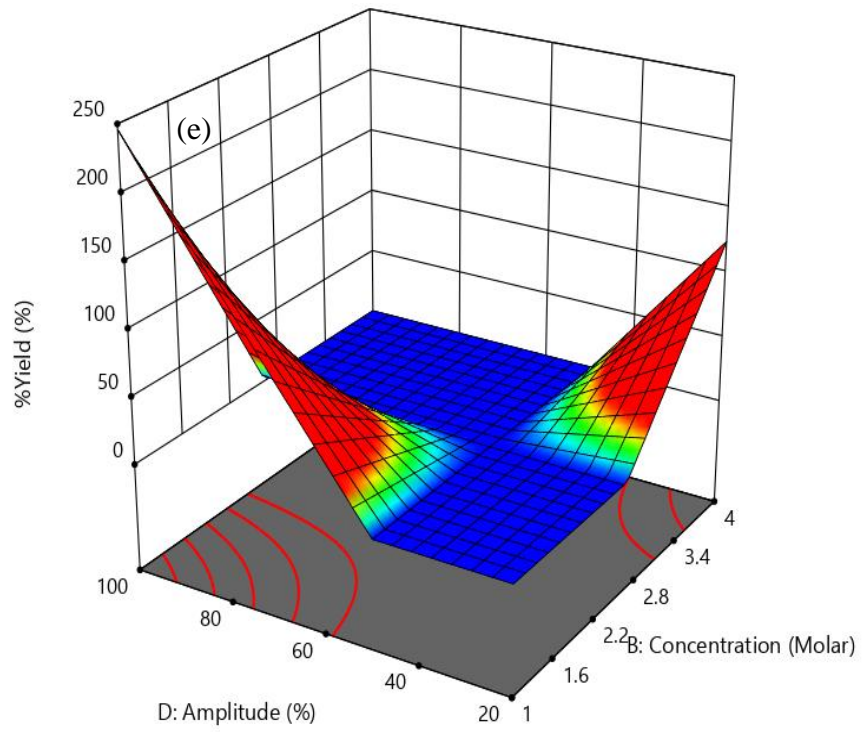
To determine optimal levels of the various factors for the extraction of silica, three – dimensional surface plots were constructed. The effect of the various factors and their mutual interaction on the percentage yield and percentage of extracted silica can be seen in the Figures 3.2, 3.3 and 3.4.

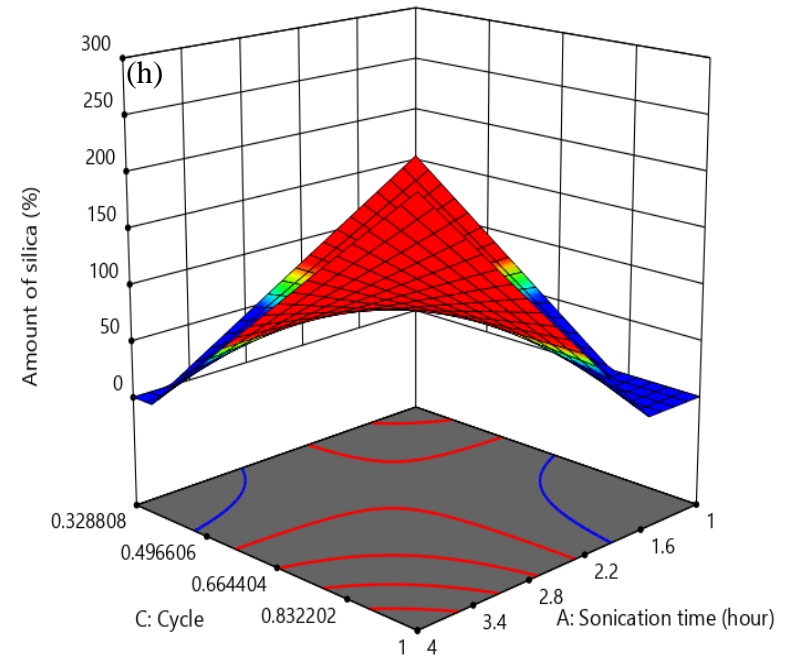
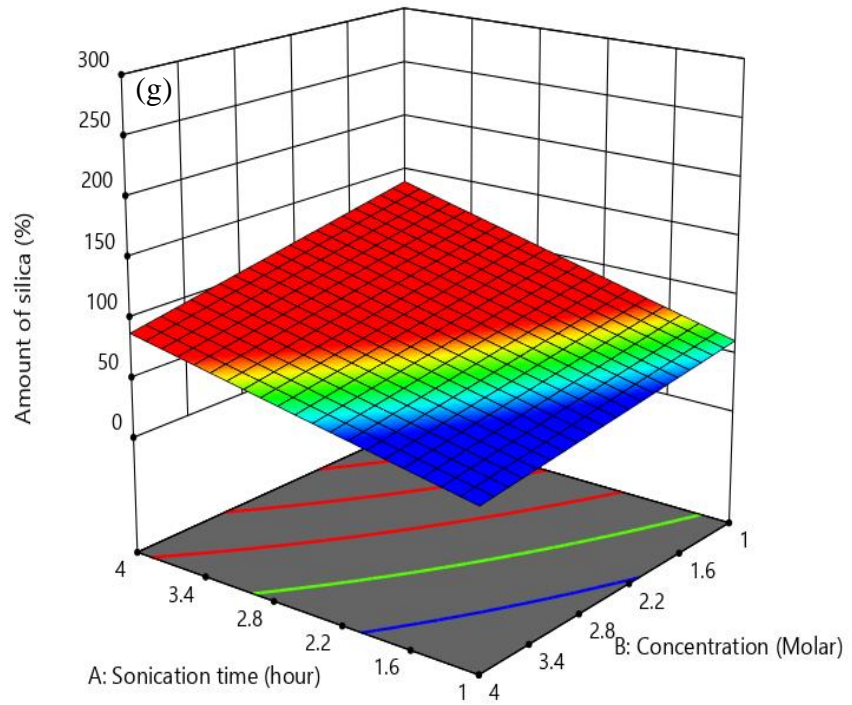
3.8.1. Alkali UAE

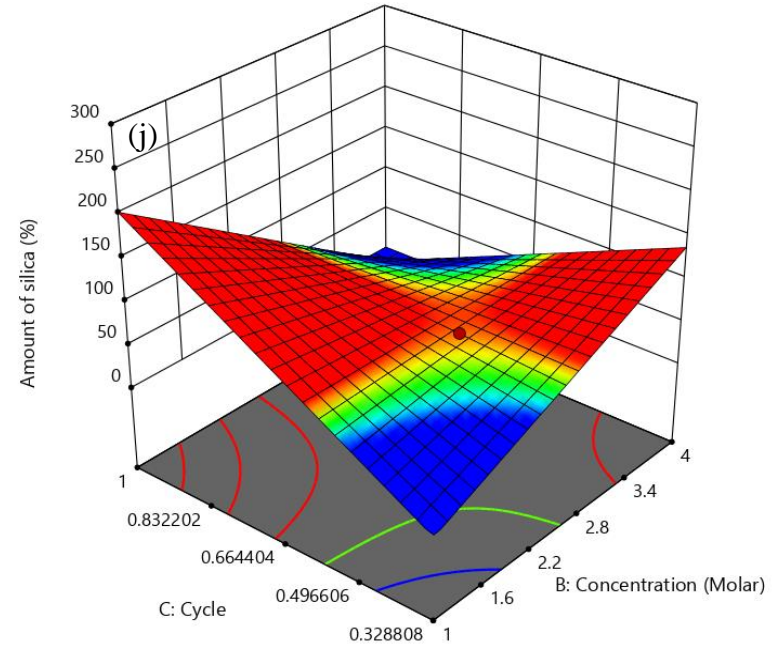
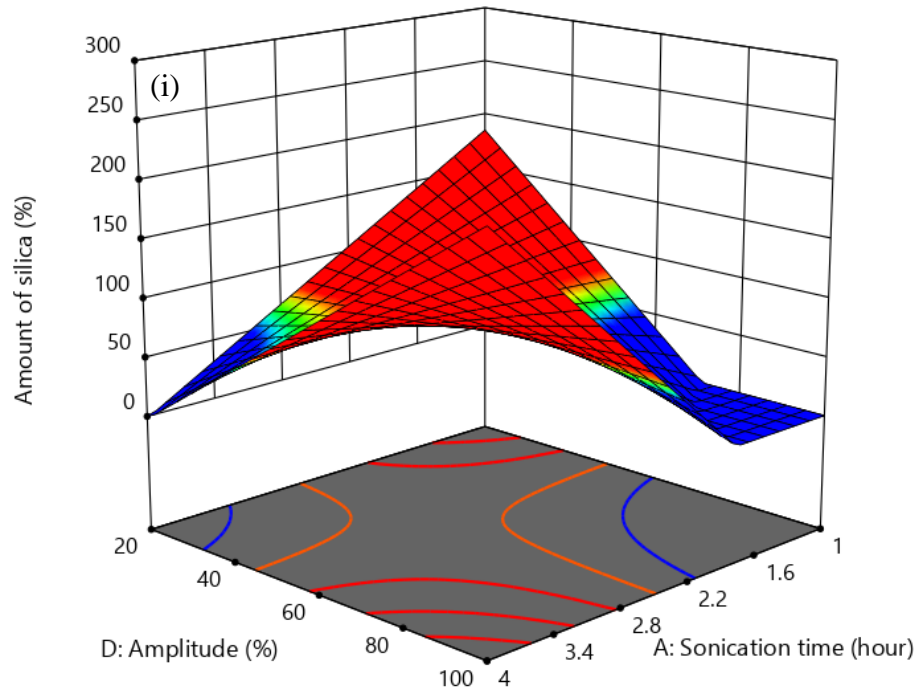
Generally during alkali extraction of silica, the alkali dissolves the silica forming soluble silicates and leaving behind impurities. Silica is then recovered from the solution by acidification. The higher the alkali concentration, and the longer the contact time or the higher the temperature, the more the silica dissolved and consequently the higher the yield of silica. From the plots of percentage yield in Figure 3.2 and amount of silica extracted increased with increase in sonication time, concentration, amplitude and cycle probably because there was a longer time for silica molecules to dissolve in NaOH to form silicates and probably because there were more NaOH molecules available to react with the silica molecules to form silicates. This is in line with previously observed trends (Jendoubi et al., 1997; Matlob et al., 2011; Qisti et al., 2017). The optimum parameters were chosen as 1.6 h for sonication time, 1 M for concentration, 0.66 for cycle and 60% amplitude.











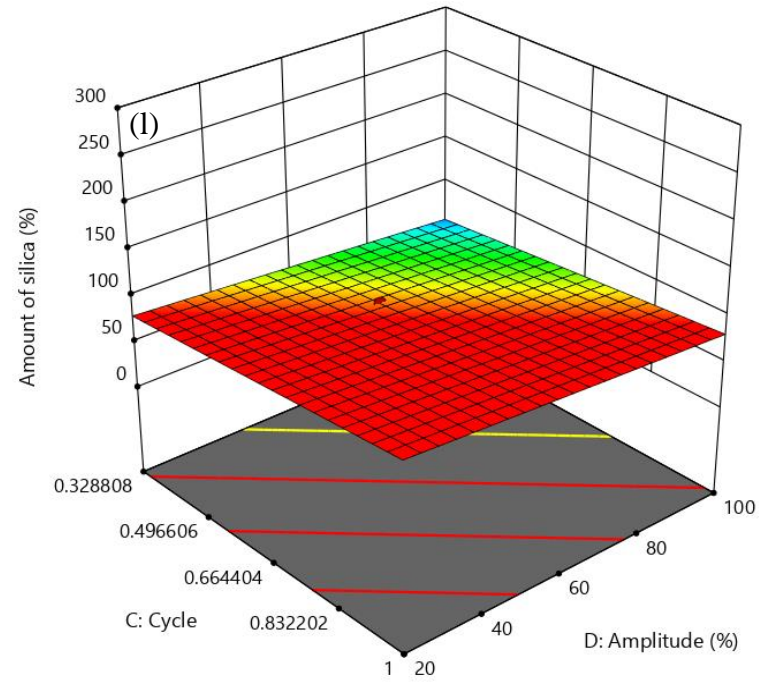
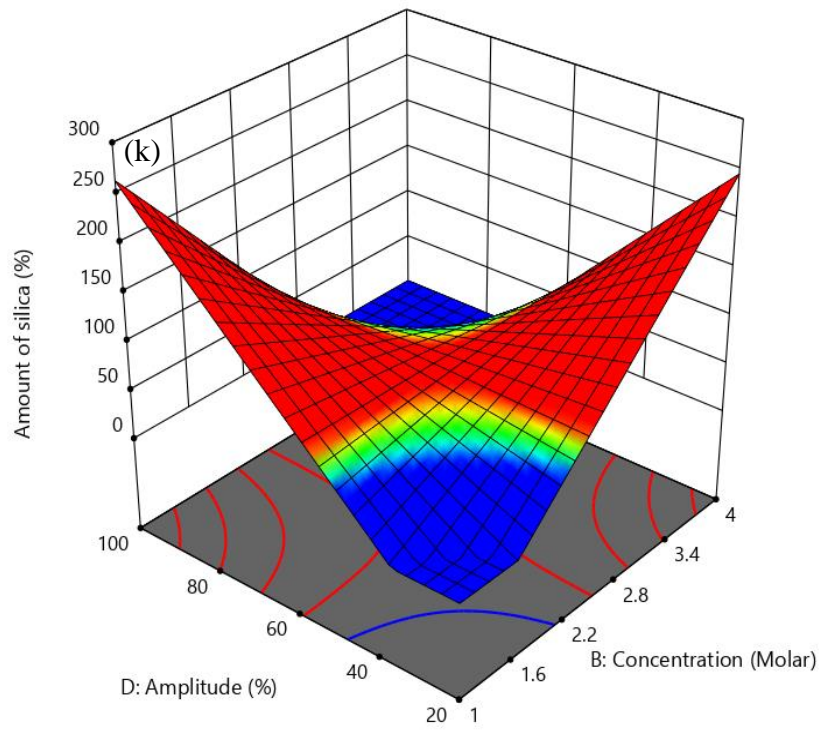
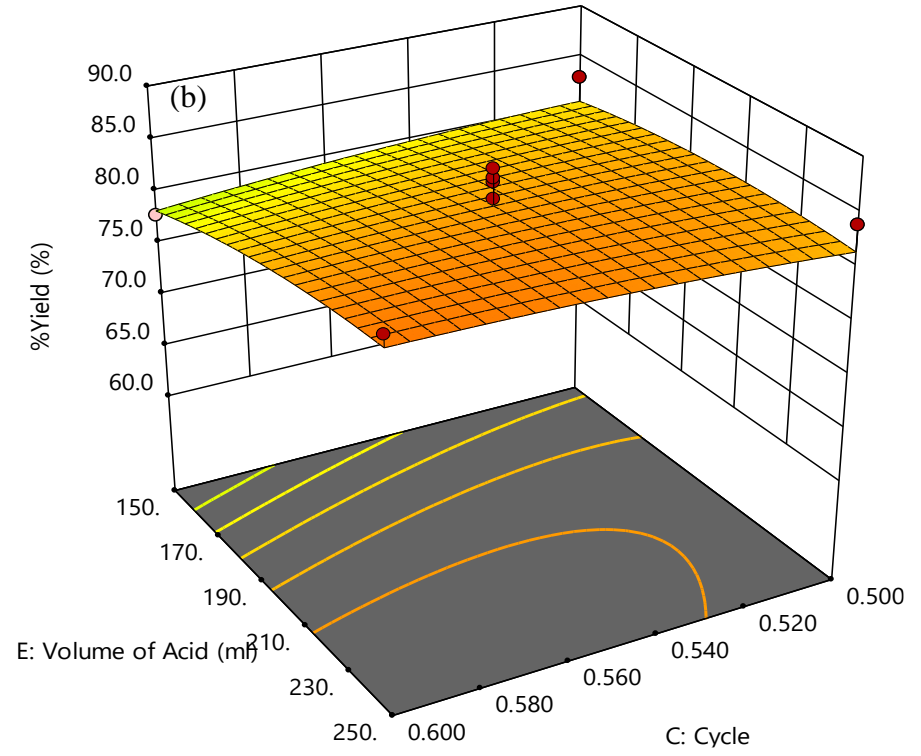
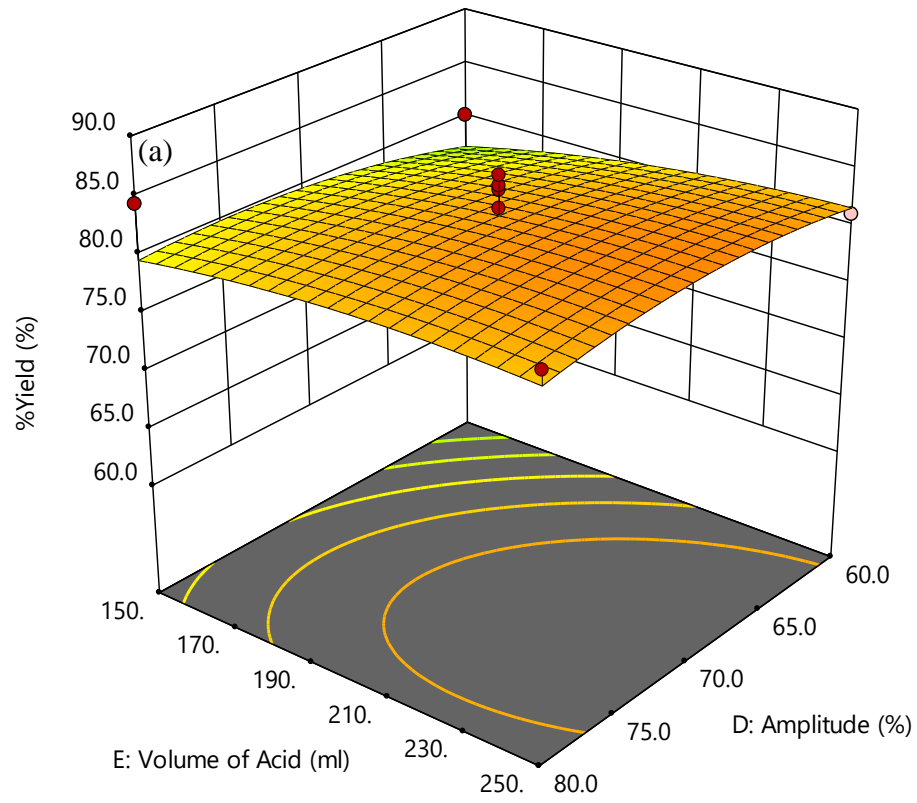
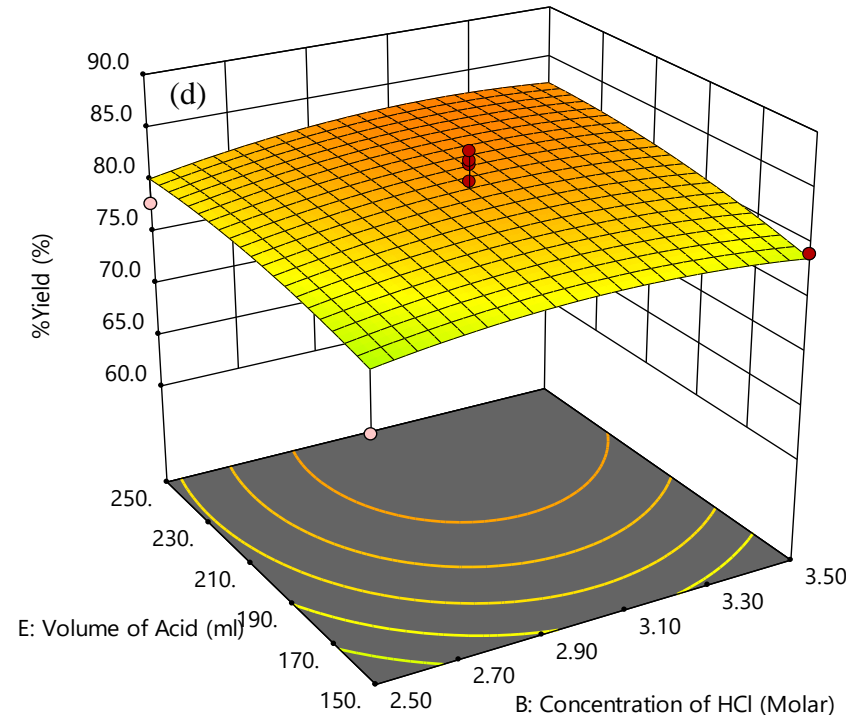
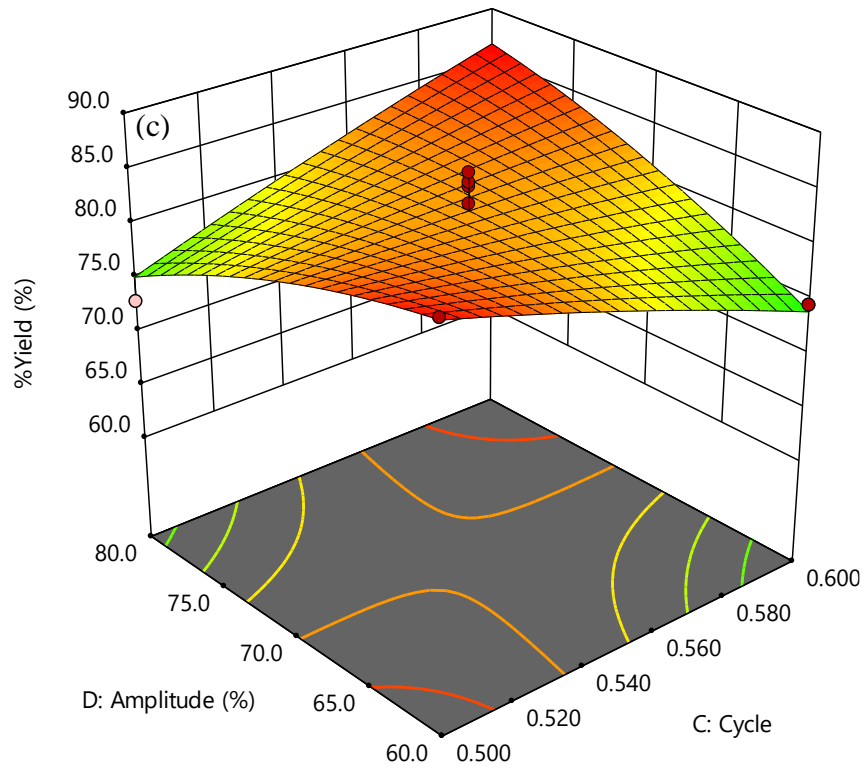


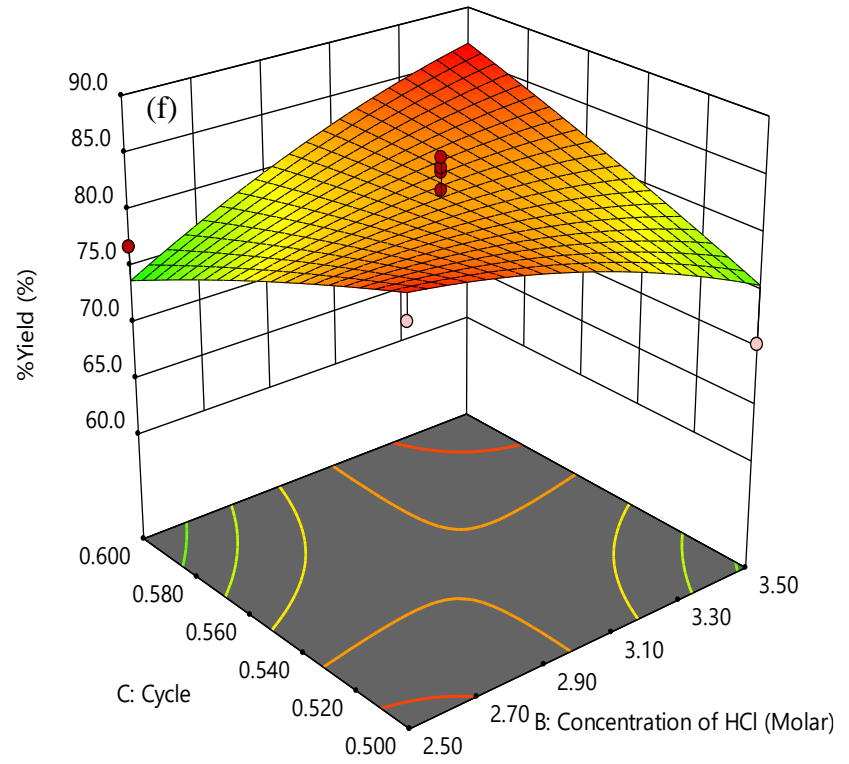
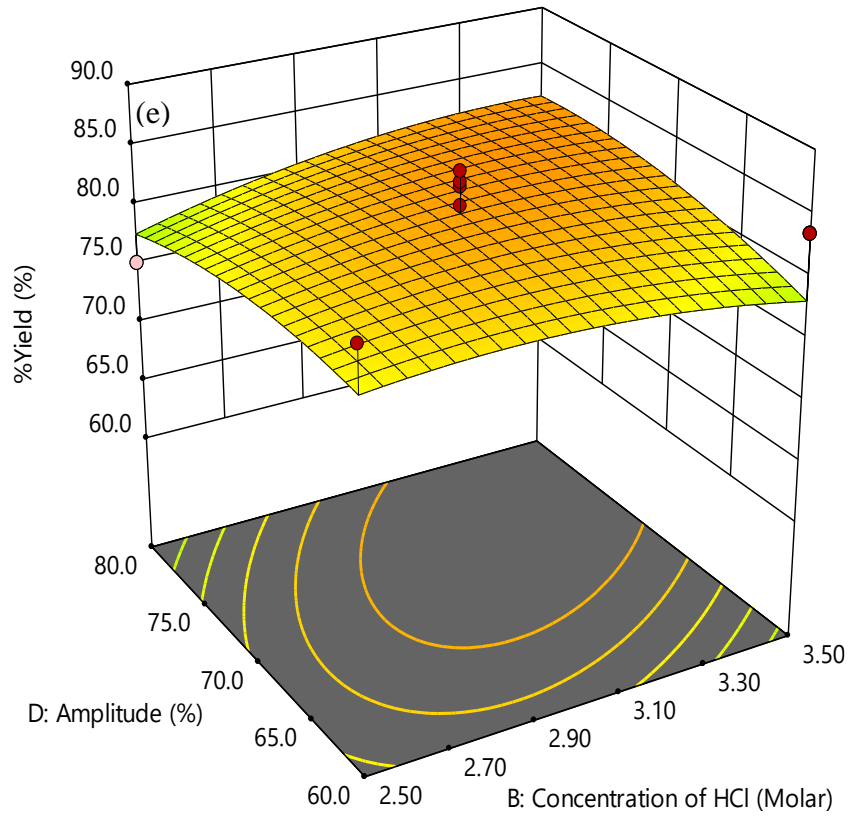
Figure 3. 2. Response surface plots for alkali UAE.

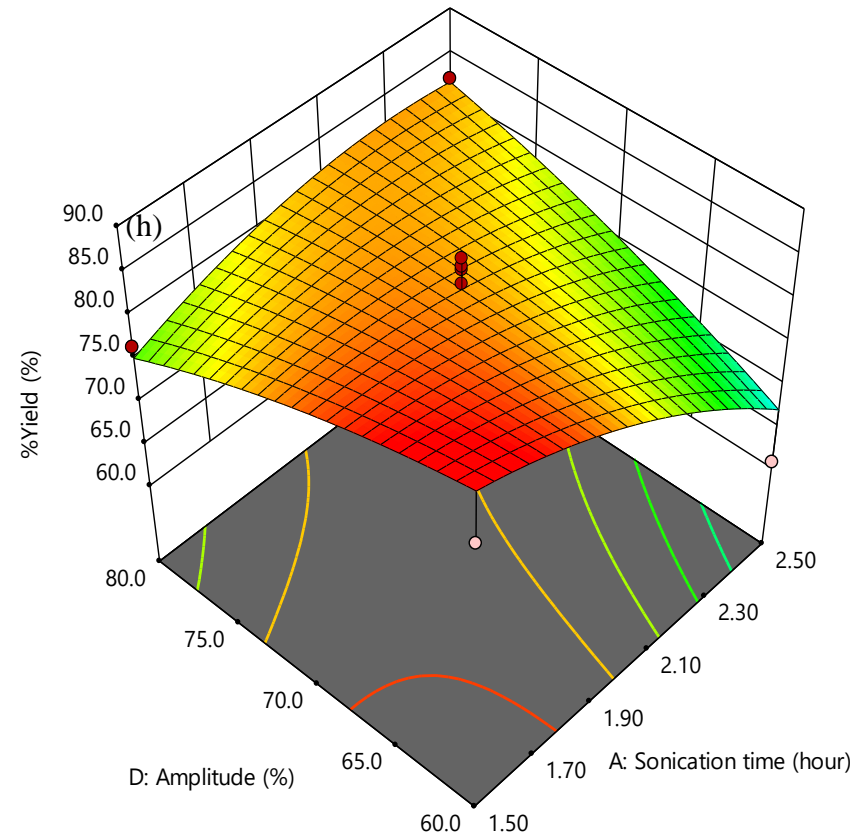
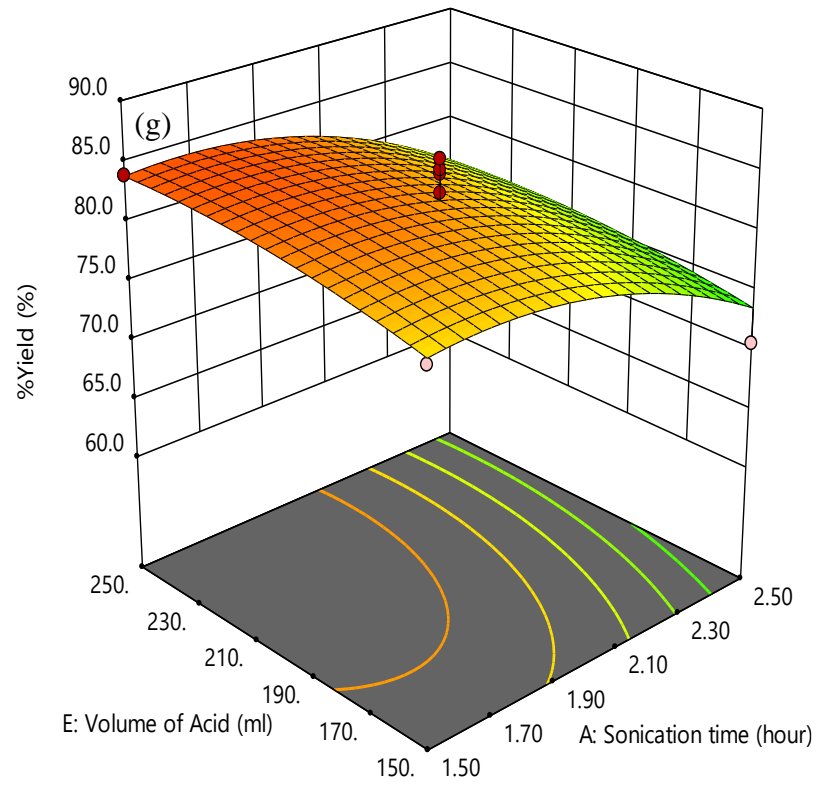
3.8.2. Acid UAE

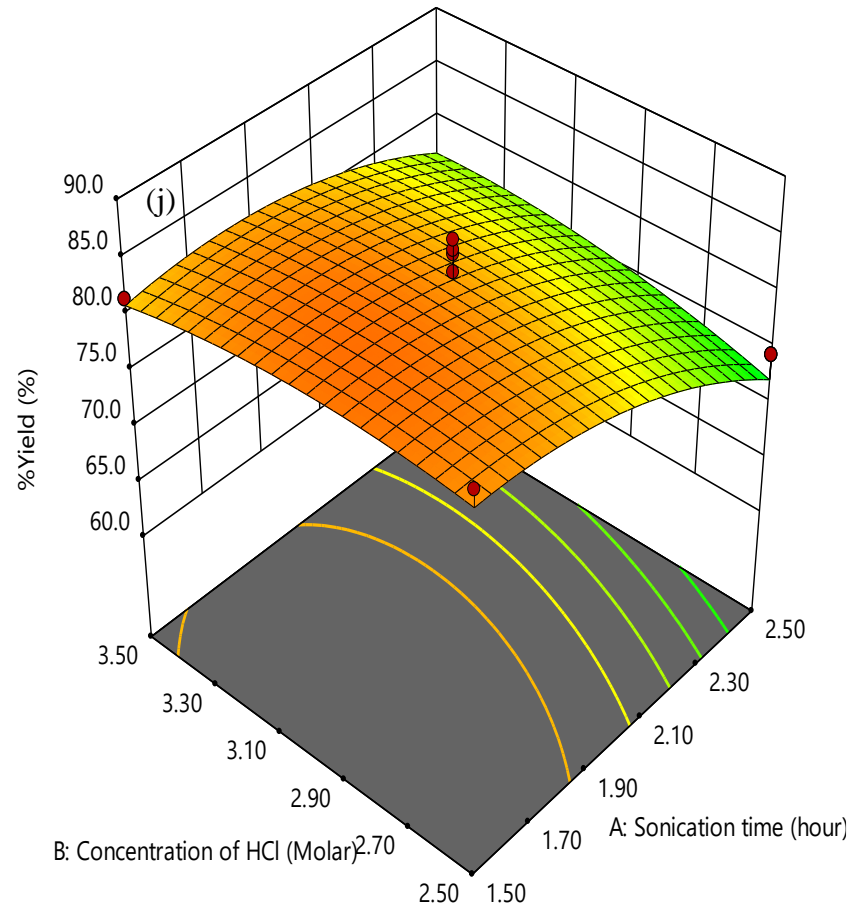
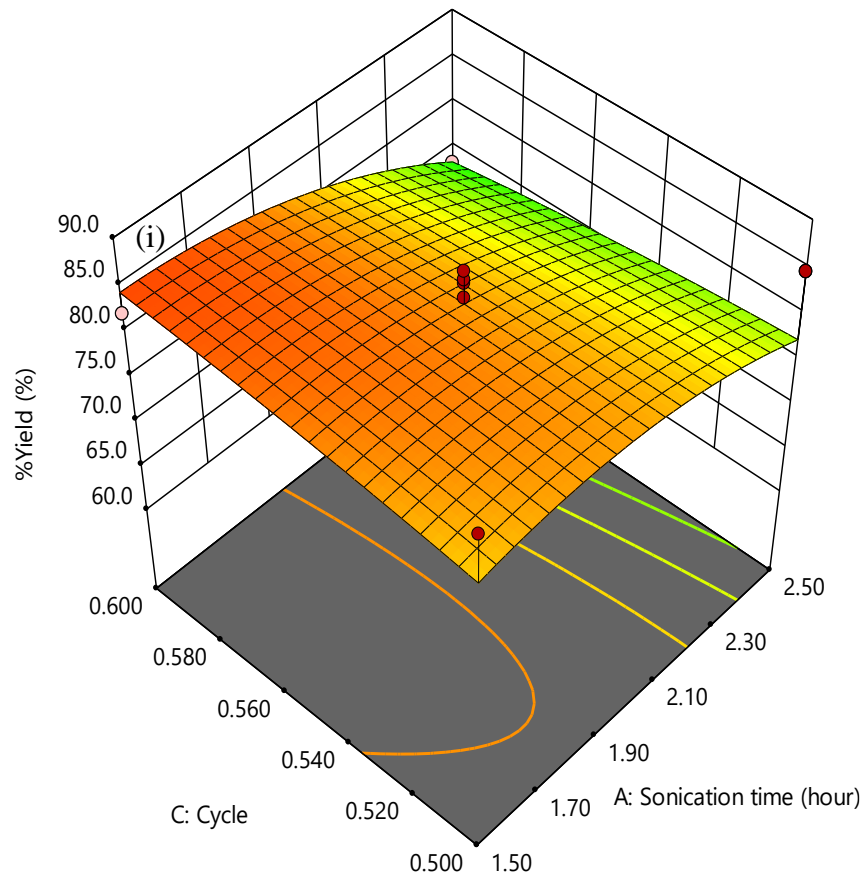
The response surface plots for the acid UAE method (Figure 3.3) showed that percentage yield increased, up to a maximum and then decreased as the volume of HCl, amplitude, concentration of HCl, sonication time increased (a, d, e, g, h and j) and it increased slightly as cycle increased (b, c, f and i), probably because HCl dissolves the impurities by chloridizing them (Kuwahara et al., 2010) thereby increasing the yield, but as more HCl is introduced or as concentration of HCl, sonication time and amplitude are increased it begins to polymerize the silica resulting in a lower yield (Gorrepati et al., 2010). This is consistent with findings by Gorrepati et al. (2010). Percentage extracted silica on the other hand, decreases up to a minimum and increases with amplitude and cycle (k, l, m, p, r and s), increases to a maximum and decreases with volume of HCl (k, l, n and q), increases with HCl concentration (n, o, p and t) and increases slightly with sonication time (q, r, s). With sonication time, volume and concentration of HCl the increase could be for same reason as the change in percentage yield while the change in percentage extracted silica as amplitude and cycle increase could be due to initial polymerization of silica due to the pockets of high temperature formed during sonication and the re-precipitation and aggregation of silica as a result of supersaturation of the solution.

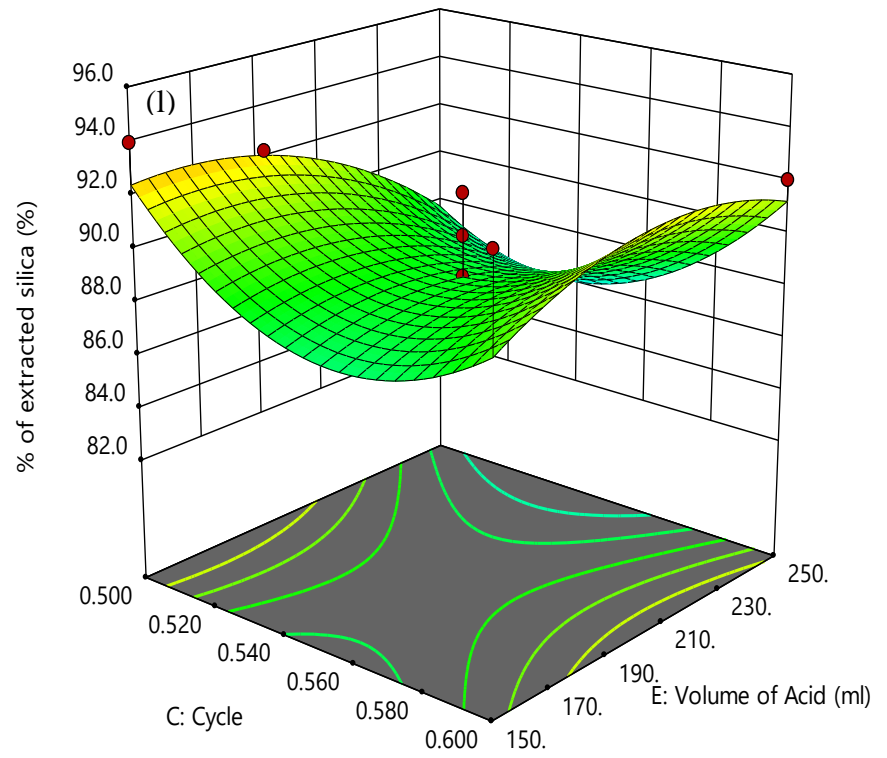
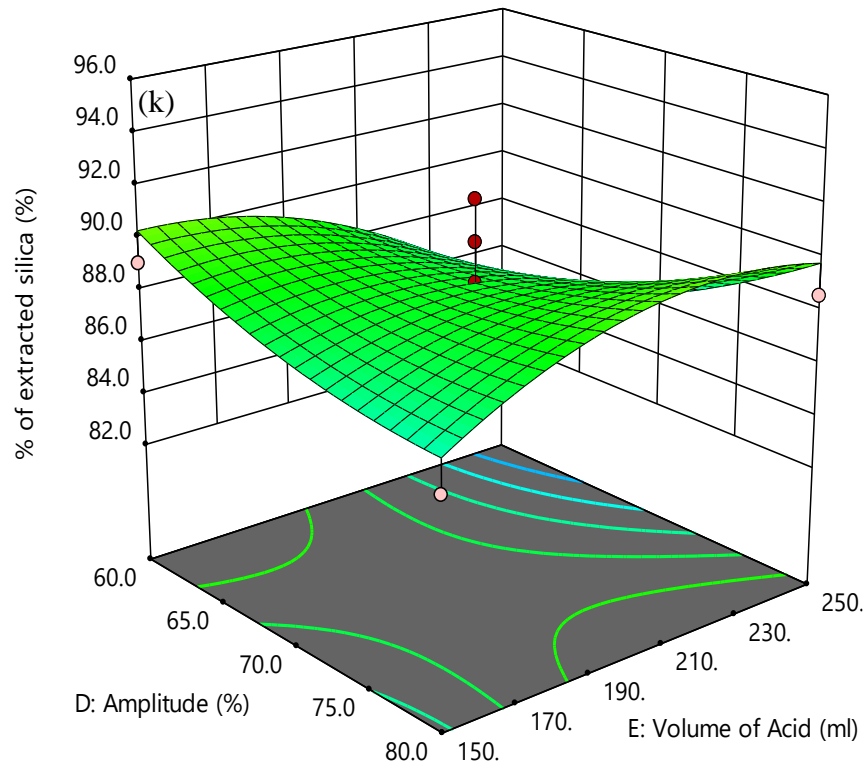


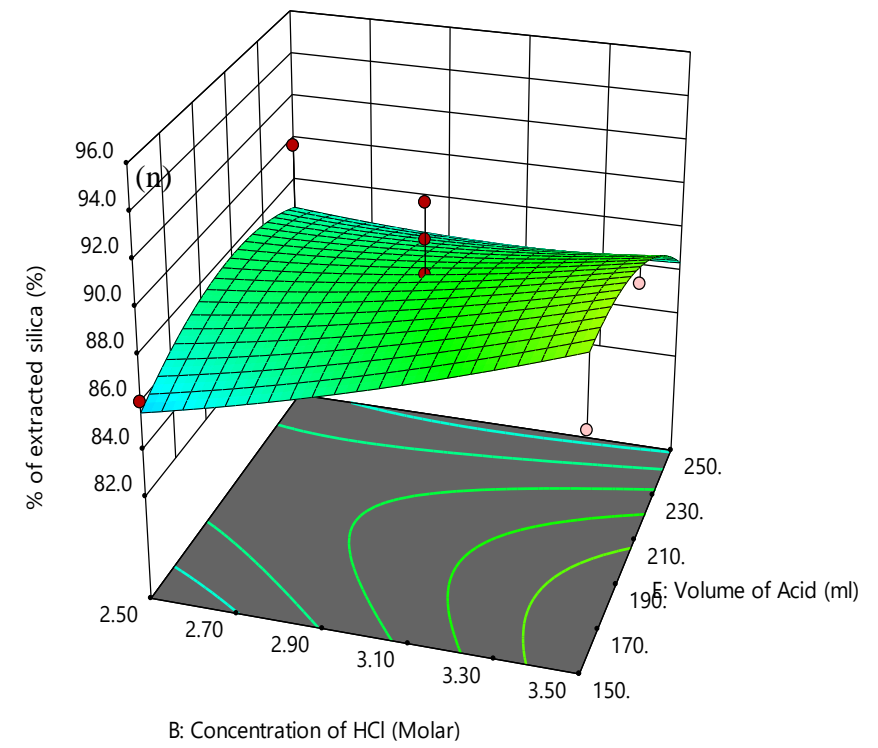
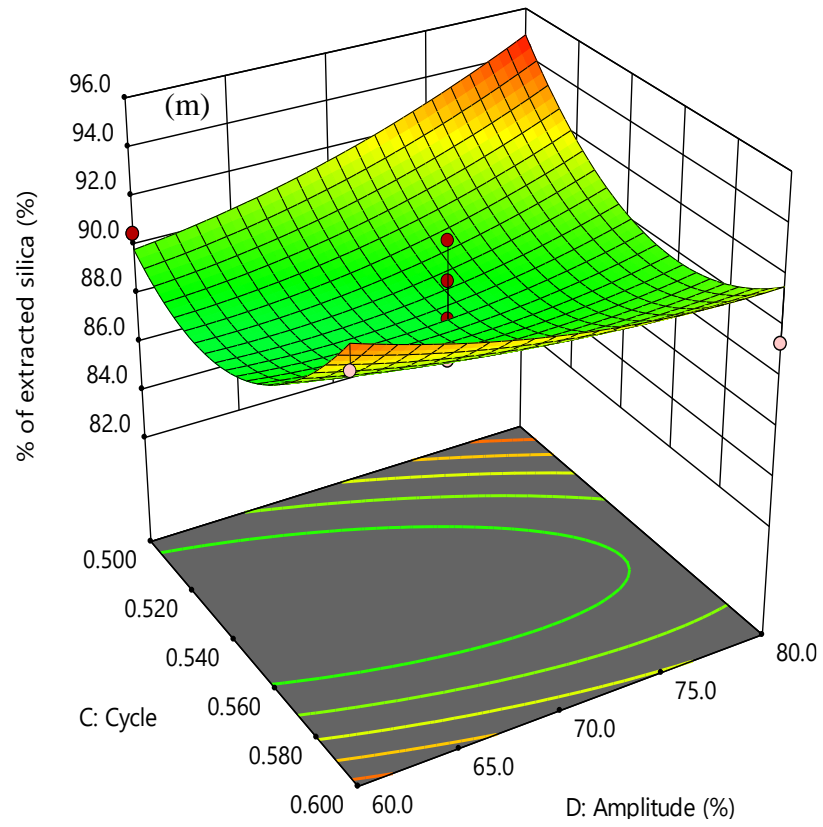


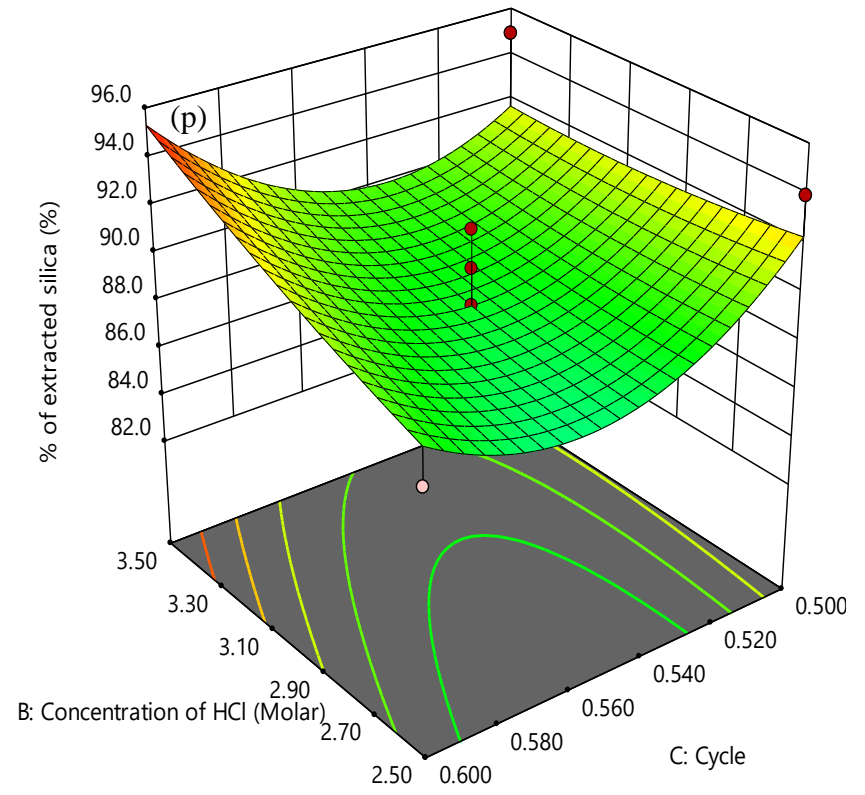
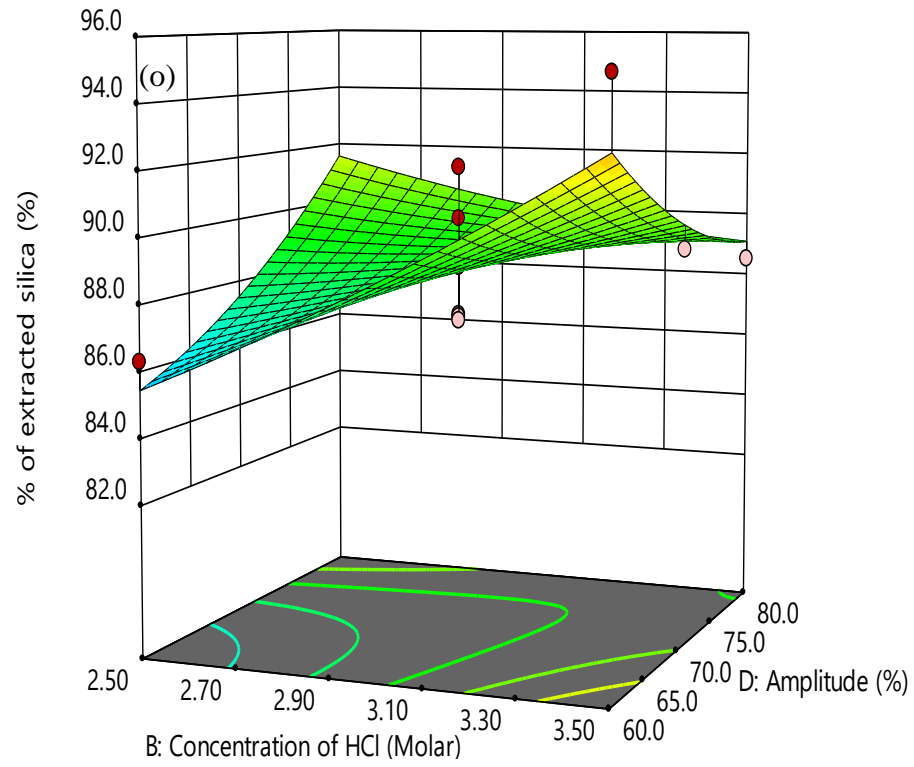


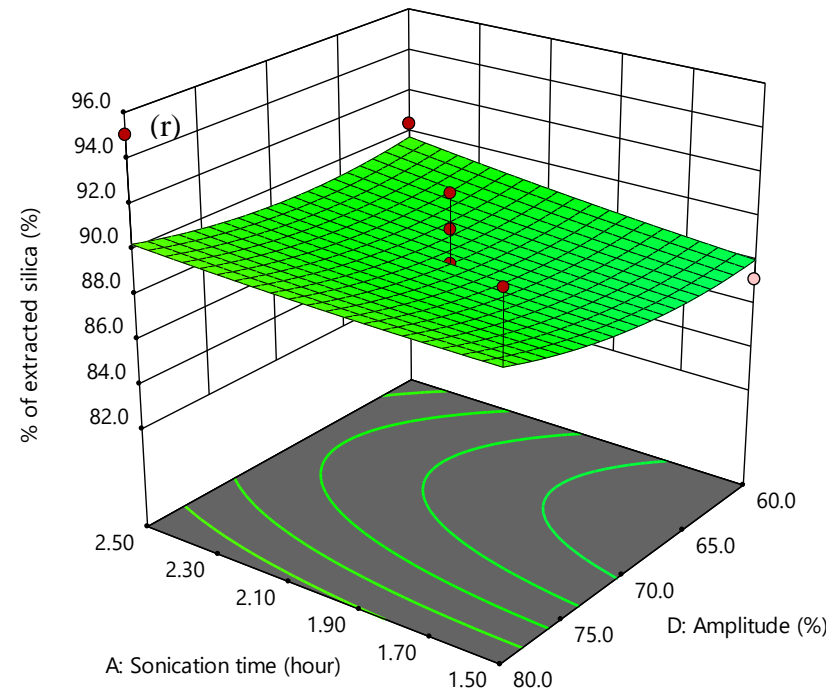
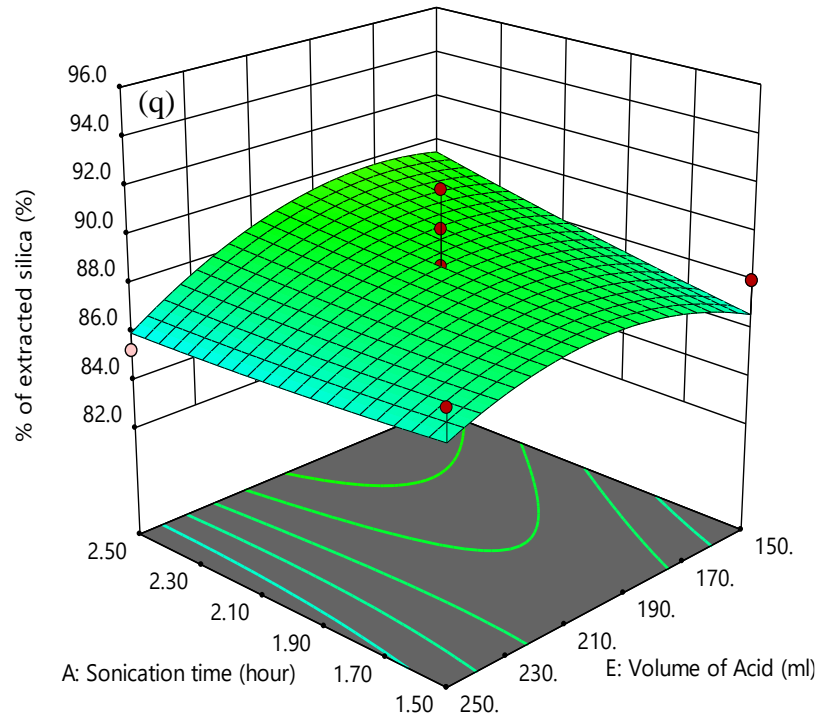












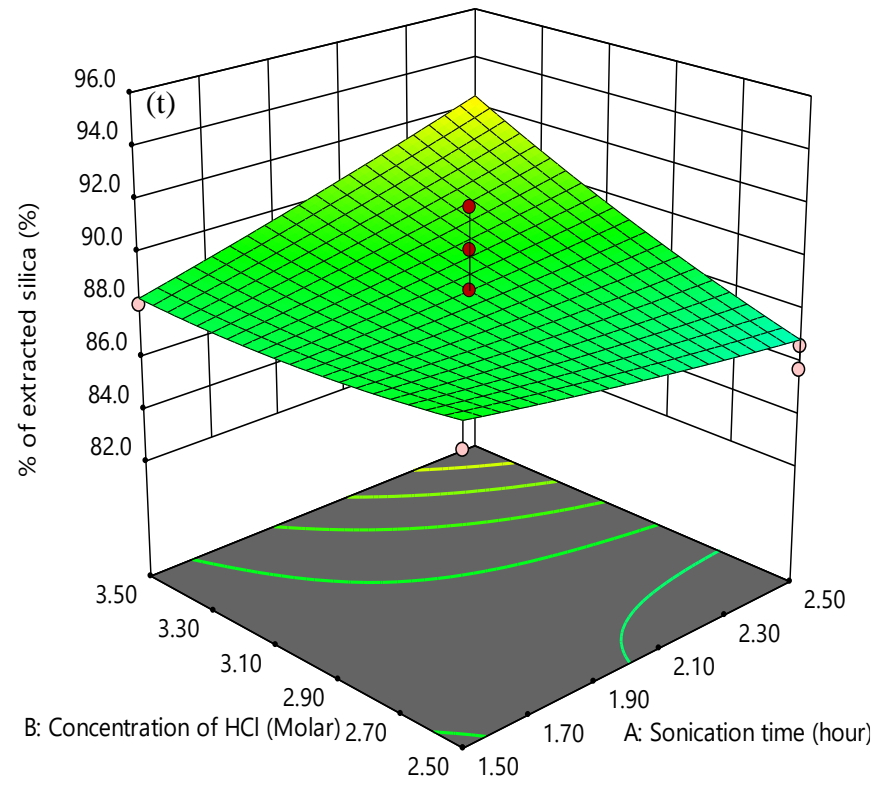
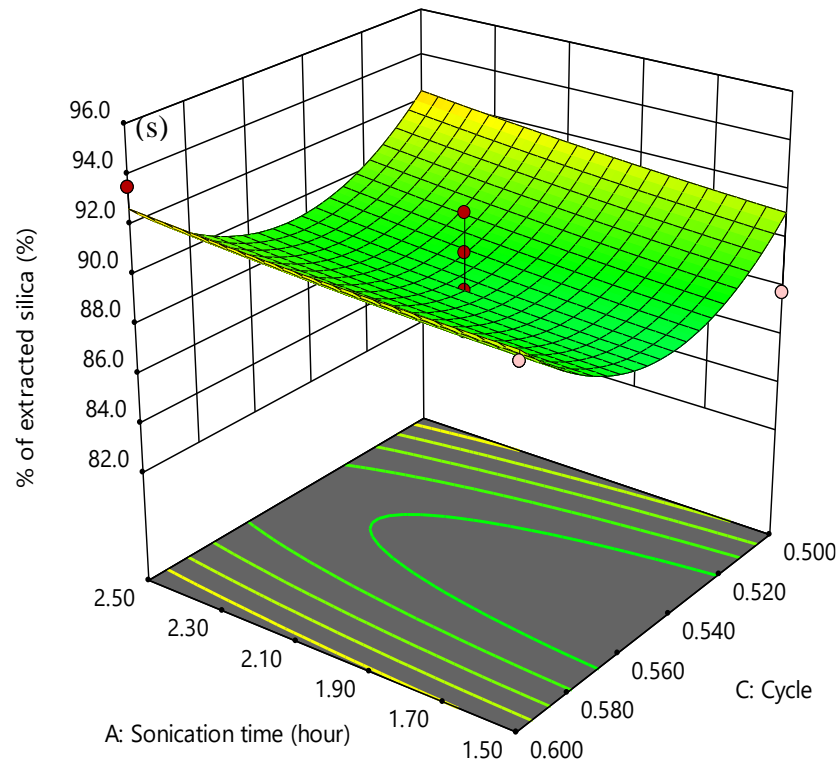


Figure 3. 3. Response Surface plots for acid UAE.

3.8.3. Conventional solvent extraction (CSE)

From the response surface plots for stirring (Figure 4), we see that percentage yield (a) and amount of silica extracted increases with NaOH concentration and stirring time as there are more NaOH molecules available and longer contact time between silica and NaOH to form silicates. In plot (b), amount of silica extracted increased, reached a maximum and began to decrease. This could be as a result of the re-precipitation of silica from the silicates making it unavailable for recovery from the filtrate. The optimum parameters were found to be 33.5 h for stirring time and 1 M NaOH concentration. These results are similar to those from previously published works (Jendoubi et al., 1997; Matlob et al., 2011; Qisti et al., 2017).

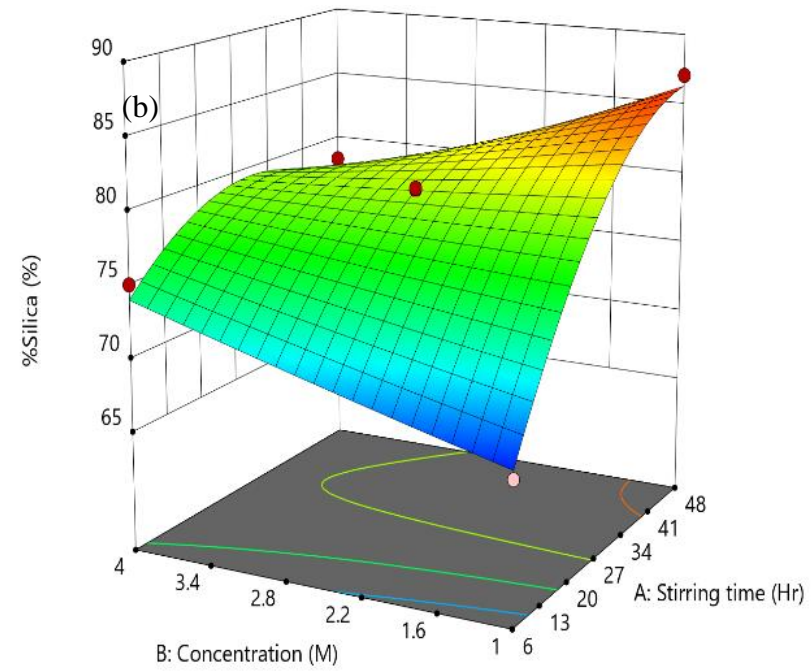
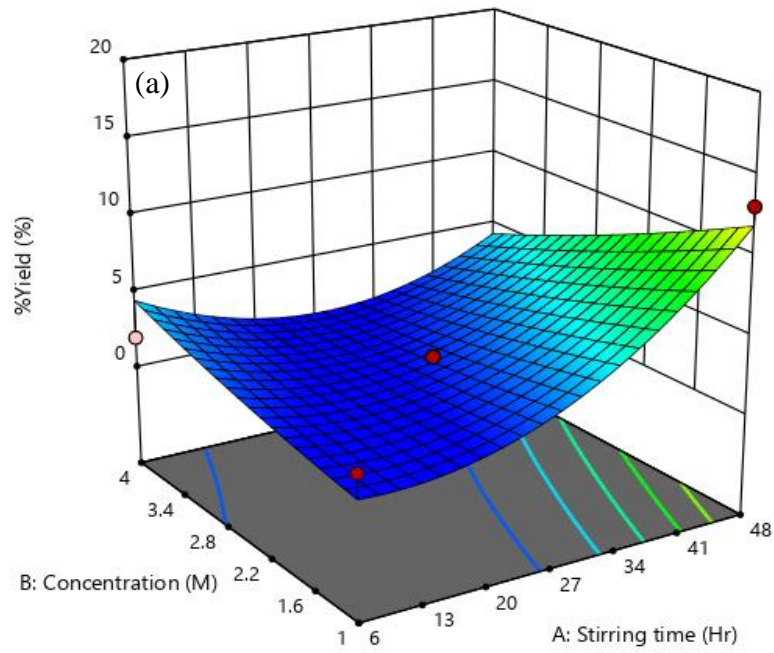


Figure 3. 4. Response surface plots for CSE.

3.9. Characterization of diatomaceous earth and extracted silica

3.9.1. Raw DE

Figure 5 (a), which shows the SEM image of raw DE (10 μm magnification), shows rectangular pores arranged in a regular pattern on each diatom and Figure 5 (b) shows the results of energy dispersion spectroscopy (EDS). The EDS results show that raw DE contains mainly Si, O and C confirming that DE is a silicate material. The C content may be due to the carbon coating during SEM analysis (Banerjee et al., 2017). This is consistent with findings by Izuagie et al. (2016b).

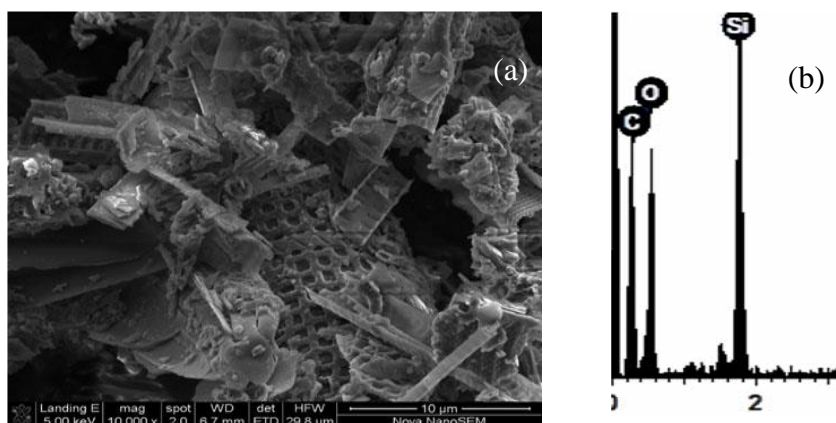


Figure 3. 5. (a) SEM and (b) EDS for raw DE.

3.9.2. Alkali UAE

The SEM image for silica sample with percentage silica (79.2%) obtained from the alkali UAE method (Sample 9, Table 3.2) is shown in Figure 3.6a. The Figure shows no visible external pores at 10 μm magnification. This may limit its application as adsorbents as opined by Tae et al. (2013). The TEM image (Figure 3.6b) shows that the silica particles exist in clusters suggesting that the silica particles are formed by aggregation brought about by attraction (possibly Van der Waals forces) (Naddaf et al., 2019) and sample size as obtained with the aid of Image-J software was 40.25 nm. The dark portions on the image may indicate the presence of pores (Ban et al., 2019). EDS results showed the sample contains O, Na and Si showing a higher Si percentage than in DE. The presence of C is as a result of the carbon tape holding the material during SEM analysis. The low Na content recorded is likely due to the use of NaOH in extraction.

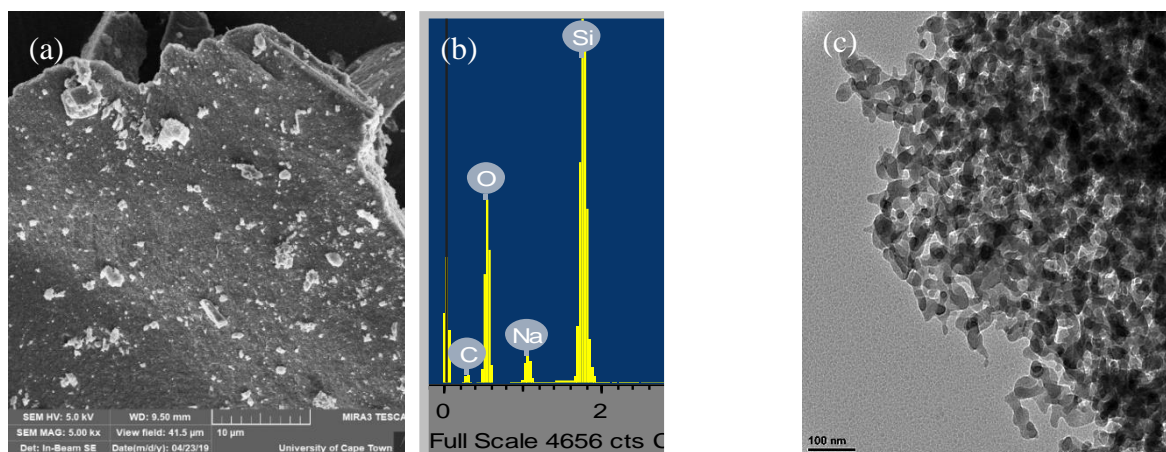


Figure 3. 6. (a) SEM (b) EDS and (c) TEM for alkali UAE.

3.9.3. Acid UAE

The morphology and chemical composition of three samples from the acid UAE method were studied. Sample 1 which corresponds to sample 25 in Table 2, had 95.1% silica (as obtained from an XRF), sample 2 had 94.3% (corresponding to sample 7 in Table 3.2). and sample 3 had 94.0% SiO_2 (sample 30 form Table 3.2). The SEM pictures of samples 1 and 3 (Figures 3.7 a1 and 3.7a3) show dot-like pores arranged in a regular pattern on rod-like particles while the picture of sample 2 (Figure 3.7a2) does not show external pores. All three SEM images show rod-like silica particles. The TEM images for samples 2 and 3 show oval shaped pores arranged in a regular pattern across razor-like surfaces with additional aggregated particles on sample 2. Sample 1 shows a dense mass of silica particles with clusters around irregular shaped pores. The EDS spectra shows that all the compounds contain mostly Si and O. Particle size as obtained from the TEM images using Image-J software were as follows: Sample 1 -35.269 nm; Sample 2- 31.512 nm and Sample 3- 38.756 nm.

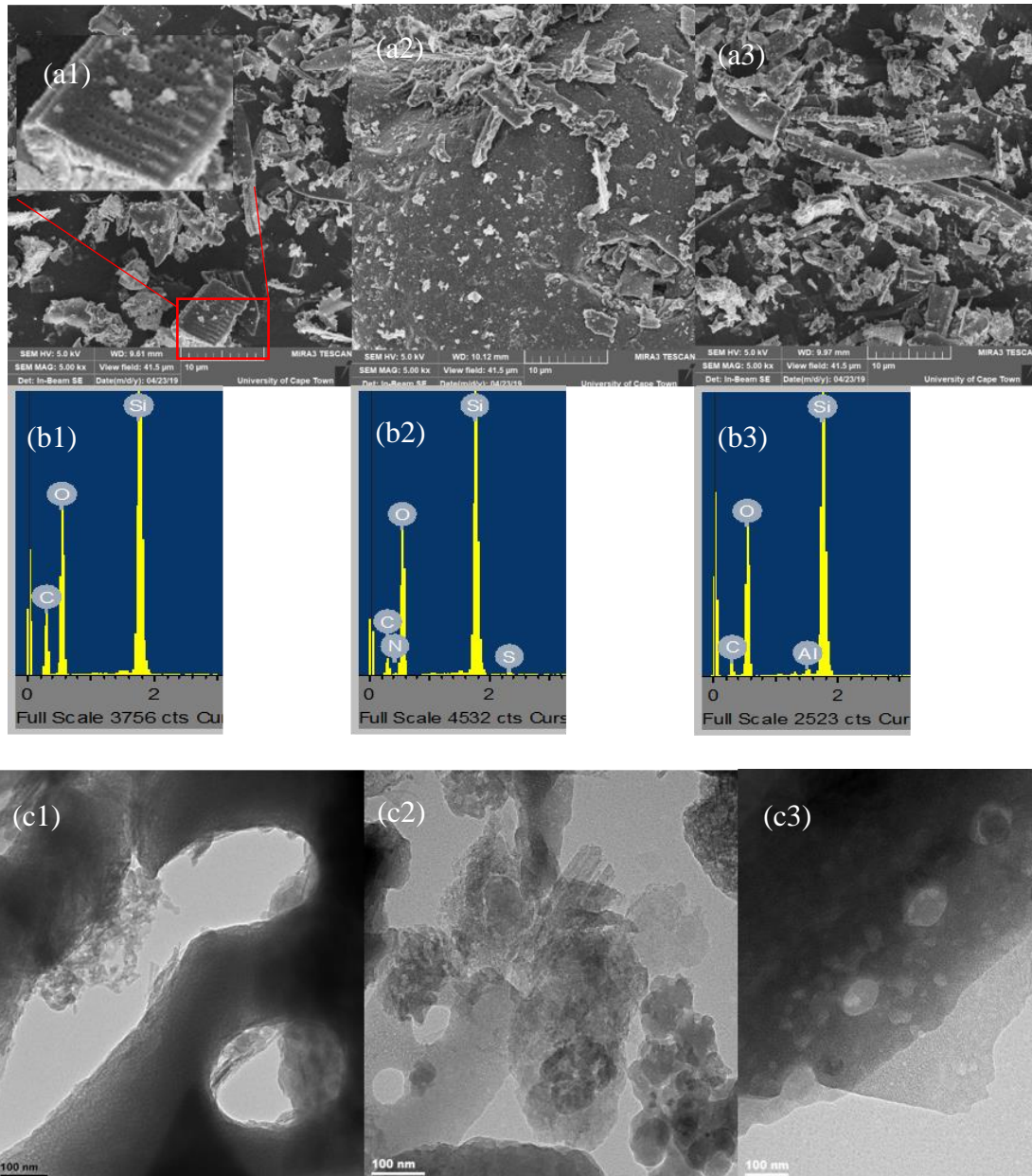


Figure 3. 7. (a) SEM (with higher magnification inset) (b) EDS (c) TEM for acid UAE.

Using the optimized conditions which were 1.99 h for sonication time, 2.82 M for concentration of HCl, 220 mL for volume, 0.524 for cycle and 72.6% amplitude, two parallel experiments were carried out. The Design expert software predicted the responses to be 76.9% for yield and 84.1% for silica percentage and the experimental results were 84.1% and 98.5% for percentage yield and percentage silica. This is consistent with the about 60% correlation observed in Figure 1 which shows that optimization parameters proposed are reliable.

3.9.4. Conventional solvent extraction (CSE)

Figures 3.8a, 3.8b and 3.8c are pictures for SEM, EDS and TEM for sample 52 (Figure 3.2) respectively. The pictures are identical to those from alkali UAE method because the methods

of synthesis are identical. The SEM image shows no external pores but the TEM image shows a well-formed pore system contained in an aggregated system similar to that in Figure 6b. Major elements present as seen in the EDS spectra are, Si, and O. The TEM image shows that silica exists as small particles which come together to form a giant particle possibly as a result of attractive forces. The calculated average particle size was 36.77 nm. The same trend was observed by Adebisi et al. (2019).

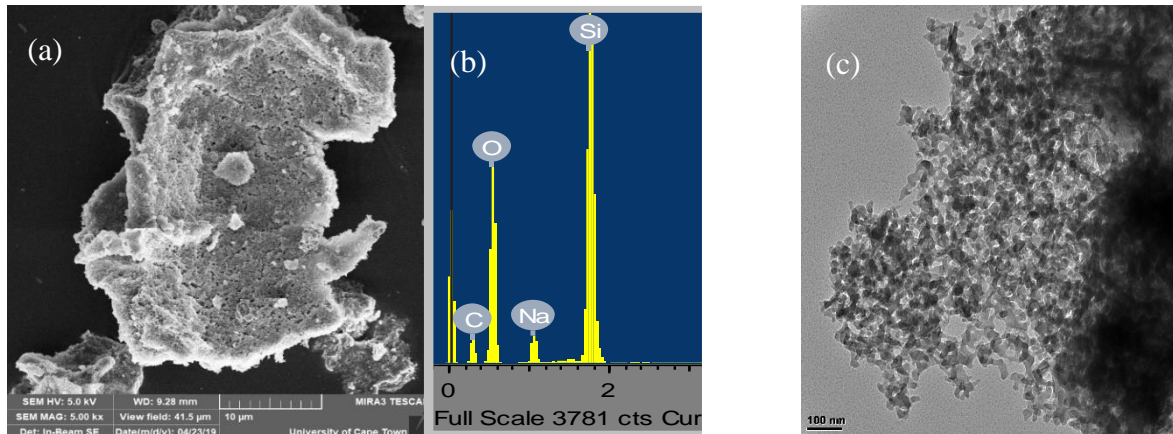


Figure 3. 8. (a) SEM (b) EDS and (c) TEM for CSE.

3.9.5. XRD plots for Alkali UAE, Acid UAE and CSE

The XRD plots in Figure 3.9 show that silica obtained from the acid UAE method (Samples 7, 25 and 30 corresponding to samples 7, 25 and 30 in Table 3.2) are mainly crystalline while samples obtained from the alkali UAE and CSE methods are amorphous. Most researchers have reported the amorphous nature of silica produced from several sources (Okoronkwo et al., 2016; Fernandes et al., 2017; Naddaf et al., 2019). This is because NaOH used in these methods as well as in the CSE and alkali UAE methods, only dissolves amorphous silica. However, Fernandes et al. (2017) reported the formation of crystalline silica at temperatures above 800°C. This would explain the crystalline phases observed in the acid UAE method.

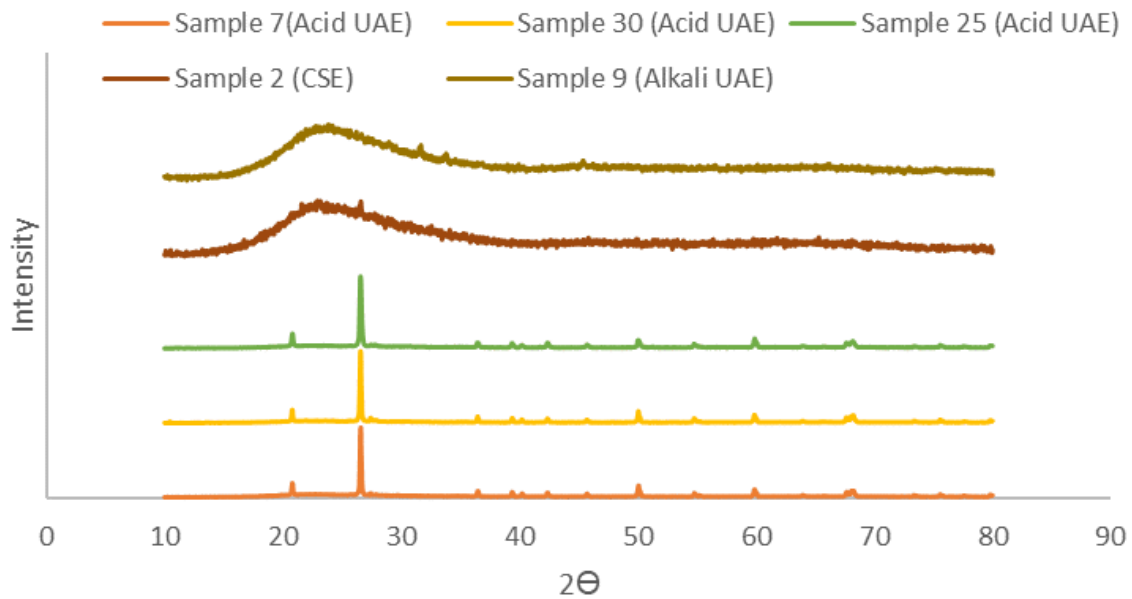


Figure 3. 9. XRD plots for acid UAE, alkali UAE and CSE.

3.10. Conclusions

Response surface methodology was successfully employed in the optimization of silica extraction from DE though the amount of silica extracted was less than that contained in DE in the CSE and alkali UAE methods probably because the time wasn't long enough or temperature not high enough to all dissolve all the silica in DE. Extraction using acids in the acid UAE method gave the best results with the recovery and purity much better. The optimum parameters for the acid UAE were found to be 1.99 h for sonication time, 2.82 M for concentration of HCl, 220 mL for volume, 0.524 for cycle and 72.6% amplitude with a desirability of 1.00. The results proved that acid leaching is an important step in the extraction and purification of silica from DE and RSM is useful technique for accurately determining the optimum conditions for extraction of silica. Also, from the results it is obvious that high quality silica can be produced from DE in high yield and so DE can be an alternative source of silica.

3.11. References

Adebisi, J.A., Agunsoye, J.O., Bello, S.A., Kolawole, F.O., Ramakokovhu, M.M., Daramola, M.O. & Hassan, S.B., 2017 Extraction of silica from sugarcane bagasse, cassava periderm and maize stalk: Proximate analysis and physico-chemical properties of wastes. *Waste Biomass Valor*, pp.1-14.

Adebisi, J.A., Agunsoye, J.O., Bello, S.A., Haris, M., Ramakokovhu, M.M., Daramola, M.O. & Hassan, S.B., 2019 Green production of silica nanoparticles from maize stalk. *Particulate Science and Technology*, 10.1080/02726351.2019.1578845, pp.1-9.

Antonides, L.E., 1998 Diatomite. *U.S. Geological Survey Mineral Commodity Summaries*, pp.56-57.

Ban, G., Song, S., Lee, H.W. & Kim, H.T., 2019 Effect of acidity levels and feed rate on the porosity of aerogel extracted from rice husk under ambient pressure. *Nanomaterials (Basel, Switzerland)*, 9, pp.300.

Banerjee, S., Dubey, S., Gautam, R.K., Chattopadhyaya, M.C. & Sharma, Y.C., 2017 Adsorption characteristics of alumina nanoparticles for the removal of hazardous dye, orange g from aqueous solutions. *Arabian Journal of Chemistry*, <https://doi.org/10.1016/j.arabjc.2016.12.016>.

Bessho, M., Fukunaka, Y., Kusuda, H. & Nishiyama, T., 2009 High-grade silica refined from diatomaceous earth for solar-grade silicon production. *Energy & Fuels*, 23, pp.4160-4165.

Box, G.E.P., Hunter, J.S. & Hunter, W.G., 2005 *Statistics for experimenters: Design, innovation and discovery*. Second Edition ed.: Wiley-Interscience: Hoboken, New Jersey United States.

Carmona, V.B., Oliveira, R.M., Silva, W.T.L., Mattoso, L.H.C. & Marconcini, J.M., 2013 Nanosilica from rice husk: Extraction and characterization. *Industrial Crops and Products*, 43, pp.291-296.

Fernandes, I.J., Calheiro, D., Sánchez, F.A.L., Camacho, A.L.D., Rocha, T.L.A.d.C., Moraes, C.A.M. & Sousa, V.C.d., 2017 Characterization of silica produced from rice husk ash: Comparison of purification and processing methods. *Materials Research*, 20, pp.512-518.

Gorrepati, E.A., Wongthahan, P., Raha, S. & Fogler, H.S., 2010 Silica precipitation in acidic solutions: Mechanism, ph effect, and salt effect. *Langmuir*, 26, pp.10467-10474.

Harish, P.R., Arumugam, A. & Ponnusami, V., 2015 Recovery of silica from various low cost precursors for the synthesis of silica gel. *Pharm. Lett.*, 7 pp.208-213.

Izuagie, A.A., Gitari, W.M. & Gumbo, J.R., 2016a Defluoridation of groundwater using diatomaceous earth: Optimization of adsorption conditions, kinetics and leached metals risk assessment. *Desalination and Water Treatment*, 57, pp.16745-16757.

Izuagie, A.A., Gitari, W.M. & Gumbo, J.R., 2016b Synthesis and performance evaluation of al/fe oxide coated diatomaceous earth in groundwater defluoridation: Towards fluorosis mitigation. *J Environ Sci Health A Tox Hazard Subst Environ Eng*, 51, pp.810-824.

Jendoubi, F., Mgaidi, A. & Maaoui, M.E., 1997 Kinetics of the dissolution of silica in aqueous sodium hydroxide solutions at high pressure and temperature. *The Canadian Journal of Chemical Engineering*, 75, pp.721-727.

Kuwahara, Y., Ohmichi, T., Kamegawa, T., Mori, K. & Yamashita, H., 2010 A novel conversion process for waste slag: Synthesis of a hydrotalcite-like compound and zeolite from blast furnace slag and evaluation of adsorption capacities. *Journal of Materials Chemistry*, 20.

Matlob, A.S., Kamarudin, R.A., Jubri, Z. & Ramli, Z., 2011 Using the response surface methodology to optimize the extraction of silica and alumina from coal fly ash for the synthesis of zeolite na-a. *Arabian Journal for Science and Engineering*, 37, pp.27-40.

Mazidi, M., Mosayebi Behbahani, R. & Fazeli, A., 2017 Screening of treated diatomaceous earth to apply as v2o5 catalyst support. *Materials Research Innovations*, 21, pp.269-278.

MohamedBakr, H.E.G.M., 2010 Diatomite: Its characterization, modifications and applications. *Asian J. Mater. Sci.*, 2 pp.121-136.

Naddaf, M., Kafa, H. & Ghanem, I., 2019 Extraction and characterization of nano-silica from olive stones. *Silicon*, 10.1007/s12633-019-00112-w.

Ogunfowokan, A.O., Ezenwafor, T.C. & Imoisili, P.E., 2011 *Synthesis of nanoporous silica membrane from corn cob ash (zea mays) by sol-gel method*. Paper presented at Nigerian materials congress (NIMACON 2011), Akure:1-7.

Okoronkwo, E.A., Imoisili, P.E., Olubayode, S.A. & Olusunle, S.O.O., 2016 Development of silica nanoparticle from corn cob ash. *Advances in Nanoparticles*, 05, pp.135-139.

Olawale, O., Akinmoladun, A., I, Oyawale, F.A. & Baba, A.O., 2012 Application of response surface methodology for optimisation of amorphous silica extracted from rice husk. *International journal of scientific & engineering research*, 3, pp.2229-5518.

Pa, F.C., Chik, A. & Bari, M.F., 2016 Palm ash as an alternative source for silica production. *MATEC Web Conf.*, 78, pp.01062.

Pilkington, J.L., Preston, C. & Gomes, R.L., 2014 Comparison of response surface methodology (rsm) and artificial neural networks (ann) towards efficient extraction of artemisinin from artemisia annua. *Industrial Crops and Products*, 58, pp.15-24.

Qisti, N., Indrasti, N.S. & Suprihatin., 2017 *Optimization of process condition of nanosilica production by hydrothermal method*. Paper presented at IOP Conference Series: Materials

Science and Engineering, Second International Conference on Chemical Engineering (ICCE) UNPAR.

Rafiee, E., Shahebrahimi, S., Feyzi, M. & Shaterzadeh, M., 2012 Optimization of synthesis and characterization of nanosilica produced from rice husk (a common waste material). *International Nano Letters*, 2, pp.29-33.

Subramanyam, B.H., Swanson, O.L., Madamanchi, N. & Norwood, S., 1994 Effectiveness of insecto, a new diatomaceous earth formulation, in supporting several stored-grain insect species. Canberra:650-659.

Tae, H., Yang D, K., Ji Y & Musaev, H.a.N., A,E, 2013 Comparative adsorption of highly porous and raw adsorbents for the elimination of copper (ii) ions from wastewaters. *Trends in chromatography*, 8, pp.97-108.

Todkar, B.S., Deorukhkar, O.A. & Deshmukh, S.M., 2016 Extraction of silica from rice husk. *Int. J. Eng. Res. Dev.*, 12, pp.69-74.

Tsai, W.T., Hsien, K.J., Chang, Y.M. & Lo, C.C., 2005 Removal of herbicide paraquat from an aqueous solution by adsorption onto spent and treated diatomaceous earth. *Bioresour Technol*, 96, pp.657-663.

Vatalis, K.I., Charalambides, G. & Benetis, N.P., 2015 Market of high purity quartz innovative applications. *Procedia Economics and Finance*, 24, pp.734-742.

Zhao, L.C., Liang, J., Li, W., Cheng, K.M., Xia, X., Deng, X. & Yang, G.L., 2011 The use of response surface methodology to optimize the ultrasound-assisted extraction of five anthraquinones from rheum palmatum l. *Molecules*, 16, pp.5928-5937.

Chapter Four: Synthesis and Evaluation of the Oil Removal Potential of 3-Bromo-Benzimidazolone Polymer Grafted Silica Gel

Abstract

Oily wastewater has become a significant issue of environmental concern and must therefore be treated before discharge into water bodies. However, current treatment methods which include biological methods, flotation, coagulation and membrane separation methods, only remove large suspended oil particles, involve the use of too many chemicals and are too expensive. Adsorption has been shown to be the most attractive method for the treatment of oily water because of its excellent oil-removal ability, cost friendliness and eco-friendliness. This work reports the successful solvent free synthesis of 3-bromo-benzimidazolone using melt condensation, its polymerization and functionalization on silica which was extracted from diatomaceous earth in our previous work. The synthesized compounds were characterized using FTIR, NMR, SEM-EDS and TEM. The FTIR and NMR spectra of the synthesized benzimidazolones showed the compounds to have several functional groups: A band due to Si–O–C at 1085.41cm^{-1} , a broad band at 3380 cm^{-1} (N–H) and chemical shifts: positive distortionless enhancement by polarization transfer (DEPT) ^{13}C peaks (indicating lack of CH_2 and CH_3 groups), ^1H NMR – 11.053 ppm (N–H), 7.086 ppm (Ar–H); ^{13}C NMR – 155.34 ppm (C=O), 101.04 ppm (C–Br) characteristic of benzimidazolones. SEM-EDS of the functionalised silica showed a rough irregular morphology with Si and O as the major elements. Carbon was also present indicating that silica was successfully functionalised with 3-bromo-benzimidazolone and TEM showed interconnected smear-like particles arranged irregularly. The functionalised silica was then applied in the treatment of oily wastewater and parameters such as initial oil concentration, adsorption dosage and time were optimized using the central composite design of response surface methodology in the design expert software. The amount of oil adsorbed was determined by measuring the total organic carbon using TOC test kits. Results showed that the optimum conditions for oil removal were 6650 mg/L oil concentration, with adsorbent dosage of 0.004 g and a contact time of 16 h. Under these conditions, the percentage adsorption was 97.9% with a desirability of 0.99. The materials were therefore seen to be applicable to field wastewaters.

Keywords: Oily wastewater, benzimidazolone, response surface methodology, silica, adsorption

4.1. Introduction

Petroleum is widely used globally, and its use is predicted to increase to about 107 million barrels daily by the year 2030. The exploration of this mineral, just like all fossil fuel extraction, requires a lot of water (Pichtel, 2016; Wilson and VanBriesen, 2012) and generates wastewater very rich in oils (Wilson and VanBriesen, 2012).

Oily wastewater is ranked high in the global environmental issues list, hence treating it is of paramount importance (Cozzarelli et al., 2017; Li et al., 2010). Coagulation, filtration with coagulation, precipitation, ozonation, ion exchange, reverse osmosis, biological methods and advanced oxidation processes have been used to treat oily wastewater in the past, but these methods have technical and economic limitations (Rashed, 2013; Yu et al., 2017; Cheng and Gong, 2018; Han et al., 2019; Noamani et al., 2019).

Adsorption is another method that has been used in the treatment of oily wastewater with advantages over other methods such as, high removal efficiency, low energy demand, less chemical investment and reusability (Dinker and Kulkarni, 2015). Over the years, several adsorbents like activated carbon, zeolites, coal, fly ash, clays and nanomagnetic particles have been used. Moazed and Viraraghavan (2005) used bentonite clay to remove oil from water and reported 70% adsorption of its weight in oil. It was also reported that the bentonite clay material had an oil removal capacity of 100%, but the materials were not successful in the removal of organic particles (Moazed and Viraraghavan, 2005). The other adsorbents listed above were found to have relatively low adsorption capacities (Dinker and Kulkarni, 2015; Pichtel, 2016). Fly ash was reported to have similar removal efficiency (70-80%). The adsorption data they obtained fitted best to Freundlich isotherm indicating adsorption on a heterogenous surface (Yan and Zhao, 1998). Li et al. (2010) used different particle sizes of three different types of coal - anthracite, lean coal and lignite to remove oil from wastewater. The results of their experiments indicated that the quantity of absorbed oil decreased with an increase in particle size. They also found anthracite to have the highest adsorption capacity (24.4 mg/g). Since the first synthesis of porous silica gels in 1968 (Stöber et al., 1968), different porous gels with different modifications and pore sizes have been synthesized by modifying the reaction conditions and parameters (Fernandes et al., 2017). This makes the materials potentially applicable in a wide range of areas. The modifications have recently been extended to organic polymers giving the materials characteristics of both organic and inorganic moieties (Nandiyanto et al., 2008; Jin et al., 2012; Wang et al., 2016).

The benzimidazole group is an integral part of many therapeutic agents with many known applications as antiviral, antihistaminic, selective nucleotide-binding oligomerization domain-containing protein 1 and angiotensin-converting-enzyme inhibitory agents (Izevbekhai et al., 2016). Benzimidazol-2-ones are an important group of benzimidazoles and have been applied as antipsychotic, antihistaminic, antihypertensive and antiviral agents among others. This group of compounds have only been applied in a few instances in remediation of wastewater. For example, Samai and Biradha (2012) successfully applied bis-benzimidazole compounds in the sorption of dyes and its derivatives have been shown to be good adsorbents of acids (Lgaz et al., 2017).

Given the frequency of use of petroleum products and the associated spills and the increasing scarcity of water, there is need for a reliable and efficient adsorbent to remove oil from water. This work was aimed at the synthesis of 3-bromobenzimidazolone derivatives of porous silica gels which has never been investigated before. The synthesis was carried out by first synthesizing the benzimidazolone through a solvent free process followed by its copolymerization with silica. For the first time, the usability of these benzimidazolone-silica hybrids in the treatment of oily wastewater is reported. The removal of oil from water using these adsorbents were optimized using response surface methodology and the optimum conditions for oil removal were obtained using this software.

4.2. Materials and methods

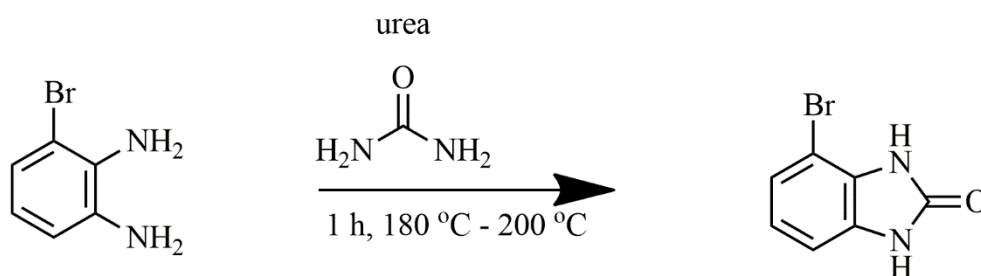
4.2.1. Chemicals and reagents

Silica previously extracted from diatomaceous earth was used after drying (Izevbekhai et al., 2019). Sodium dodecyl sulphate, 3 – bromo – 1, 2 – benzenediamine, urea and ammonium persulphate were of analytical grade and obtained from Sigma – Aldrich (St Louis, USA), NaOH and HCl was obtained from Rochelle Chemicals (Johannesburg, South Africa). Milli-Q water from Millipore S.A.S (Molsheim, France) ($18.2 \mu\text{s}/\text{cm}$ at 25°C) was also used in all dilutions. Tea bags were obtained from retail outlets in Thohoyandou, South Africa. Vacuum pump oil was obtained from Telstar technologies (Barcelona, Spain). Telstar Lyoquest-55 freeze dryer (Shanghai, China) was used to freeze dry all samples and spectroquant UV spectrophotometer from Merck Group (Germiston, South Africa) was used for total organic carbon testing and Stuart reciprocating shaker (Staffordshire, UK) was used for shaking and ALPHA FT-IR spectrophotometer from Bruker Pty (Sandton, South Africa) was used in functional group analysis.

Synthetic oily wastewater (SOWW) was prepared using the method described by Shoba et al. (2018). Vacuum pump oil was mixed with sodium dodecyl sulphate (90:1 v/w) in 1 L of water, sonicated for 5 min at an amplitude of 75% and cycle of 0.5 to obtain a homogenous solution.

4.2.2. Synthesis of benzimidazolone

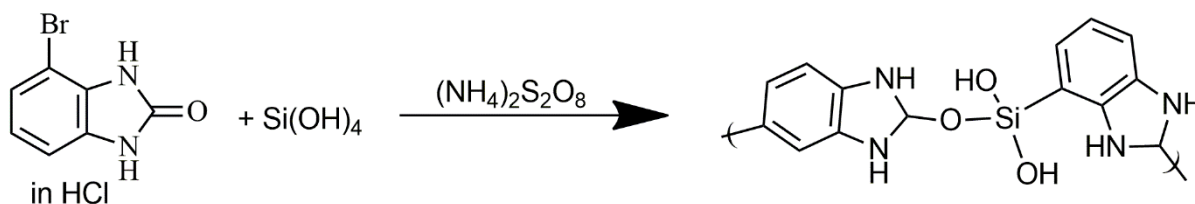
Benzimidazolone were prepared by modifying the method described by Mavrova et al. (2016), Izevbekhai et al. (2018) and Yang et al. (2009). 1 mole of 3-bromo-1,2-benzenediamine, was mixed thoroughly with 1 mole of urea by crushing in a mortar and heated at 190°C for 1 h over a sand bath as shown in reaction Scheme 4.1. The reaction mixture was then allowed to cool to room temperature, it was then dissolved in 10% NaOH, filtered and the filtrate extracted with 35% HCl, filtered, dried and then characterized using FT – IR and NMR.



Scheme 4.1. Synthesis of 3-bromo-benzimidazolone.

4.2.3. Polymerization of 3-bromo benzimidazolone

Prepared 3-bromo-benzimidazolone was polymerized by modifying the method described by Mdlalose et al. (2017). Silica and benzimidazolone (mole ratio 2:1) were dissolved in 50 mL, 0.1 M HCl and stirred in a beaker over ice bath for 3 h. A volume of 25 mL 0.6 M ammonium persulphate in HCl was then added dropwise into the reaction mixture and stirring was continued for 24 h (Scheme 4.2). The reaction was then quenched by the addition of acetone and filtered. The filtrate was evaporated to dryness at 60°C to obtain solutes which were characterized and used in adsorption experiments.



Scheme 4.2. Polymerization of 3- bromo benzimidazolone.

4.2.4. Response surface optimization of oil removal

The synthesized polymer was used in the optimization tests. Variable amounts of adsorbent were placed in tea bags whose contents had previously been carefully emptied out (Fig 1). The tea bags were then sealed using a plastic sealer and placed in 10 mL of SOWW. The setup was allowed to stand ‘undisturbed’ for some time. After this, the solution was filtered and the TOC of the treated and untreated SOWW was measured using a spectroquant UV spectrophotometer. The equilibrium adsorption was calculated using Equation (4.1) and percentage removal using Equation (4.2).

$$Q_e = \left(\frac{C_i - C_f}{m} \right) V \quad (4.1)$$

$$\% \text{ Removal} = \left(\frac{C_i - C_f}{C_i} \right) 100 \quad (4.2)$$

where C_i and C_f are the oil concentrations (mg/L) before and after treatment with adsorbent respectively; V (L) is the volume of the solution and m (g) is the mass of the adsorbent.



Figure 4. 1. (a) sealed empty tea bag (b) sealed tea bag containing adsorbents.

4.2.5. Experimental design

For the purposes of optimization of oil removal, the weight of the adsorbent, oil concentration and contact time were varied using the central composite design in the response surface methodology (RSM) software. The range of optimized parameters are listed in Table 4.1.

Table 4. 1. Range of optimized parameters.

Parameter	Low	High
Oil concentration (mg/L)	192	9250
Sorbent dosage (g)	0.0011	0.004
Contact time (h)	16.0	60.5

4.3. Results and discussion

4.3.1. Functional group analysis

Fig 4.2 shows the FT-IR spectra of 3-bromo-1,2-diaminobenzene, urea and the synthesised 3-bromo-benzimidazolone. The spectrum for 3-bromo-1,2-diaminobenzene exhibited bands at 620 cm^{-1} due to C-Br, 797 cm^{-1} , 1060 cm^{-1} (CH out of plane), 1234 cm^{-1} , 1295 cm^{-1} (CH plane), 1367 cm^{-1} , 1625 cm^{-1} (C-N stretching vibration), 1456 cm^{-1} , 1573 cm^{-1} and 1738 (aromatic C=C) as well as 3282 cm^{-1} and 3371 cm^{-1} due to N-H bonds. The product (3-bromo-benzimidazolone) showed distinctive bands, for example, the bands at 1458 cm^{-1} and 1599 cm^{-1} are characteristic of the C=C stretching of the benzene ring (Ramadhan et al., 2018), band at 3117 cm^{-1} is characteristic of N-H stretching bands of benzimidazoles (Abdolmaleki and Bazayar, 2013). This band was seen to be broad probably due to OH groups formed as a result of tautomerism in the benzimidazolone ring and also as a result of intra-molecular hydrogen bonding (Abdeldjebar et al., 2019). Also worthy of note was the fact that the band for asymmetric N-H stretching seen in the spectrum for 3-bromo-1,2-diaminobenzene, was absent in the 3-bromobenzimidazolone spectrum because the primary NH_2 group (amine) in the former becomes a secondary NH group (amine) in the later. There was also an observed red shift in band for the C=O group in urea from 1678 cm^{-1} to 1629 cm^{-1} . This could have been as a result of increased electronegativity of the oxygen atom (with contributions from tautomerism) and a subsequent increase in intra-molecular hydrogen bonding leading to the observed red shift in wavelength. FT-IR analysis of the 3-bromo benzimidazolone polymer showed the presence of Si-O-C bond at about 1085.41 cm^{-1} (Kasinathan et al., 2010; Tian et al., 2010). The transmission band was broad with shoulders indicating that there was also contribution from C-H out of plane band. There was also a broad band of N-H bond between $3172 - 3380\text{ cm}^{-1}$ (Abdolmaleki and Bazayar, 2013) and there was a shift and a decrease in the intensity of C=O band from 1629 cm^{-1} to 1680 cm^{-1} possibly because of the formation of a bond with Si. As a result of increased conjugation, a decrease in intensity and a shift in the C-N band from 1454 cm^{-1} to 1499 cm^{-1} was also observed (Anand and Muthusamy, 2017). A

decrease in the intensity and number of CH out of plane bands of the benzene ring was noticed. This could be attributed to the formation of phenylene units through polycondensation (Anand and Muthusamy, 2017).

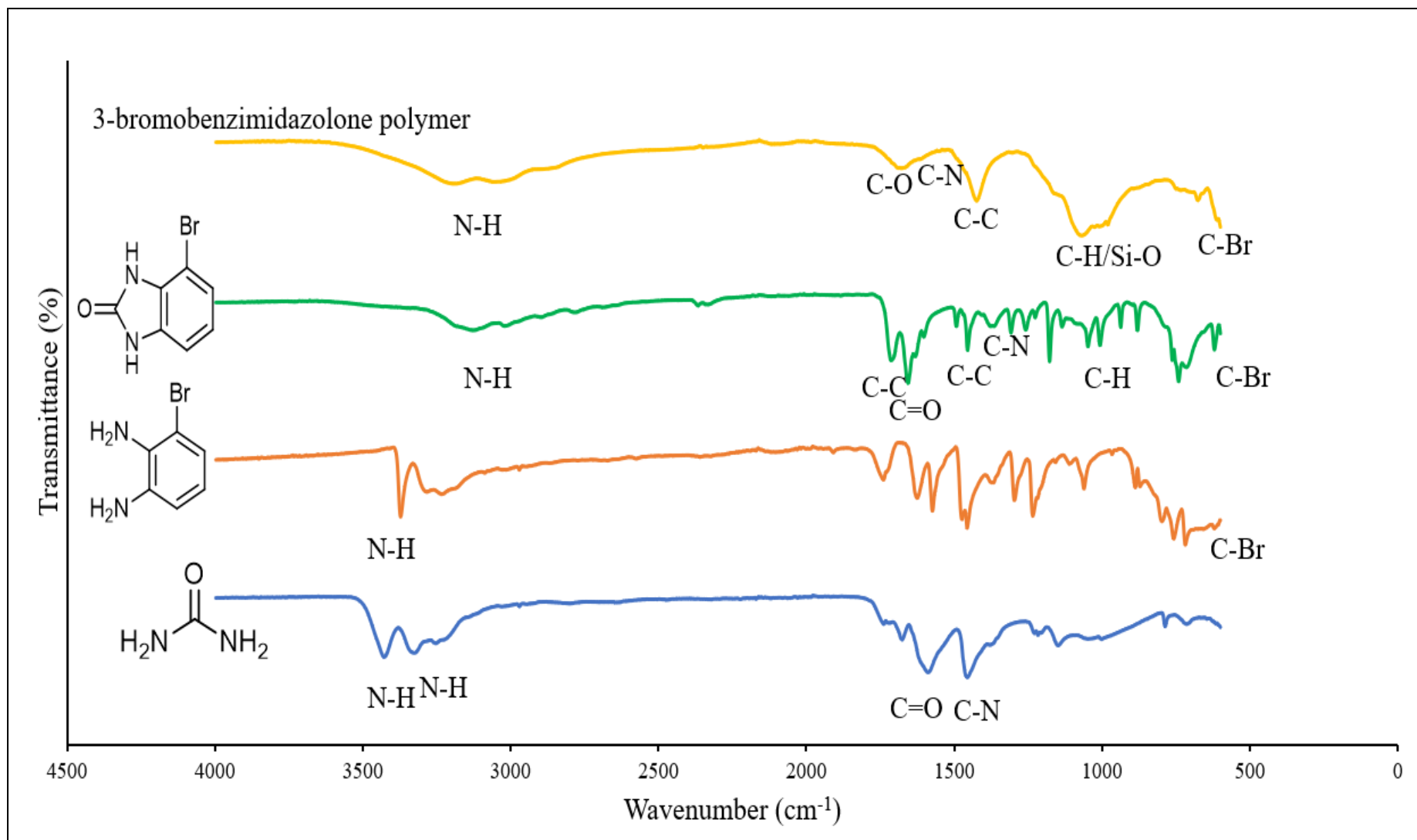


Figure 4. 2. FTIR spectra for Urea, 3- bromo-1,2-phenylenediamine, 3- bromobenzimidazolone and 3-bromobenzimidazolone polymer.

4.3.2. Structure elucidation of 3-bromo benzimidazolone polymer

The ^1H NMR peaks in Figure 4.3 (a) shows chemical shifts of Ar-H at 6.9 ppm and 7.0 ppm (El-Naggar et al., 2018). Chemical shifts at this position is usually due to immobile protons (Zhang and Yan, 2010). This therefore suggested electron redistribution in the benzimidazole ring and confirmed that tautomerism exists in the benzimidazolone ring and could have caused the broad transmission band observed on the spectrum for the 3 -bromo benzimidazolone. It also shows chemical shifts of N-H at 11.0 and 10.9 ppm (El-Naggar et al., 2018). The ^{13}C NMR peaks on Figure 4.3 (b) indicated chemical shifts for a total of seven carbon atoms. This is in line with the chemical formula $\text{C}_7\text{H}_5\text{BrN}_2\text{O}$, of 3-bromo-benzimidazolone. The chemical shifts were assigned as follows: C=O at 155.3 ppm, C-N at 131.09 ppm and 129.6 ppm, Ar C-H at 123.5 ppm, 122.4 ppm and 108.1 ppm and C-Br at 101.04 ppm (Smith, 2008). The chemical shifts on the ^{13}C NMR are confirmed by the DEPT (Figure 4.3 (c)) chemical shifts. These had all positive amplitude which indicated that all seven carbon atoms present in the ^{13}C NMR were CH. The absence of negative amplitudes shows the absence of CH_2 peaks (Eberhard, 2002) confirming that all C atoms in the bromo benzimidazolone are unsaturated.

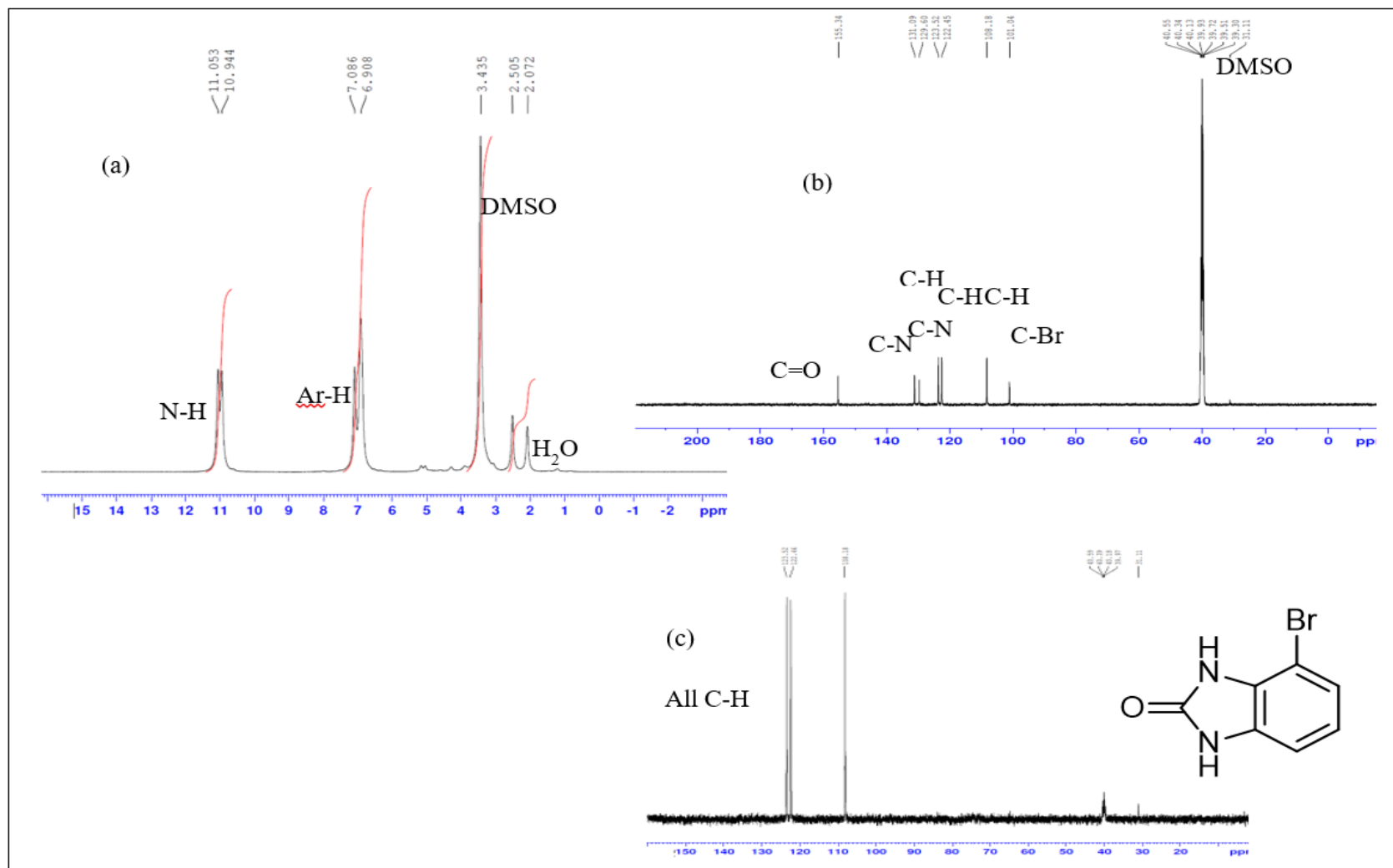


Figure 4. 3. (a) ^1H , (b) ^{13}C and (c) DEPT NMR of 3- bromo-benzimidazolone.

4.3.3. Morphological studies

As seen in the TEM image of the modified silica (Figure 4.4 (d)) shows an oily like surface as a result of its recovery from solution. On the SEM image on Figure 4.4 (b), pores are evident on the surface of razor-like crystals of silica. The SEM of the 3- bromo benzimidazolone modified silica (Figure 4.4 (e)) showed a rough surface with clearly defined pores which shows it could be a good adsorbent. The EDX the unmodified silica (Figure 4.4 (c)) shows silicon and oxygen as major elements while the benzimidazolone modified silica (Figure 4.4 (f)) shows the presence of silicon and oxygen from silica, nitrogen from the benzimidazolone ring and other unreacted elements from the synthesis.

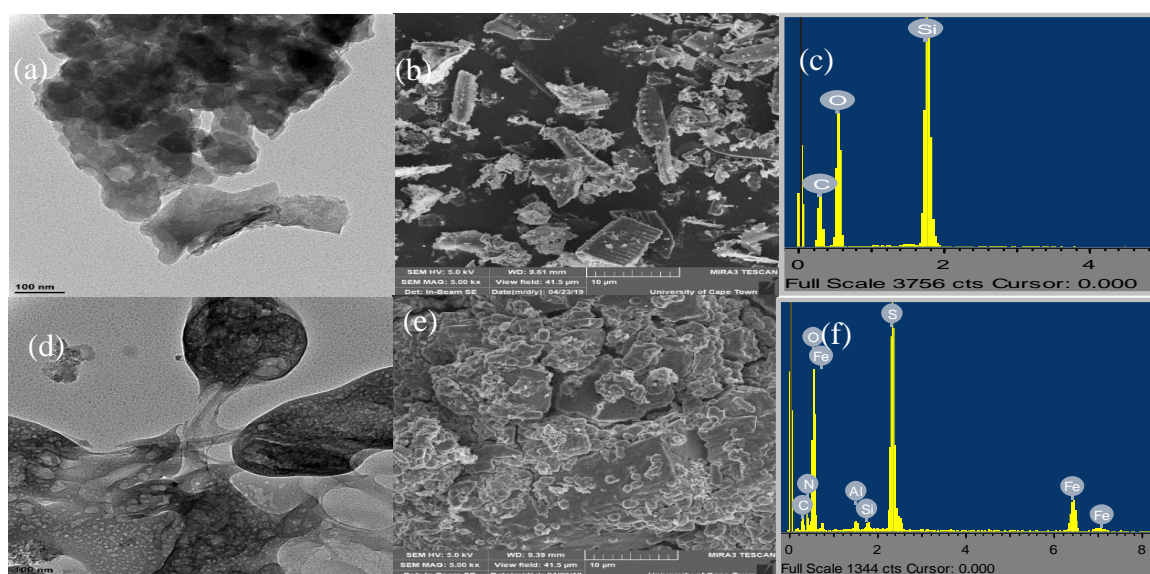


Figure 4. 4. TEM, SEM and EDX of (a) unmodified silica (b) 3- bromo-benzimidazolone modified silica.

4.3.4. Response surface experiments and model fitting

Modelling experiments were done using the quadratic model of the central composite design of the response surface methodology (RSM), varying three reaction parameters, namely initial oil concentration (mg/L), adsorbent dosage (g) and contact time (h). The actual percentage removal as calculated using equation 4.2 are presented in Table 4.2 and pictures of the optimization experiments are shown in Figure 4.5. From the pictures in Figure 4.5, the colour of the adsorbent treated water had an inverse relationship with the percentage oil adsorption. The more intense the colour, the lower the percentage removal and vice versa. The trends observed in the table are as described in the response surface plots.

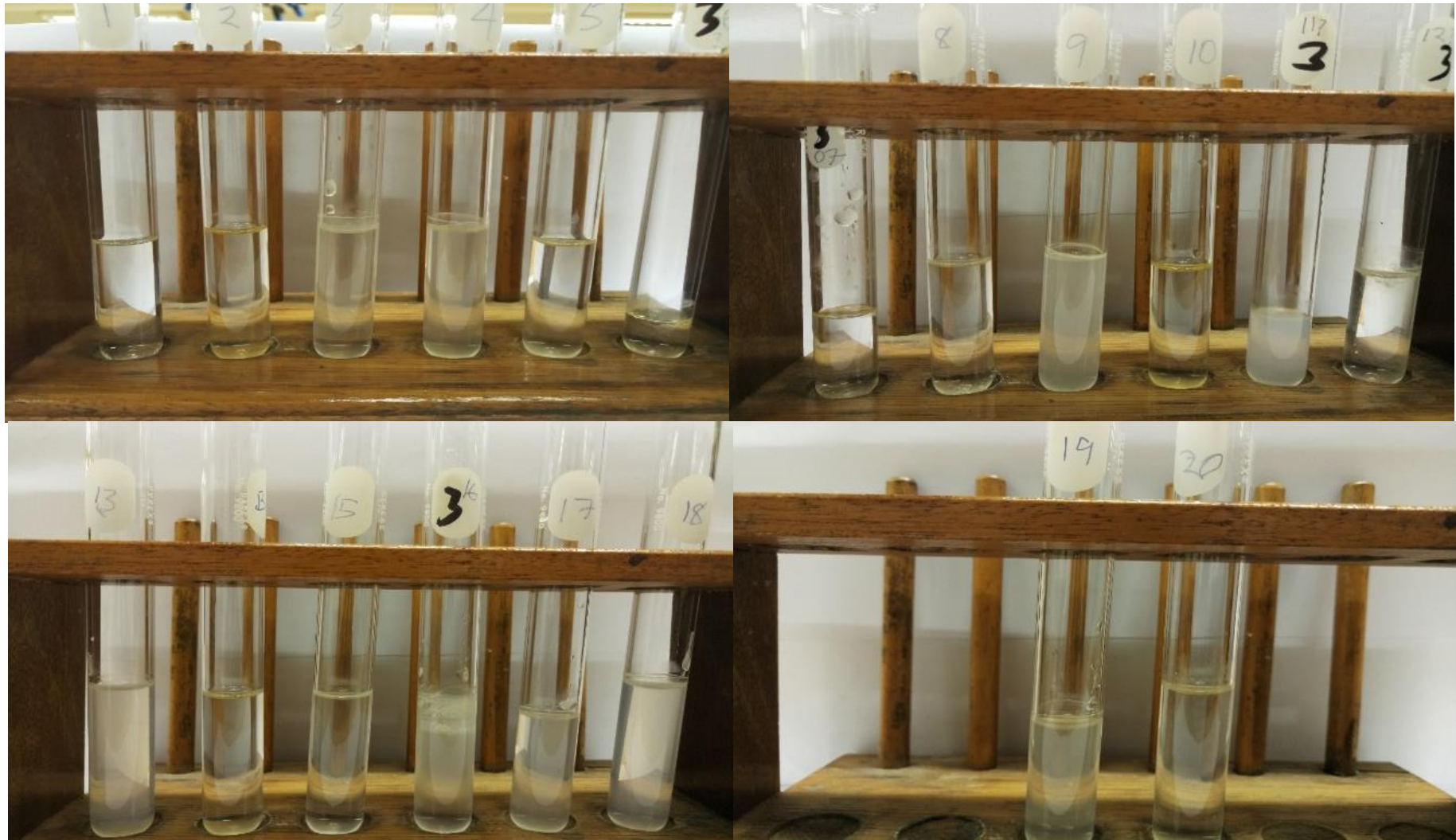


Figure 4. 5. Pictures of adsorbent treated synthetic oily wastewater (Experimental conditions are as presented in Table 2).

Table 4. 2. RSM design and the actual values of responses.

Run	Oil concentration (mg/L)	Sorbent dosage (g)	Contact time (h)	Percentage adsorption
1	9250	0.0026	38.2	97.1
2	9250	0.0045	38.2	97.9
3	704	0.0011	16.0	75.7
4	9250	0.0026	38.2	98.1
5	704	0.0040	60.5	75.5
6	6650	0.0011	60.5	96.7
7	6650	0.0040	60.5	96.0
8	704	0.0040	16.0	76.5
9	7200	0.0026	38.2	96.8
10	9250	0.0001	38.2	98.2
11	9250	0.0026	38.2	97.8
12	6650	0.0040	16.0	97.9
13	9250	0.0026	38.2	98.3
14	9250	0.0026	75.6	98.1
15	704	0.0011	60.5	75.7
16	6650	0.0011	16.0	97.4
17	9250	0.0026	38.2	98.2
18	9250	0.0026	38.2	98.2
19	9250	0.0026	0.85	97.7
20	192	0.0026	38.2	14.6

The model predictions for percentage removal of oil from synthetic oily wastewater was compared with the values obtained from experiments and plotted in Figure 4.6 to obtain a straight line, with most points distributed on the line and a few very close to the line. The coefficient of determination R^2 was found to be 0.99 indicating that predicted and actual values were in good agreement and

that the quadratic polynomial model chosen was sufficient to represent the design space, and is able to explain the relationship between the responses and significant variables (Ani et al., 2019; Zhao et al., 2011).

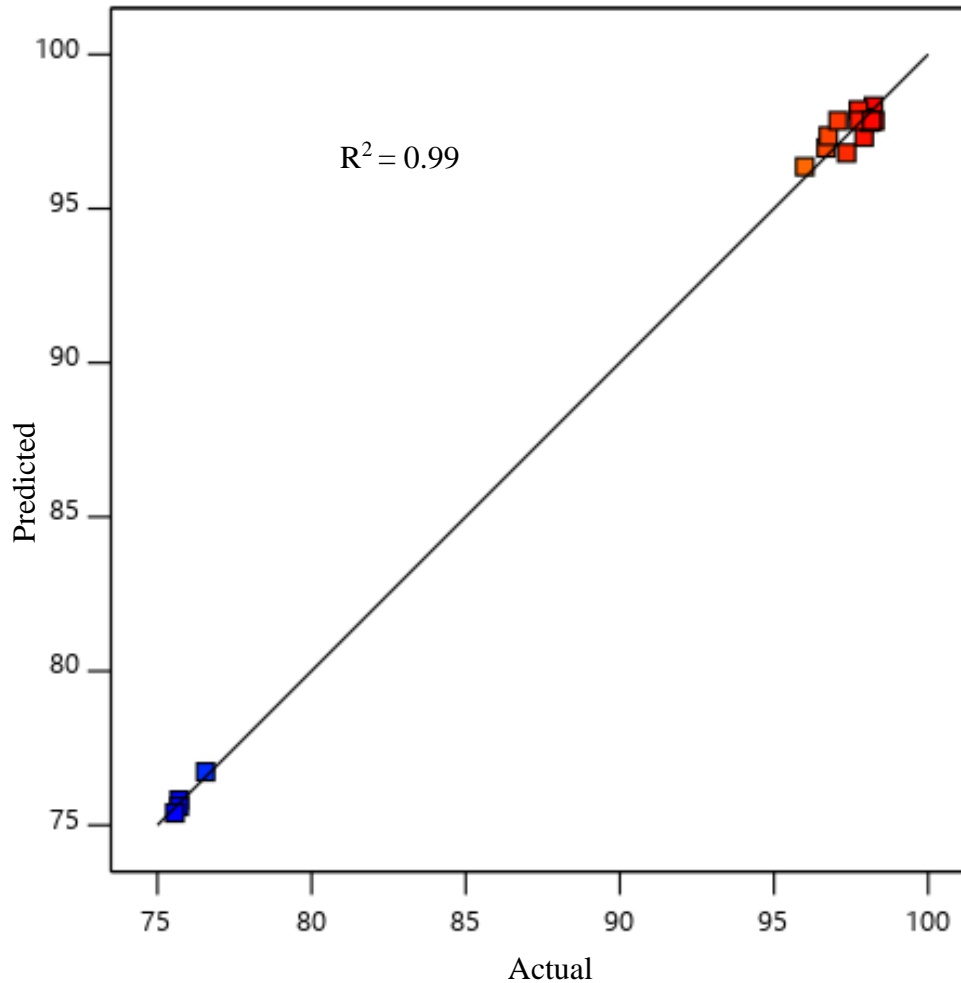


Figure 4. 6. Comparison between values predicted by response surface methodology (RSM) model and experimentally determined values.

4.3.4.1. Regression model and analysis of variance (ANOVA)

In order to ascertain the significance of the model and the model terms, analysis of variance (ANOVA) was carried out (Table 4.3). It was observed that the quadratic polynomial model used to represent percentage adsorption was significant (p – value less than 0.05 and high F -value) which means that the model was sufficient to represent the design space just like a line of best fit. The lack of fit P -value, which was high and therefore not significant, further proved that the model

was good. Only initial oil concentration and its quadratic function had an effect on the percentage oil removal.

Table 4. 3. ANOVA for model and model terms.

Source	% Removal	
	F-value	p-value
Model	561.73	< 0.0001
A-Oil concentration	815.58	< 0.0001
B-sorbent dosage	0.2294	0.6434
C-contact time	0.0189	0.8938
AB	0.6528	0.4400
AC	0.5746	0.4678
BC	2.15	0.1763
A ²	364.55	< 0.0001
B ²	0.4508	0.5188
C ²	0.1251	0.7317
Lack of fit	2.02	0.2296

4.3.4.2. Effect of oil concentration and sorbent dosage

As seen from the response surface plot in Figure 4.7, an increase in initial oil concentration caused an increase in percentage adsorption up to a maximum and started to decrease. This could be because as the oil concentration is increased, larger oil droplets are formed by the coming together of smaller droplets due to the coagulative effect of the adsorbents. These large oil droplets become trapped in the pores of the adsorbent and settle at the base, leaving the water clear (Carlos et al., 2001; Ishak and Ayoub, 2019). This could also be as a result of the introduction of new binding sites as the dosage is increased but as these get saturated, the adsorption capacity begins to reduce (Hassan et al., 2019; Rahdar et al., 2019; Syuhada et al., 2017). With adsorbent dosage, there is a slight increase in adsorption capacity as the adsorbent dosage is increased as a result of increase in new binding sites.

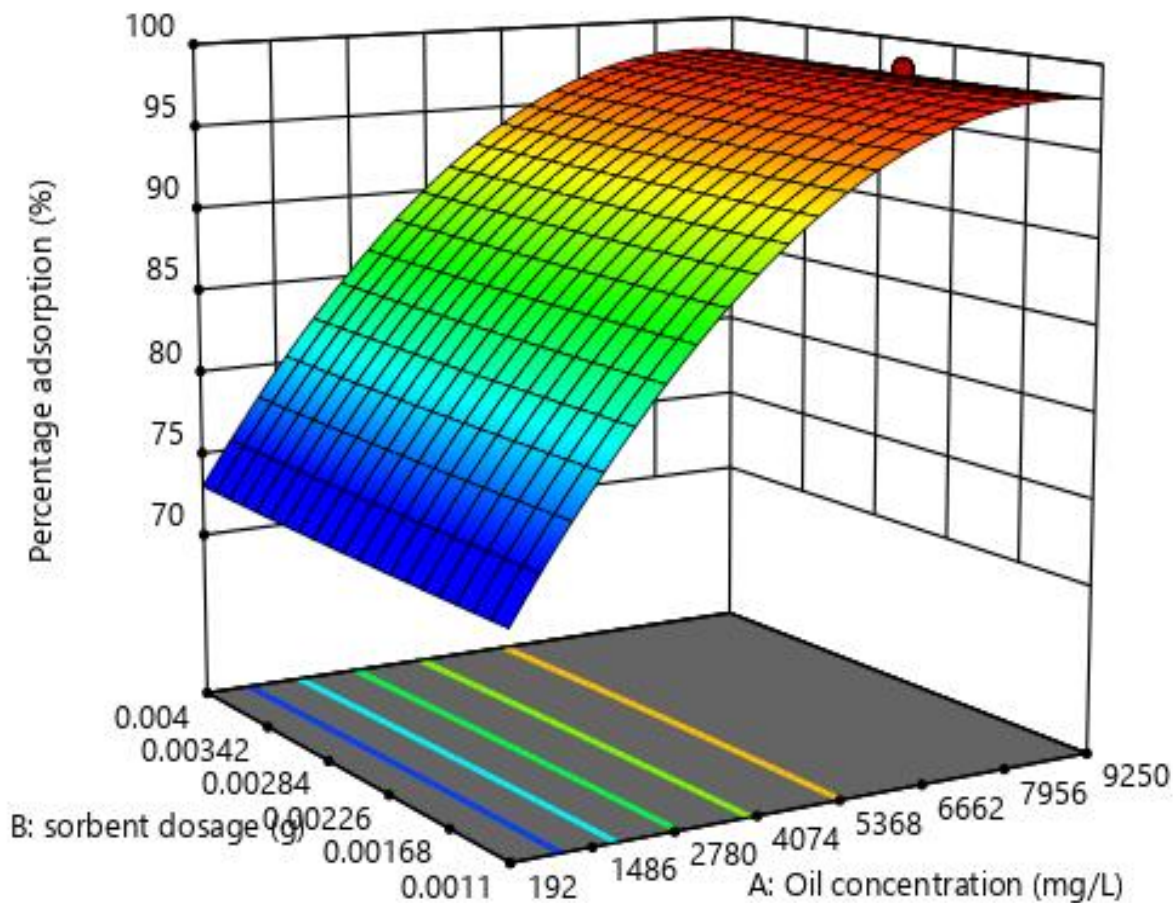


Figure 4. 7. Response surface plot for the effect of initial oil concentration and adsorbent dosage on percentage adsorption.

4.3.4.3. Effect of oil concentration and time

As can be seen from the response surface plots in Figure 4.8, percentage oil removal increased with time, this was because there was an increased chance of positive interaction between the adsorbent and oil as the adsorbent stayed longer in contact with the solution (Hassan et al., 2019).

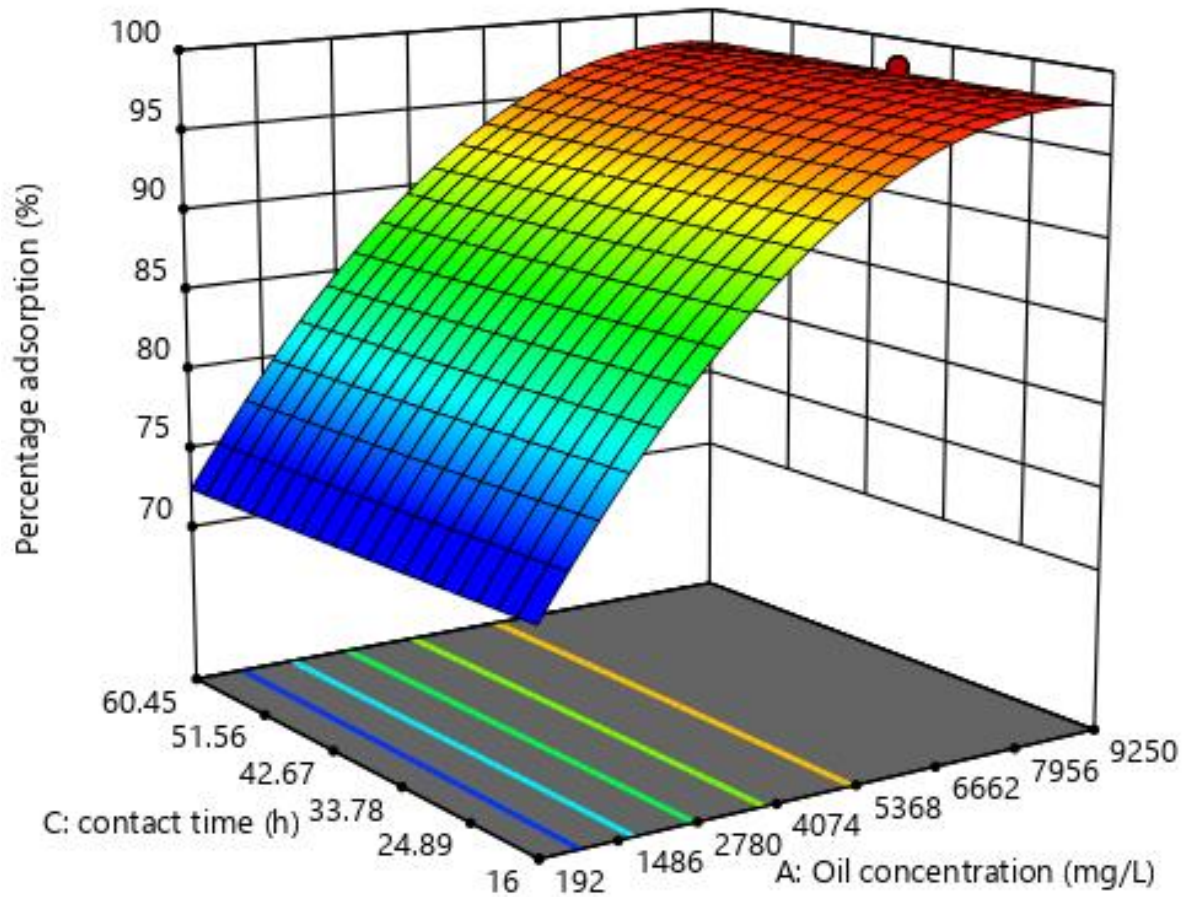


Figure 4. 8. Response surface plot for the effect of initial oil concentration and time on percentage adsorption.

4.3.4.4. Effect of adsorbent dosage and time

The response surface plot for effect of adsorbent dose and time on percentage adsorption in Figure 4.9 shows a slight increase in percentage adsorption with time and adsorbent dosage. As the dosage was increased, more binding sites were made available and as time was increased, there was more time for the oil molecules to interact with the binding sites (Rahdar et al., 2019).

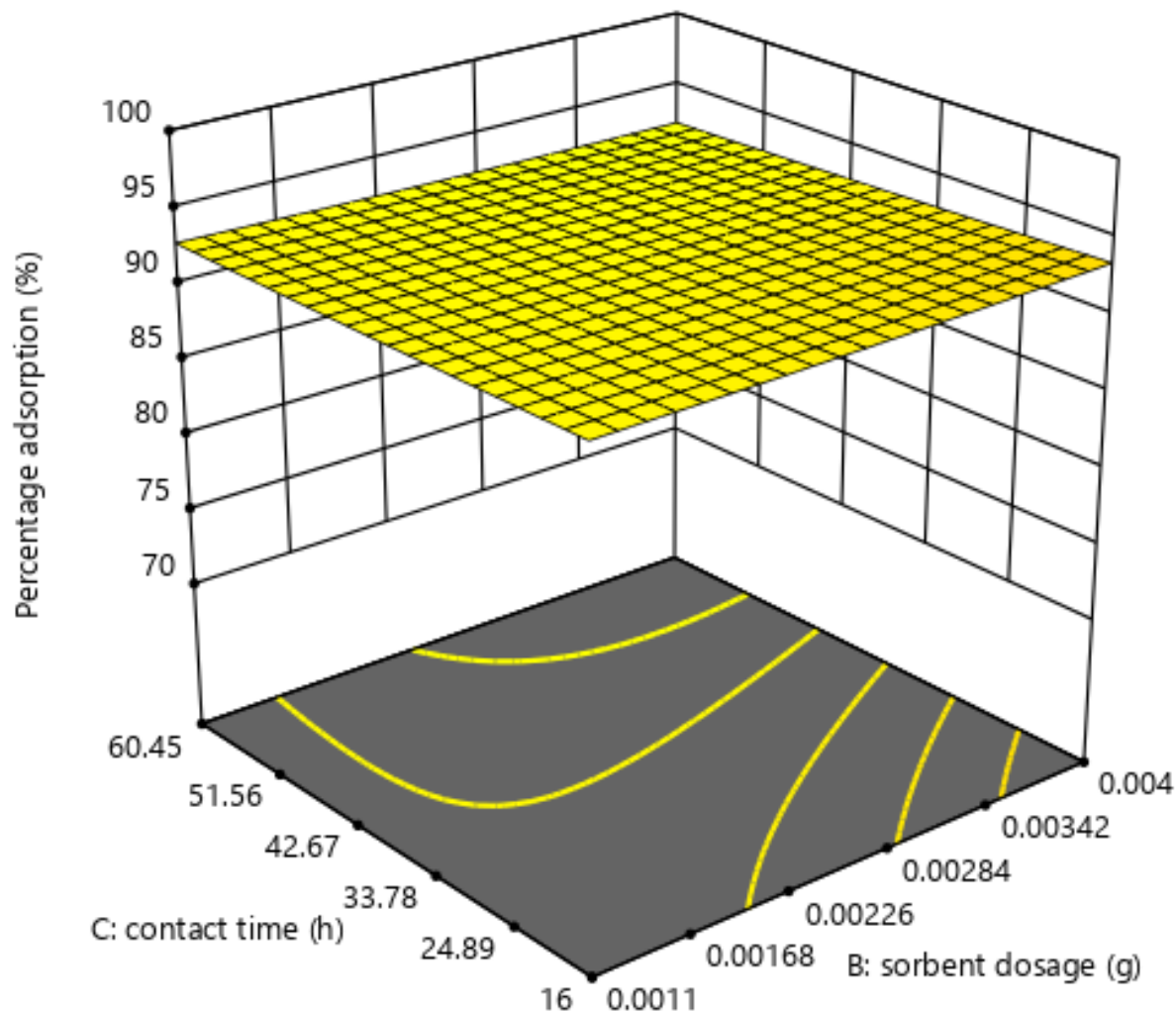


Figure 4.9. Response surface plot for the effect of contact time and adsorbent dosage on percentage adsorption.

4.4. Conclusion

In this study, 3- bromo-benzimidazolone polymer was successfully synthesized by first synthesizing the benzimidazolone via a solvent free process. The synthesized bromo benzimidazolone was then functionalized on pre-extracted silica gels as an oil sorbent material. The oil adsorption performance of this polymer – silica sorbent material in synthetic oily wastewater (SOWW) was then optimized using response surface methodology. It was found that the central composite model chosen was adequate to represent the relationship between the optimized parameters: initial oil concentration, adsorbent dosage and contact time. The results demonstrated that oil removal by adsorption onto benzimidazolone modified silica is feasible. The

adsorption and percentage removal were found to be dependent on the adsorbent dose, initial oil concentration and contact time with initial oil concentration being the major determinant of oil adsorption. The optimum conditions for removal of oil from synthetic oily wastewater using silica functionalized with benzimidazolone were as follows 6650 mg/L oil concentration, with adsorbent dosage of 0.004 g and a duration of 16 h. The percentage oil adsorption using these optimum conditions was found to be 97.9%. Given the percentage oil removal, the optimum duration of adsorption and the fact that oil adsorption takes place without stirring or shaking or any form of mechanical agitation, the benzimidazolone modified silica adsorbent can be applied in field wastewaters.

4.5. References

- Abdeldjebar, H., Belmiloud, Y., Djitli, W., Achour, S., Brahimi, M. & Tangour, B., 2019 Proton transfer in the benzimidazolone and benzimidazolthione tautomerism process catalyzed by polar protic solvents. *Progress in Reaction Kinetics and Mechanism*, 44, pp.143-156.
- Abdolmaleki, A. & Bazyar, Z., 2013 Preparation and characterization of poly(benzimidazole-amide)/zno nanocomposites using silane coupling agent. *Polymer-Plastics Technology and Engineering*, 52, pp.1542-1549.
- Anand, S. & Muthusamy, A., 2017 Optical, thermal and electrical properties of polybenzimidazoles derived from substituted benzimidazoles. *Journal of Molecular Structure*, 1148.
- Ani, J.U., Okoro, U.C., Aneke, L.E., Onukwuli, O.D., Obi, I.O., Akpomie, K.G. & Ofomatah, A.C., 2019 Application of response surface methodology for optimization of dissolved solids adsorption by activated coal. *Applied Water Science*, 9, pp.60.
- Carlos, G., Juan, C., Wang, S., Luis, G., Mohan, R.S. & Ovadia, S., 2001 Oil-water separation in liquid-liquid hydrocyclones (llhc) -experiment and modeling.1-10.
- Cheng, X.-N. & Gong, Y.-W., 2018 Treatment of oily wastewater from cold-rolling mill through coagulation and integrated membrane processes. *Environmental Engineering Research*, 23, pp.159-163.
- Cozzarelli, I.M., Skalak, K.J., Kent, D.B., Engle, M.A., Benthem, A., Mumford, A.C., Haase, K., Farag, A., Harper, D., Nagel, S.C., Iwanowicz, L.R., Orem, W.H., Akob, D.M., Jaeschke, J.B., Galloway, J., Kohler, M., Stoliker, D.L. & Jolly, G.D., 2017 Environmental signatures and effects of an oil and gas wastewater spill in the williston basin, north dakota. *Science of The Total Environment*, 579, pp.1781-1793.
- Dinker, M.K. & Kulkarni, P.S., 2015 Recent advances in silica-based materials for the removal of hexavalent chromium: A review. *Journal of Chemical and Engineering Data*, 60, pp.2521-2540.
- Eberhard, B., 2002 *Structure elucidation by nmr in organic chemistry - a practical guide*. West Sussex: John Wiley and sons Ltd.

El-Naggar, M., Eldehna, W.M., Almahli, H., Elgez, A., Fares, M., Elaasser, M.M. & Abdel-Aziz, H.A., 2018 Novel thiazolidinone/thiazolo[3,2-a]benzimidazolone-isatin conjugates as apoptotic anti-proliferative agents towards breast cancer: One-pot synthesis and in vitro biological evaluation. *Molecules (Basel, Switzerland)*, 23, pp.1420.

Fernandes, I.J., Calheiro, D., Sánchez, F.A.L., Camacho, A.L.D., Rocha, T.L.A.d.C., Moraes, C.A.M. & Sousa, V.C.d., 2017 Characterization of silica produced from rice husk ash: Comparison of purification and processing methods. *Materials Research*, 20, pp.512-518.

Han, Zhang, Chu, Chen & Zhou, 2019 Research progress and prospects of marine oily wastewater treatment: A review. *Water*, 11, pp.2517.

Hassan, A.A., Naeem, H.T. & Hadi, R.T., 2019 A comparative study of chemical material additives on polyacrylamide to treatment of waste water in refineries. *IOP Conference Series: Materials Science and Engineering*, 518, pp.062003.

Ishak, K.E.H.K. & Ayoub, M.A., 2019 Predicting the efficiency of the oil removal from surfactant and polymer produced water by using liquid–liquid hydrocyclone: Comparison of prediction abilities between response surface methodology and adaptive neuro-fuzzy inference system. *IEEE Access*, 7, pp.179605-179619.

Izevbekhai, O., Mavrova, A. & Anichina, K., 2016 *Design and synthesis of 1, 3- disubstituted benzimidazol-2-ones using solid - liquid phase transfer catalysis*. Paper presented at 13th National Poster Session for Young Scientists, Students and Doctorate Students, University of Chemical Technology and Metallurgy, Sofia, Bulgaria:21.

Izevbekhai, O., Anichina-Zarkova, K., Mavrova, A., Vutchev, D., Popova-Daskalova, G., Yancheva, D. & Stoyanov, S., 2018 Design, synthesis and antitrichinellosis activity of 1,3-disubstituted benzimidazol-2-ones. Edirne, Turkey:237.

Izevbekhai, O.U., Gitari, W.M. & Tavengwa, N.T., 2019 *Optimization of silica extraction from diatomaceous earth using response surface methodology*. Paper presented at 20th WaterNet/WARFSA/GWPSA Symposium, Indaba Hotel, Spa & Conference Centre Fourways, Johannesburg, South Africa:1-10.

Jin, H.X., Dong, B., Wu, B. & Zhou, M.H., 2012 Oil absorptive polymers: Where is the future? *Polymer-Plastics Technology and Engineering*, 51, pp.154-159.

Kasinathan, A., Rama, R. & Sivakumar, G., 2010 Extraction, synthesis and characterization of nanosilica from rice husk ash. *International Journal of Nanotechnology and Applications*, 4, pp.61-66.

Lgaz, H., El Aoufir, Y., El Bakri, Y., Zarrouk, A., Salghi, R., Warad, I., Ramli, Y., Guenbour, A., Essassi, E.M. & Oudda, H., 2017 Understanding the adsorption of benzimidazole derivative as corrosion inhibitor for carbon steel in 1 m hcl: Experimental and theoretical studies. *Journal of Materials and Environmental Sciences*, 8.

Li, X., Zhang, C. & Liu, J., 2010 Adsorption of oil from waste water by coal: Characteristics and mechanism. *Mining Science and Technology (China)*, 20, pp.778-781.

Mavrova, A., Dimov, S. & Izevbekhai, O., 2016 Synthesis of some novel benzimidazol-2-onederivatives Dubai, UAE:13-15.

Mdlalose, L., Balogun, M., Setshedi, K., Tukulula, M., Chimuka, L. & Chetty, A., 2017 Synthesis, characterization and optimization of poly(p-phenylenediamine)-based organoclay composite for cr(vi) remediation. *Applied Clay Science*, 139, pp.72-80.

Moazed, H. & Viraraghavan, T., 2005 Use of organo-clay/anthracite mixture in the separation of oil from oily waters. *Energy Sources*, 27, pp.101-112.

Nandiyanto, A.B.D., Iskandar, F. & Okuyama, K., 2008 Nanosized polymer particle-facilitated preparation of mesoporous silica particles using a spray method. *Chemistry Letters*, 37, pp.1040-1041.

Noamani, S., Niroomand, S., Rastgar, M. & Sadrzadeh, M., 2019 Carbon-based polymer nanocomposite membranes for oily wastewater treatment. *npj Clean Water*, 2, pp.20.

Pichtel, J., 2016 Oil and gas production wastewater: Soil contamination and pollution prevention. *Applied and Environmental Soil Science*, 2016, pp.1-24.

Rahdar, S., Taghavi, M., Khaksefidi, R. & Ahmadi, S., 2019 Adsorption of arsenic (v) from aqueous solution using modified saxaul ash: Isotherm and thermodynamic study. *Applied Water Science*, 9, pp.87-95.

Ramadhan, D., Warsito & dhiaul iftitah, E., 2018 Microwave-assisted synthesis of benzimidazole derivatives from citronellal in kaffir lime (citrus hystrix dc.) oil. *IOP Conference Series: Materials Science and Engineering*, 299, pp.012076.

Rashed, M.N., 2013 Adsorption technique for the removal of organic pollutants from water and wastewater. In: Rashed, M.N. (ed.). *Organic pollutants-monitoring, risk and treatment*. Rijeka, Croatia: InTech Publisher.

Samai, S. & Biradha, K., 2012 Chemical and mechano responsive metal–organic gels of bis(benzimidazole)-based ligands with cd(ii) and cu(ii) halide salts: Self sustainability and gas and dye sorptions. *Chemistry of Materials*, 24, pp.1165-1173.

Shoba, B., Jeyanthi, J. & Vairam, S., 2018 Synthesis, characterization of cellulose acetate membrane and application for the treatment of oily wastewater. *Environ Technol*, 10.1080/09593330.2018.1543353, pp.1-16.

Smith, D., 2008 Dihydrobenzimidazoles, benzimidazolones, benzimidazolethiones, and related compounds

Stöber, W., Fink, A. & Bohn, E., 1968 Controlled growth of monodisperse silica spheres in the micron size range. *Journal of Colloid and Interface Science*, 26, pp.62-69.

Syuhada, N., Mohd Ghazi, R. & Ismail, N., 2017 Response surface methodology optimization of oil removal using banana peel as biosorbent. *Malaysian Journal of Analytical Sciences*, 21, pp.1101-1110.

Tian, R., Seitz, O., Li, M., Hu, W., Chabal, Y.J. & Gao, J., 2010 Infrared characterization of interfacial si–o bond formation on silanized flat sio₂/si surfaces. *Langmuir*, 26, pp.4563-4566.

Wang, C.Y., Li, L. & Zheng, S.X., 2016 Synthesis and characterization of mesoporous silica monoliths with polystyrene homopolymers as porogens. *RSC Advances*, 6, pp.105840-105853.

Wilson, J.M. & VanBriesen, J.M., 2012 Research articles: Oil and gas produced water management and surface drinking water sources in pennsylvania. *Environmental Practice*, 14, pp.288-300.

Yan, H., L. & Zhao, D.F., 12(3), , 1998 Application of the fly ash absorption to dispose of petroleum in oil refining wastewater. *Arid Environmental Monitoring.*, 12, pp.139-144.

Yang, Z., Wang, J., Li, L., Ye, C. & Liu, H., 2009 Cheminform abstract: Synthesis and characteristic of 5,6-dinitro and 5,6-diaminobenzimidazolone-2. *Journal of Heterocyclic Chemistry - J HETEROCYCL CHEM*, 46, pp.788-790.

Yu, L., Han, M. & He, F., 2017 A review of treating oily wastewater. *Arabian Journal of Chemistry*, 10, pp.S1913-S1922.

Zhang, D. & Yan, L., 2010 Probing the acid–base equilibrium in acid–benzimidazole complexes by 1h nmr spectra and density functional theory calculations. *The Journal of Physical Chemistry B*, 114, pp.12234-12241.

Zhao, L.C., Liang, J., Li, W., Cheng, K.M., Xia, X., Deng, X. & Yang, G.L., 2011 The use of response surface methodology to optimize the ultrasound-assisted extraction of five anthraquinones from rheum palmatum l. *Molecules*, 16, pp.5928-5937.

Chapter Five: Application of Synthesized Acetylated Silica in the Remediation of Oily Wastewater

Abstract

Acetylated materials have been applied successfully in oily water remediation with some degree of success. Many of these materials which have been acetylated are, however, from seasonal fruits and other plant parts. This work reports the successful acetylation of silica extracted from diatomaceous earth by refluxing silica and acetic anhydride using 1% N-bromosuccinimide as a catalyst. The functionalization was confirmed by the presence of absorption bands at 1406 cm^{-1} (C-O) and 1568 cm^{-1} (C=O) on an IR spectrum and the presence of C, Si, and increased amount of O on the EDX spectrum. The synthesized materials were applied in the optimization of the removal of oil from synthetic oily wastewater using response surface methodology giving a percentage oil removal of 99.7%. The optimum conditions for oil removal were as follows; 7867 mg/L oil concentration, with adsorbent dosage of 0.001 g and a duration of 21.6 h, and the adsorption capacity under these conditions was found to be 1039 mg/g. The outcomes proved that acetylated silica is an excellent material for oil adsorption and can therefore be used in oil spill clean-ups.

Keywords: oily wastewater, response surface methodology, adsorption, silica, acetylated silica

5.1. Introduction

Many economies of the world are becoming increasingly dependent on oil. As a result, there is increased exploration, transportation and consumption of oil with associated risk of oil spills at each stage. These spills lead to a stress on the environment, causing death to marine organisms, leading to shortage of water and giving it a top spot on the environmental issues list (Azzam and Madkour, 2008; Asadpour et al., 2016; Asadpour et al., 2019). Research in recent years, has been geared towards finding the best method to reverse the impacts of pollution arising from oil exploration and use especially in the area of oily water remediation. Methods which have been employed include mechanical methods such as skimming and in situ burning (Adebajo et al., 2003), the use of oil dispersants (Angelova et al., 2011), bioremediation methods (Zahed et al., 2010) and the use of oil sorbents (Asadpour et al., 2013).

However, the use of adsorbent materials is becoming increasingly popular because of the ease of use, affordability and effectiveness of these materials (Asadpour et al., 2013; Liu and Wang, 2019; Vocciante et al., 2019). Adsorbent materials can either be synthetic organic polymers, inorganic materials or organic natural polymers (Adebajo et al., 2003). Synthetic organic polymers like polyurethane usually have high adsorption potential but are non-biodegradable (Adebajo et al., 2003). Inorganic materials like organoclays are biodegradable but have low adsorption capacities (Asadpour et al., 2014; Carmody et al., 2007). Organic adsorbents on the other hand, are relatively cheap, easily accessible and have been shown to have high adsorption capacities (Annunciado et al., 2005; Asadpour et al., 2013).

Silica, a major component of the ubiquitous diatomaceous earth (Bessho et al., 2009), can also be mined from ores and has been extracted from agricultural wastes like rice husk (Rafiee et al., 2012; Carmona et al., 2013; Todkar et al., 2016; Fernandes et al., 2017), sugarcane bagasse (Harish et al., 2015; Adebisi et al., 2017), palm ash (Pa et al., 2016) and corn cob (Ogunfowokan et al., 2011; Okoronkwo et al., 2016). It has found application in several areas such as solar energy systems and in water filtration. Silica has proven to be an excellent adsorbent and has been applied in the treatment of water contaminated with gasoline and diesel (Ning, 2010; Syed et al., 2011; Gilak et al., 2015; Alkindy et al., 2019; Noamani et al., 2019; Zhang et al., 2019). There have also been studies using silica functionalized with petroleum vacuum residues in the treatment of oily water and oily brines at different pH values (Franco Ariza et al., 2014). Two major drawbacks of these studies however were pH adjustments and the use of mechanical shakers to aid adsorption which are not achievable in actual oil spills. The search for a cost-effective and practicable adsorbent is still on with many researchers coming up with different materials.

In a bid to find the perfect adsorbent, this study looks at the modification of silica with acetyl groups, the optimization of oil removal from synthetic oily wastewater using the central composite design of the response surface methodology software without the application of mechanical shakers/ stirrers or pH adjustment so as to make it applicable in actual field treatments.

5.2. Materials and Methods

5.2.1. Chemicals and reagents

Silica previously extracted from diatomaceous earth (Izevbekhai et al., 2019) was used after drying to a constant weight. Acetic anhydride, acetone, ethanol and ethyl acetate were of analytical grade and obtained from Rochelle Chemicals (Johannesburg, South Africa). N-bromosuccinimide was also of analytical grade and obtained from Sigma – Aldrich (St Louis, USA). Sodium dodecyl sulphate was obtained from Sigma – Aldrich (St Louis, USA) and vacuum pump oil was obtained from Telstar technologies (Barcelona, Spain). Milli-Q water from Millipore S.A.S (Molsheim, France) ($18.2 \mu\text{S}/\text{cm}$ at 25°C) was also used in all dilutions. Telstar Lyoquest-55 freeze dryer (Shangai, China) was used to freeze dry all samples, spectroquant UV spectrophotometer from Merk Group (Germiston, South Africa) was used for total organic carbon testing. Tea bags were obtained from retail outlets in Thohoyandou, South Africa and ALPHA FT-IR spectrophotometer from Bruker Pty (Sandton, South Africa) was used in functional group analysis.

5.2.2. Acetylation of silica

Acetylation was done by modifying the methods of Nwadiogbu et al. (2014) and Nwadiogbu et al. (2018). To 1 mmol of the pre-prepared silica, 5 mmol of acetic anhydride was added. This mixture was refluxed over an oil bath at 100°C for 30 h using 1% N- bromosuccinimide as catalyst. After which, the resulting solution was decanted while still hot. The solute was then washed with 2 mL each of acetone, ethanol and water and freeze-dried.

5.2.3. Characterization

The resulting residue from acetylation was characterized using a Bruker Alpha IR spectrophotometer (Randburg, South Africa). Scanning electron microscope and energy dispersion X-ray spectroscopy (EDX) FEI Nova NanoSEM 230 with field emission gun, (Eindhoven, Netherlands) was used to examine the morphology and elemental composition of the prepared adsorbent and silica before modification. A FEI T20 absorption electron microscope (TEM with a CCD camera embedded (2048X2048) was used for further morphological evaluation.

5.2.4. Preparation of synthetic oily wastewater

Synthetic oily wastewater (SOWW) was prepared using the method described by Shoba et al. (2018). Vacuum pump oil was mixed with sodium dodecyl sulphate (90:1, v/w) in 1 litre of water,

sonicated for 5 min at an amplitude of 75% and cycle of 0.5 to obtain a homogenous solution. This oily wastewater was used in the optimization experiments.

5.2.4.1. Response surface optimization of oil removal

Optimization was done by placing variable amount of adsorbent (0.001 g - 0.004 g) in a tea bag, whose tea leaves had previously been emptied out (Figure 5.1). The bag was then sealed using a plastic sealer and placed in the SOWW (192 mg/L – 9250 mg/L), it was allowed to stand undisturbed for a pre-set time (16 h – 60.5 h) which was also varied. After this, the solution was filtered and the total organic carbon was measured for the initial SOWW and adsorbent treated SOWW using a spectroquant UV spectrophotometer. The equilibrium adsorption was calculated from equation 1.1 and percentage removal from equation (5.2).

$$Q_e = \left(\frac{(C_i - C_f)}{m} \right) V \quad (5.1)$$

$$\% \text{ Removal} = \left(\frac{(C_i - C_f)}{C_i} \right) 100 \quad (5.2)$$

where C_i and C_f are the oil concentrations (mg/L) before and after treatment with adsorbent respectively; V (L) is the volume of the solution, m (g) is the mass of the adsorbent and Q_e is the equilibrium adsorption capacity per milligram dry weight of the adsorbent.



Figure 5. 1. (a) sealed empty tea bag (b) sealed tea bag containing adsorbents.

5.2.5. Experimental design

Experiments for optimization of oil removal without shaking were done by varying the weight of the adsorbent, oil concentration and contact time using the central composite design in the response surface methodology (RSM) software. The range of optimized parameters are listed in Table 5.1.

Table 5. 1. Range of optimized parameters.

Parameter	Minimum	Maximum
Oil concentration (mg/L)	192	9250
Sorbent dosage (g)	0.0011	0.004
Contact time (h)	16.0	60.5

5.3. Results and Discussion

5.3.1. Characterization of synthesized adsorbent

Figure 5.2 represents the infra-red spectra for silica and acetylated silica. The absorption band at 1406.18 cm^{-1} was due to C – O, the absorption band at 1568.37 cm^{-1} was due to C = O and the band at 1042 cm^{-1} was most likely due to Si – O. The absence of peak at 1715 cm^{-1} showed that there were no unreacted acetic anhydride and the absence of peaks around $1840 - 1760\text{ cm}^{-1}$ indicated that the acetylated products are free from acetic acid by-products. These results are in line with what was observed by Nwadiogbu et al. (2016) who illustrated that the presence of the carbonyl bands are key to successful acetylation when they reported the acetylation of corn cobs. El Boustani et al. (2015) also observed same peaks when they studied the effect of acetylation on the fibres of flax and wood pulp using sulphuric acid as catalyst. Onwuka et al. (2019) had similar findings as well during the acetylation of cocoa pods, pride of Barbados pods and empty oil palm fruit bunch.

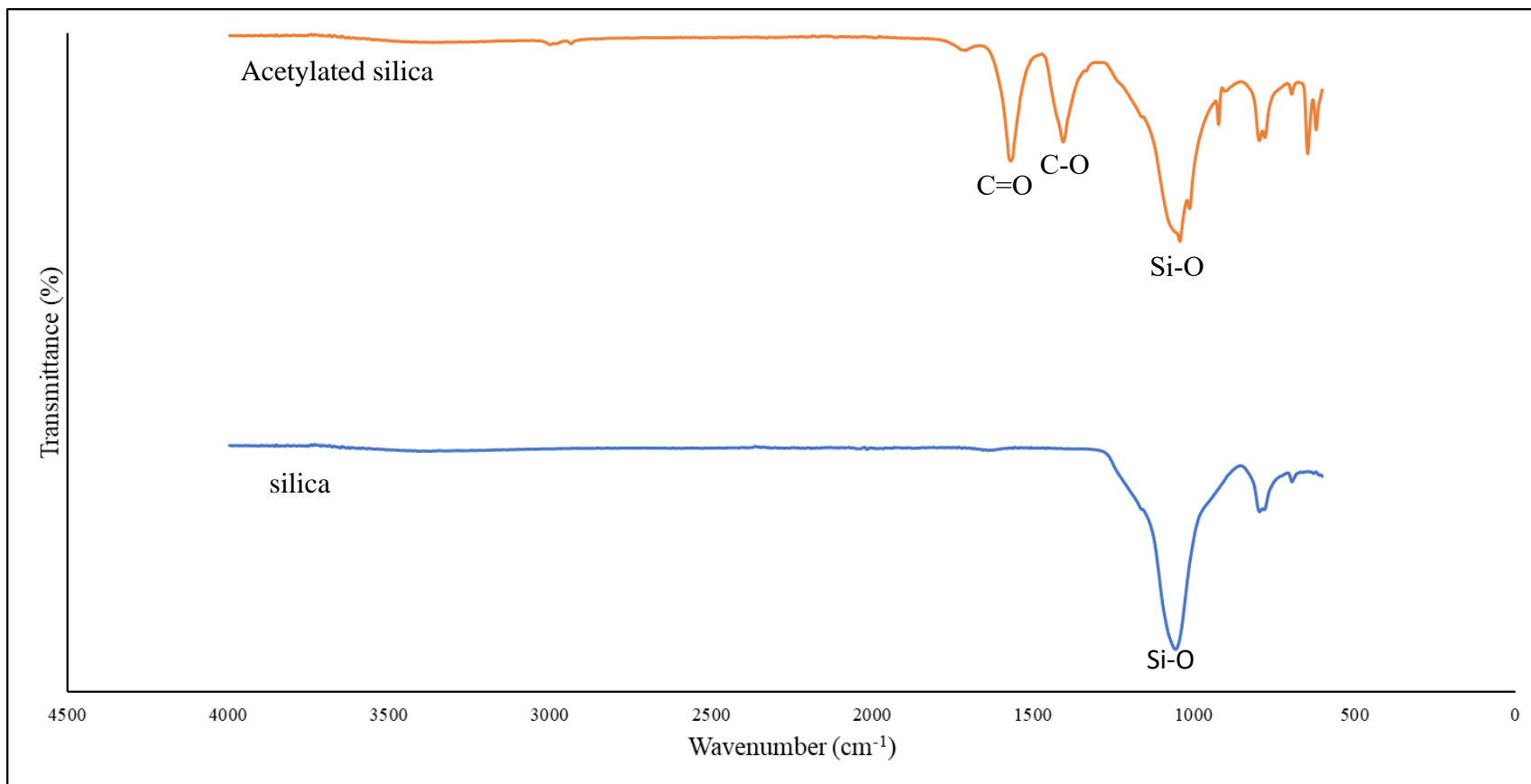


Figure 5. 2. FT-IR spectra of raw silica and acetylated silica.

Figure 5.3 is the XRD spectra of silica and the modified silica. The plots for both the raw silica and acetylated silica had identical diffraction patterns with no new peaks formed. As can be seen from the plots, sharp peaks present at $2\Theta = 26$ indicated that the material was crystalline. It is also worthy of note, that acetylation did not change the crystalline nature of silica suggesting that acetylation occurred on the surface of silica. This is contrary to observations made by Nwadiogbu et al. (2018) who discovered that acetylation led to the conversion of crystalline phases into amorphous phases. This disparity can however be explained by the fact that their material was mainly cellulose and as they correctly opined, acetylation of cellulose materials leads to a decrease in crystallinity (Kosaka et al., 2005). Dong et al. (2017), however reported similar findings to those obtained in this study when they prepared acetylated cellulose nanocrystals using phosphoric acid as solvent. Also, Liu et al. (2019) reported that the XRD patterns on silica gel and acetylated silica gel had identical diffraction patterns with no new crystals formed. This is consistent with findings in this study.

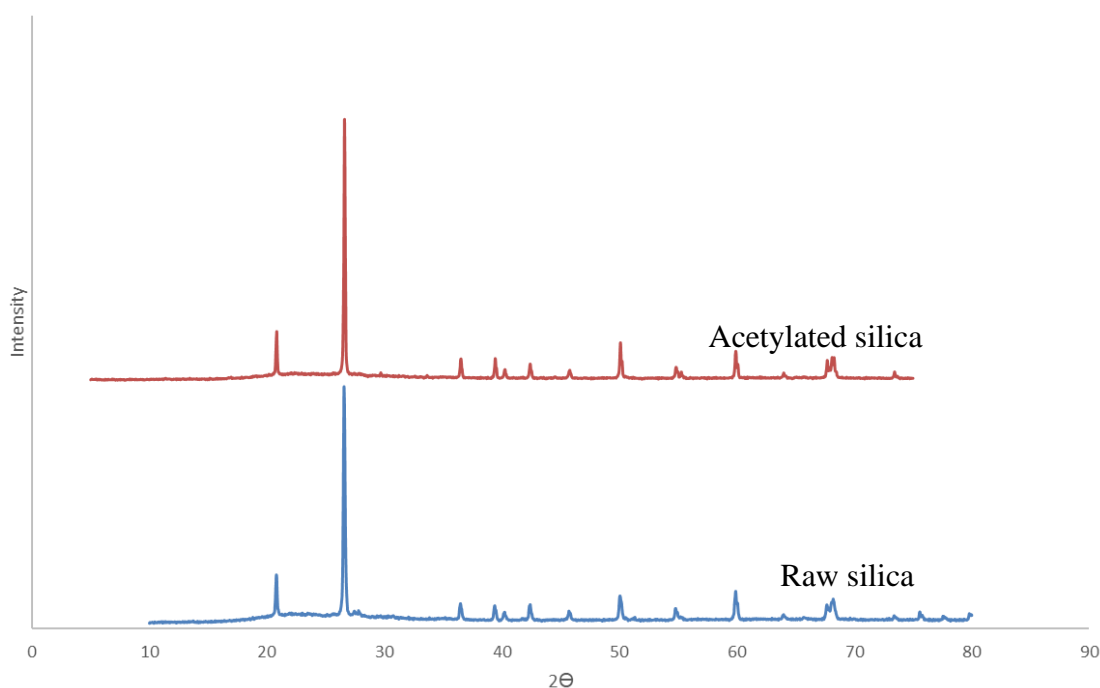


Figure 5. 3. XRD plots of raw and acetylated silica.

Figure 5.4(a) shows the TEM, SEM and EDX pictographs of the unmodified silica and the corresponding acetylated silica (Figure 5.4(b)). It was evident that the external pores visible on the surface SEM images of the former were no longer present on the surface of the acetylated silica but have been replaced with a bit of wrinkles and grooves most likely because of the

conversion of hydroxyl groups on the surface of silica to more bulky acetyl groups leading to a closure of most of the external pores indicating successful functionalization (Onwuka et al., 2018). The EDX indicated that the unmodified silica had silicon, oxygen and carbon which most likely came from the coating material and the acetylated silica has increased intensity of oxygen and carbon as a result of the introduction of acetyl groups. TEM images shows that the acetylated silica particles were aggregated. This same trend has been observed by other researchers (Onwuka et al., 2016; Wang et al., 2012).

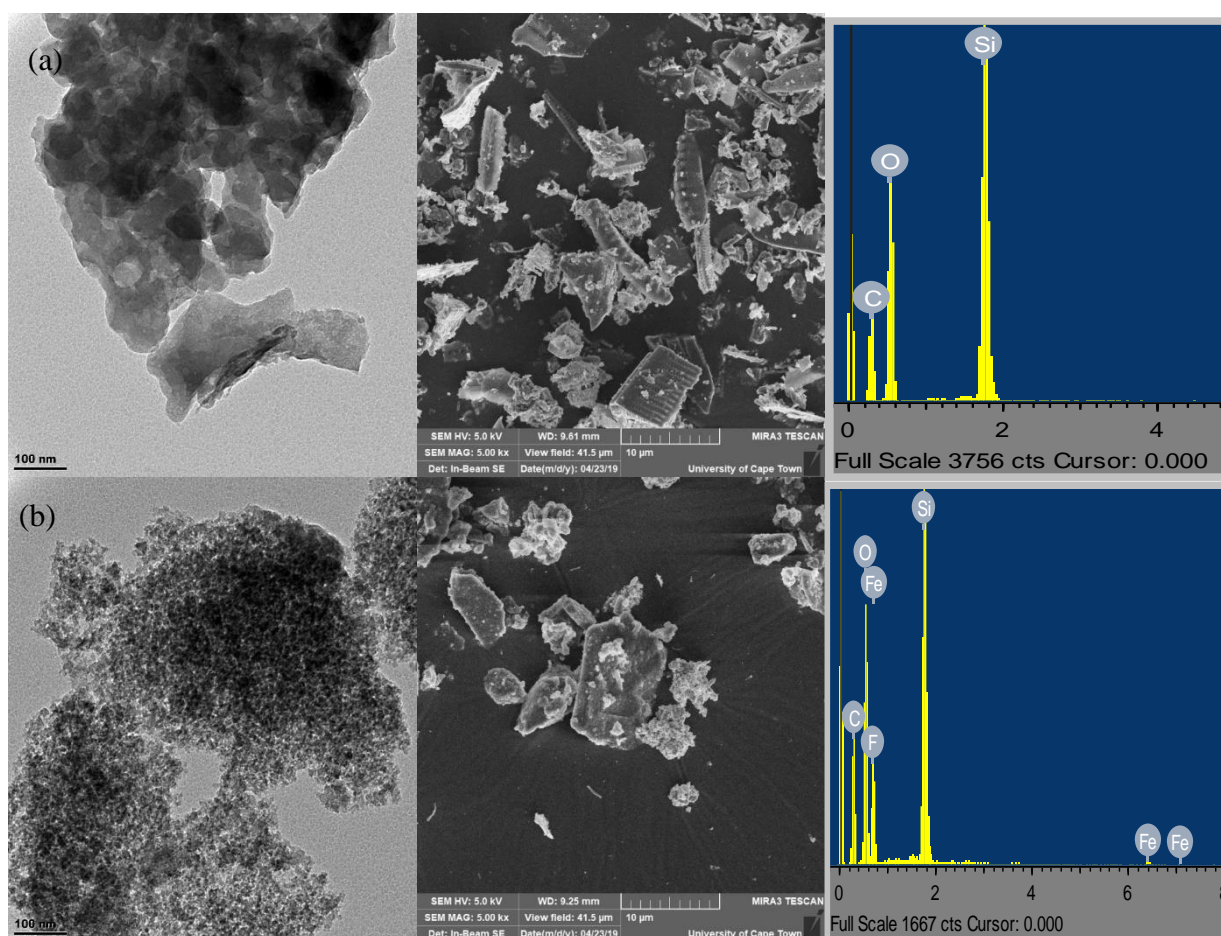


Figure 5. 4. TEM, SEM and EDX micrographs of (a) raw silica (b) acetylated silica.

5.3.2. RSM experiments and model fitting

Quadratic model of the central composite design of the response surface methodology (RSM), a statistical software that allows for estimation of interactions including quadratic effects, was used for modelling experiments. Three reaction parameters were varied as indicated in Table 5.1: namely, initial oil concentration (mg/L), adsorbent dosage (g) and contact time (h). The actual percentage removal as calculated using equation 1.2 are presented in Table 5.2 which had 20 runs and pictorial representation of the optimization experiments presented Figure 5.5.

It was seen that changes in the optimized parameters were reflected as changes in colour intensity of the SOWW in Figure 5.5.



Figure 5. 5. Pictures of adsorbent treated synthetic oily wastewater (Experimental conditions are as presented in Table 2).

Table 5. 2. RSM design and the actual values of responses.

Run	Oil concentration (mg/L)	Sorbent dosage (g)	Contact time (h)	Percentage adsorption
1	6650	0.004	16.0	15.6
2	9250	0.003	38.2	97.6
3	9250	0.003	38.2	97.3
4	9250	0.003	0.85	98.3
5	9250	0.003	38.2	97.6
6	704	0.001	16.0	95.2
7	9250	0.005	38.2	97.5
8	704	0.004	16.0	62.6
9	192	0.003	38.2	19.3
10	704	0.004	60.5	57.4
11	6650	0.001	60.5	95.5
12	9250	0.003	38.2	97.6
13	9250	0.003	38.2	92.5
14	9250	0.0001	38.2	97.8
15	9250	0.002	75.6	97.6
16	9250	0.002	38.2	99.4
17	7250	0.003	38.2	95.9
18	704	0.001	60.5	68.0
19	6650	0.004	60.5	96.3
20	6650	0.001	16.0	96.4

The model predictions for percentage removal of oil from SOWW was compared with the values obtained from experiments and plotted in Figure 6 to obtain a straight line with most of the points close to the line. The coefficient of determination R^2 was 0.96 indicating that predicted and actual values were in good agreement and that the quadratic polynomial model chosen was sufficient to represent the design space, and was able to explain the relationship between the responses and significant variables (Olawale et al., 2012; Adebisi et al., 2017; Syuhada et al., 2017).

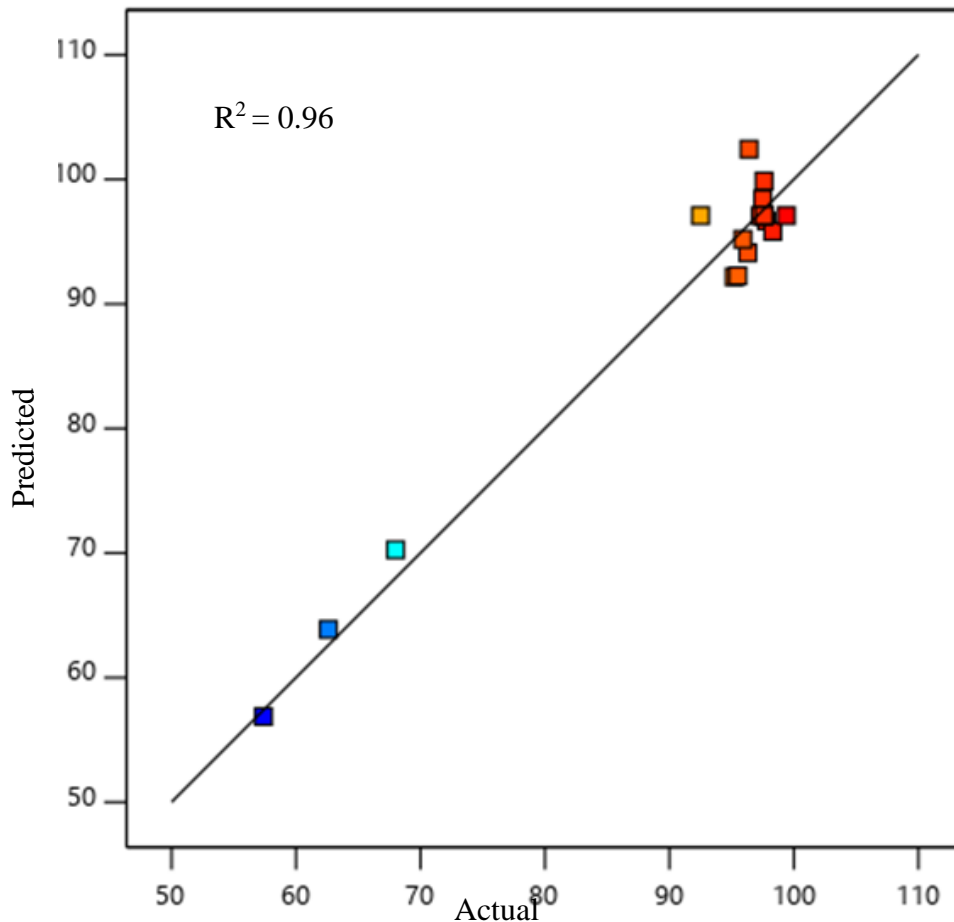


Figure 5. 6. Comparison between values predicted by response surface methodology (RSM) model and experimentally determined values.

5.3.3. Regression model and analysis of variance (ANOVA)

In order to investigate the significance of the model and the model terms, analysis of variance (ANOVA), an essential test used to determine the adequacy and significance of a model was carried out (Table 5.3). ANOVA determines the significance or otherwise of a model by dividing the variation of the results into two sources, distinguishing model variations from experimental error. It is then able to determine and show if variation from the model is significant when compared to the variation due to residual error with the aid of the Fisher's F-test value also known as F-value (ratio between the mean square of the model and the residual error) (Kasiri et al., 2013; Segurola et al., 1999). P-value is another tool used in ANOVA that helps determine if a model term is significant or not. The smaller the p-value, the more significant the factor is. Generally the smaller the p-value, the less likely the observed trends occurred by chance (Sawyer, 2009).

It was discovered that the quadratic polynomial model used to represent percentage adsorption was significant (p – value < 0.05 and high F - value). The lack of fit p -value was found to be greater than 0.05 indicating that the model fits and further confirmed that the model chosen was adequate to show how concentration, adsorbent dosage, and contact time affected the percentage removal of oil. Only initial oil concentration, adsorbent dosage and contact time and their interaction influenced the percentage oil removed.

Table 5. 3. ANOVA for model and model terms.

Source	% Removal	
	F-value	p-value
Model	23.64	< 0.0001
A-Oil concentration	140.65	< 0.0001
B-sorbent dosage	22.26	0.0015
C-contact time	8.52	0.0193
AB	20.77	0.0019
AC	12.33	0.0080
BC	6.54	0.0338
A ²	5.15	0.0530
B ²	0.0251	0.8781
C ²	0.0686	0.8001
Lack of fit	5.02	0.0572

5.3.4. Effect of oil concentration and sorbent dosage

As seen from the response surface plot in Figure 5.7, percentage adsorption increased steadily up to 99%, which was the maximum with an increase in initial oil concentration and then decreased to 93% with a further increase in initial oil concentration. When initial oil concentration was increased, the oil droplets increased and passed into the pores of the adsorbent easily, hence the initial increase in percentage adsorption (Carlos et al., 2001; Ishak and Ayoub, 2019; Sahu and Singh, 2019). A point was reached however, when the size of the oil droplets equalled the size of the adsorbent pores. At this point, there was maximum or effective adsorption but as the size of the oil droplets became greater than the size of the adsorbent pores, less oil was adsorbed and there was a subsequent decrease in percentage adsorption. Also, as adsorbent dosage was increased, percentage adsorption increased slightly. The reason for this observed trend was as a result of the introduction of new binding sites on the adsorbents (Hassan et al., 2019; Rahdar et al., 2019).

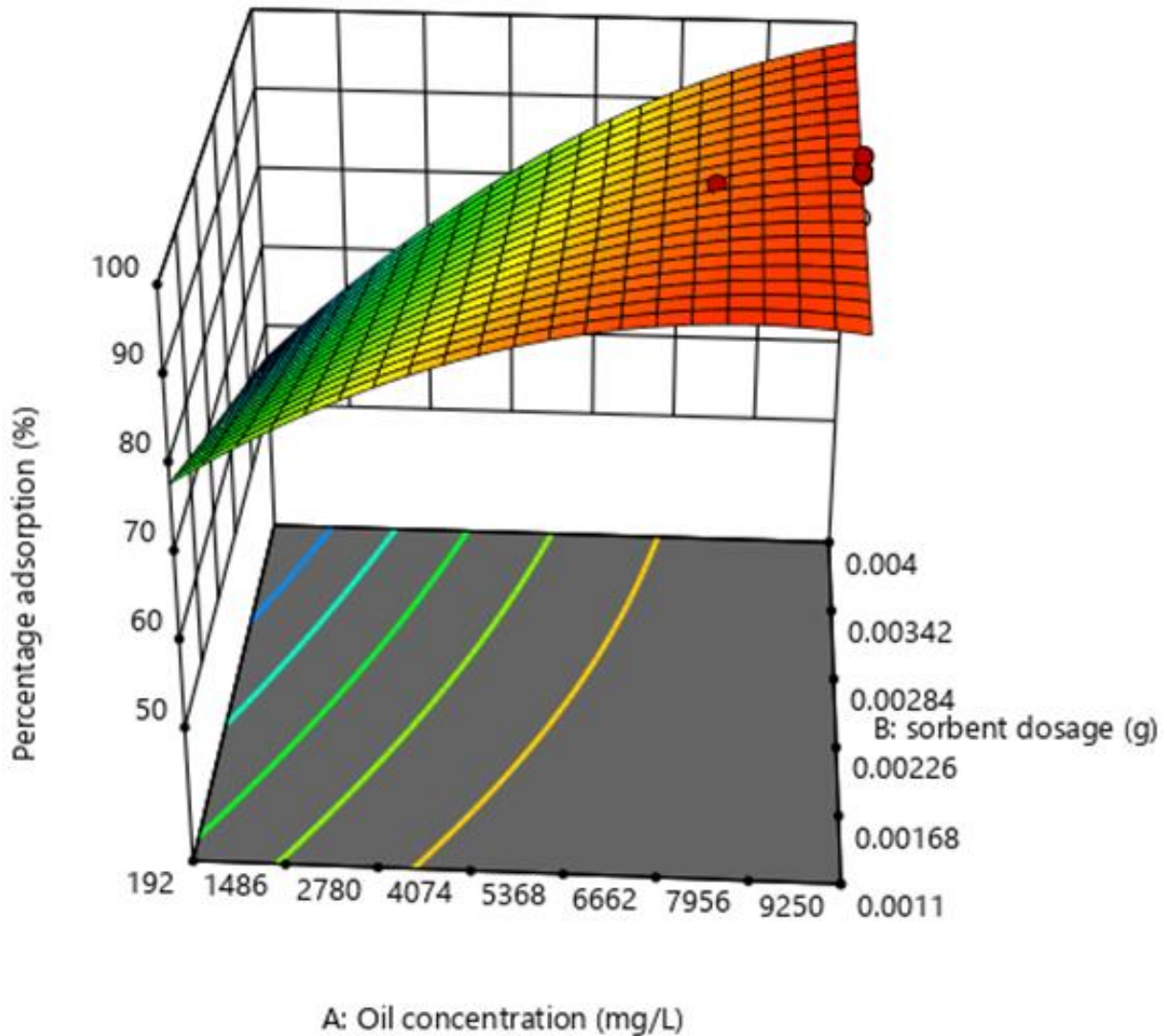


Figure 5. 7. Response surface plots for the effect of changes in oil concentration and adsorbent dosage on percentage adsorption.

5.3.5. *Effect of oil concentration and time*

As can be seen from the response surface plots in Figure 5.8, percentage oil removal increased with time, this was because there was an increased chance of positive interaction between the adsorbent and oil as the adsorbent stayed longer in contact with the solution (Hassan et al., 2019). The effect of oil concentration is as discussed in section 5.3.4.

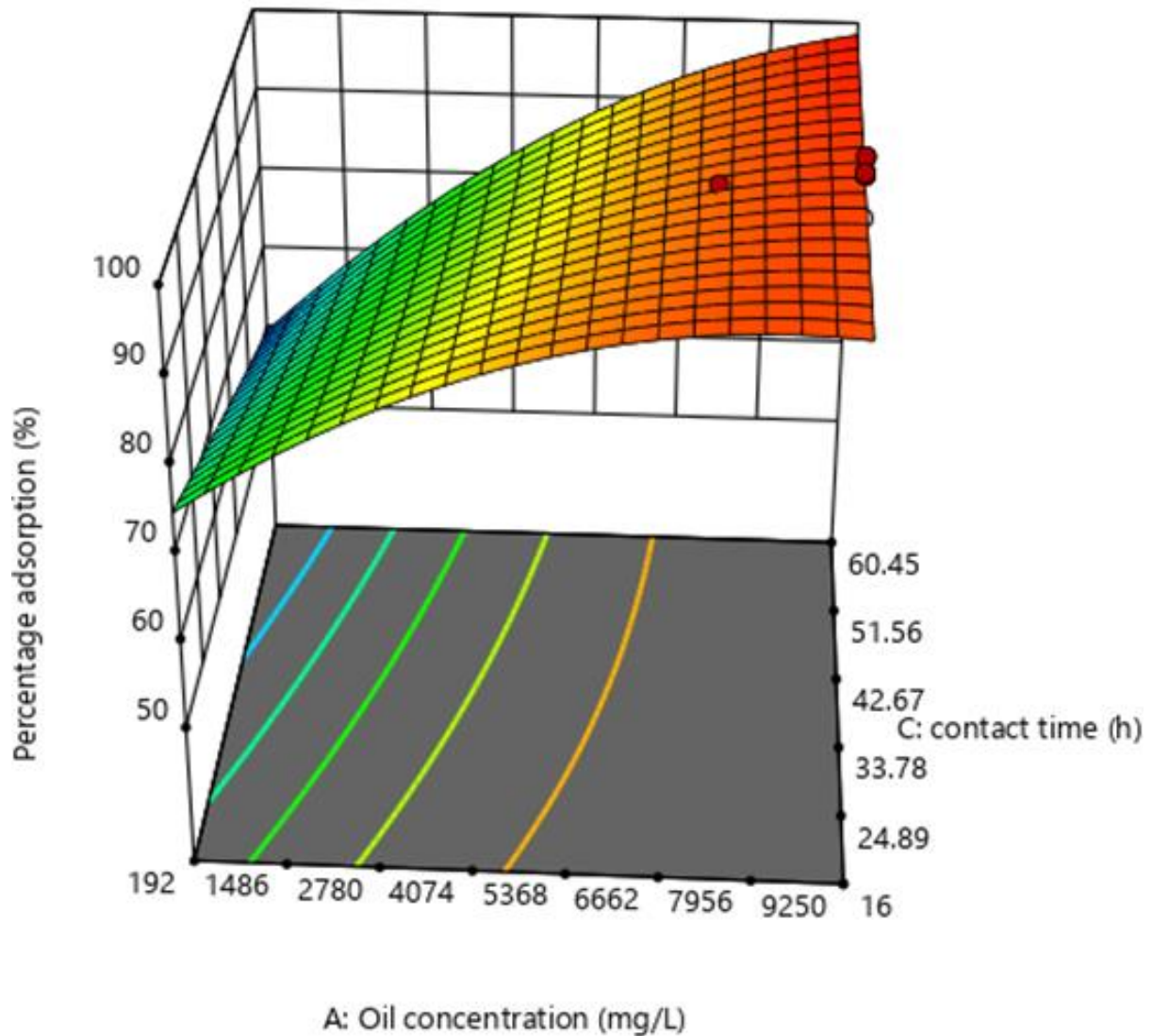


Figure 5. 8. Response surface plots for the effect of changes in initial oil concentration and contact time on percentage adsorption.

5.3.6. Effect of adsorbent dosage and time

The response surface plot for effect of adsorbent dose and time on percentage adsorption in Figure 5.9 shows an increase in percentage adsorption with time. With adsorbent dosage, percentage adsorption increased, a maximum was reached, and it decreased. As the dosage was increased, more binding sites were made available and as time was increased, there was more time for the oil molecules to interact with the binding sites. Therefore, at higher dosages, more oil was adsorbed since there are more empty binding sites (Rahdar et al., 2019).

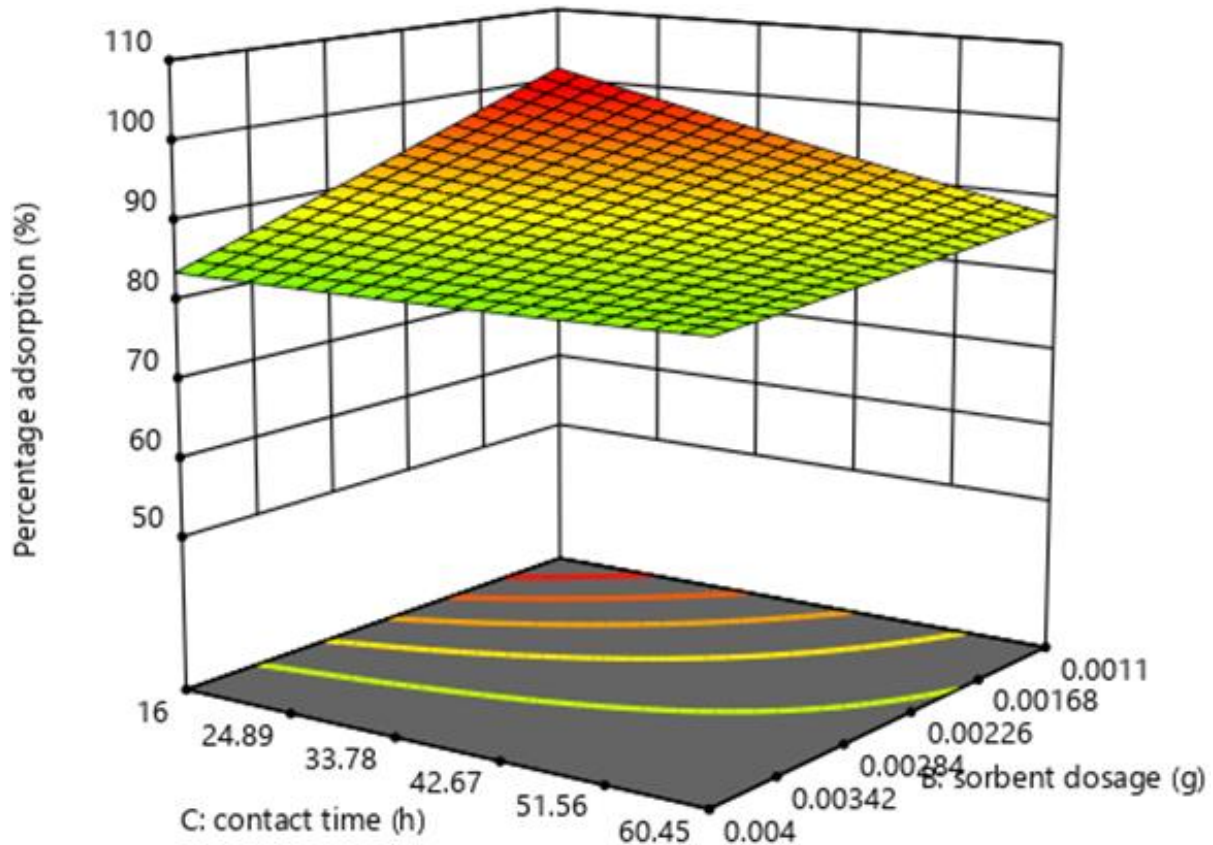


Figure 5. 9. Response surface plots for the effect of changes in contact time and adsorbent dosage on percentage adsorption.

5.4. Conclusion

Acetylated silica has been synthesized using acetic anhydride producing a material with a wrinkled, groove-like surface. Response surface optimization revealed that oil adsorption using this material depended largely on initial oil concentration, adsorbent dosage and contact time. The optimum conditions for the removal of oil from SOWW using acetylated silica were as follows: 7867 mg/L oil concentration, with adsorbent dosage of 0.001 g and a duration of 21.6 h with a desirability of 1.00. The percentage oil adsorption was found to be 99.3%, meaning that 99% of oil contained in an oily wastewater sample was adsorbed by the acetylated silica under these conditions and the adsorption capacity under these conditions was found to be 1039 mg/g. On-going studies also show that mechanical pressure applied on the adsorbent followed by oven drying at 60°C released the adsorbed oil giving the adsorbent a potential for reuse. Oil adsorption using acetylated silica was carried out without pH adjustments or stirring/ shaking making the material applicable in the treatment of field wastewater.

5.5. References

- Adebajo, M.O., Frost, R.L., Kloprogge, J.T., Carmody, O. & Kokot, S., 2003 Porous materials for oil spill cleanup: A review of synthesis and absorbing properties. *Journal of Porous materials*, 10, pp.159-170.
- Adebisi, J.A., Agunsoye, J.O., Bello, S.A., Kolawole, F.O., Ramakokovhu, M.M., Daramola, M.O. & Hassan, S.B., 2017 Extraction of silica from sugarcane bagasse, cassava periderm and maize stalk: Proximate analysis and physico-chemical properties of wastes. *Waste Biomass Valor*, pp.1-14.
- Alkindy, M.B., Naddeo, V., Banat, F. & Hasan, S.W., 2019 Synthesis of polyethersulfone (pes)/go-sio2 mixed matrix membranes for oily wastewater treatment. *Water Science and Technology*, 10.2166/wst.2019.347, pp.1-10.
- Angelova, D., Uzunov, I., Uzunova, S., Gigova, A. & Minchev, L., 2011 Kinetics of oil and oil products adsorption by carbonized rice husks. *Chemical Engineering Journal*, 172, pp.306-311.
- Annunciado, T., Sydenstricker, T. & Amico, S., 2005 Experimental investigation of various vegetable fibers as sorbent materials for oil spills. *Marine pollution bulletin*, 50, pp.1340-1346.
- Asadpour, R., Sapari, N.B., Tuan, Z.Z., Jusoh, H., Riahi, A. & Uka, O.K., 2013 Application of sorbent materials in oil spill management: A review. *Caspian Journal of Applied Sciences Research*, 2, pp.46-58.
- Asadpour, R., Sapari, N.B., Isa, M.H. & Orji, K.U., 2014 Enhancing the hydrophobicity of mangrove bark by esterification for oil adsorption. *Water Science and Technology*, 70, pp.1220-1228.
- Asadpour, R., Sapari, N.B., Isa, M.H. & Kakooei, S., 2016 Acetylation of oil palm empty fruit bunch fiber as an adsorbent for removal of crude oil. *Environmental Science and Pollution Research*, 23, pp.11740-11750.
- Asadpour, R., Sapari, N.B., Hasnain Isac, M. & Kakooei, S., 2019 Further study of adsorption of crude oils onto acetylated corn silk and its kinetics and equilibrium isotherm. *International Journal of Engineering*, 32, pp.229-235.
- Azzam, R. & Madkour, T., 2008 Molecular design, synthesis and analysis of new hydrophobic seafoams with augmented uptake capacity. *International Journal of Energy and Environment*, 2, pp.56-65.
- Bessho, M., Fukunaka, Y., Kusuda, H. & Nishiyama, T., 2009 High-grade silica refined from diatomaceous earth for solar-grade silicon production. *Energy & Fuels*, 23, pp.4160-4165.

Carlos, G., Juan, C., Wang, S., Luis, G., Mohan, R.S. & Ovadia, S., 2001 Oil-water separation in liquid-liquid hydrocyclones (llhc) -experiment and modeling.1-10.

Carmody, O., Frost, R., Xi, Y. & Kokot, S., 2007 Adsorption of hydrocarbons on organo-clays—implications for oil spill remediation. *Journal of Colloid and Interface Science*, 305, pp.17-24.

Carmona, V.B., Oliveira, R.M., Silva, W.T.L., Mattoso, L.H.C. & Marconcini, J.M., 2013 Nanosilica from rice husk: Extraction and characterization. *Industrial Crops and Products*, 43, pp.291-296.

Dong, F., Yan, M., Jin, C. & Li, S., 2017 Characterization of type-ii acetylated cellulose nanocrystals with various degree of substitution and its compatibility in pla films. *Polymers*, 9, pp.346-360.

El Boustani, M., Brouillette, F., Lebrun, G. & Belfkira, A., 2015 Solvent-free acetylation of lignocellulosic fibers at room temperature: Effect on fiber structure and surface properties. *Journal of Applied Polymer Science*, 132, pp.1-8.

Fernandes, I.J., Calheiro, D., Sánchez, F.A.L., Camacho, A.L.D., Rocha, T.L.A.d.C., Moraes, C.A.M. & Sousa, V.C.d., 2017 Characterization of silica produced from rice husk ash: Comparison of purification and processing methods. *Materials Research*, 20, pp.512-518.

Franco Ariza, C., Martínez, M., Benjumea, P., Patiño, E. & Cortés, F., 2014 Water remediation based on oil adsorption using nanosilicates functionalized with a petroleum vacuum residue. *Adsorption Science & Technology*, 32, pp.197-208.

Gilak, S., Mosavian, M. & Rohani Bastami, T., 2015 Functionalized magnetite / silica nanocomposite for oily wastewater treatment. *Advances in environmental research*, 4, pp.69-81.

Harish, P.R., Arumugam, A. & Ponnusami, V., 2015 Recovery of silica from various low cost precursors for the synthesis of silica gel. *Pharm. Lett.*, 7 pp.208-213.

Hassan, A.A., Naeem, H.T. & Hadi, R.T., 2019 A comparative study of chemical material additives on polyacrylamide to treatment of waste water in refineries. *IOP Conference Series: Materials Science and Engineering*, 518, pp.062003.

Ishak, K.E.H.K. & Ayoub, M.A., 2019 Predicting the efficiency of the oil removal from surfactant and polymer produced water by using liquid–liquid hydrocyclone: Comparison of prediction abilities between response surface methodology and adaptive neuro-fuzzy inference system. *IEEE Access*, 7, pp.179605-179619.

Izevbekhai, O.U., Gitari, W.M. & Tavengwa, N.T., 2019 *Optimization of silica extraction from diatomaceous earth using response surface methodology*. Paper presented at 20th WaterNet/WARFSA/GWPSA Symposium, Indaba Hotel, Spa & Conference Centre Fourways, Johannesburg, South Africa:1-10.

Kasiri, M.B., Modirshahla, N. & Mansouri, H., 2013 Decolorization of organic dye solution by ozonation; optimization with response surface methodology. *International Journal of Industrial Chemistry*, 4, pp.3-10.

Kosaka, P.M., Kawano, Y., Salvadori, M.C. & Petri, D.F.S., 2005 Characterization of ultrathin films of cellulose esters. *Cellulose*, 12, pp.351-359.

Liu, J. & Wang, X., 2019 A new method to prepare oil adsorbent utilizing waste paper and its application for oil spill clean-ups. *BioResources*, 14, pp.3886-3898.

Liu, Y.-H., Meng, Z.-Y., Wang, J.-Y., Dong, Y.-F. & Ma, Z.-C., 2019 Removal of siloxanes from biogas using acetylated silica gel as adsorbent. *Petroleum Science*, 16, pp.920-928.

Ning, R.Y., 2010 Reactive silica in natural waters — a review. *Desalination and Water Treatment*, 21, pp.79-86.

Noamani, S., Niroomand, S., Rastgar, M. & Sadrzadeh, M., 2019 Carbon-based polymer nanocomposite membranes for oily wastewater treatment. *npj Clean Water*, 2, pp.20.

Nwadiogbu, J.O., Okoye, P.A.C., Ajiwe, V.I. & Nnaji, N.J.N., 2014 Hydrophobic treatment of corn cob by acetylation: Kinetics and thermodynamics studies. *Journal of Environmental Chemical Engineering*, 2, pp.1699-1704.

Nwadiogbu, J.O., Ajiwe, V.I.E. & Okoye, P.A.C., 2016 Removal of crude oil from aqueous medium by sorption on hydrophobic corncobs: Equilibrium and kinetic studies. *Journal of Taibah University for Science*, 10, pp.56-63.

Nwadiogbu, J.O., Ajiwe, V.I.E. & Okoye, P.A.C., 2018 Removal of crude oil from aqueous medium by sorption on hydrophobic corncobs: Equilibrium and kinetic studies. *Journal of Taibah University for Science*, 10, pp.56-63.

Ogunfowokan, A.O., Ezenwafor, T.C. & Imoisili, P.E., 2011 *Synthesis of nanoporous silica membrane from corn cob ash (zea mays) by sol-gel method*. Paper presented at Nigerian materials congress (NIMACON 2011), Akure:1-7.

Okoronkwo, E.A., Imoisili, P.E., Olubayode, S.A. & Olusunle, S.O.O., 2016 Development of silica nanoparticle from corn cob ash. *Advances in Nanoparticles*, 05, pp.135-139.

Olawale, O., Akinmoladun, A., I, Oyawale, F.A. & Baba, A.O., 2012 Application of response surface methodology for optimisation of amorphous silica extracted from rice husk. *International journal of scientific & engineering research*, 3, pp.2229-5518.

Onwuka, J.C., Agbaji, E.B., Ajibola, V.O. & Okibe, F.G., 2016 Kinetic studies of surface modification of lignocellulosic delonix regia pods as sorbent for crude oil spill in water. *Journal of applied research and technology*, 14, pp.415-424.

Onwuka, J.C., Agbaji, E.B., Ajibola, V.O. & Okibe, F.G., 2018 Treatment of crude oil-contaminated water with chemically modified natural fiber. *Applied Water Science*, 8, pp.86-90.

Onwuka, J.C., Agbaji, E.B., Ajibola, V.O. & Okibe, F.G., 2019 Thermodynamic pathway of lignocellulosic acetylation process. *BMC Chemistry*, 13, pp.79.

Pa, F.C., Chik, A. & Bari, M.F., 2016 Palm ash as an alternative source for silica production. *MATEC Web Conf.*, 78, pp.01062.

Rafiee, E., Shahebrahimi, S., Feyzi, M. & Shaterzadeh, M., 2012 Optimization of synthesis and characterization of nanosilica produced from rice husk (a common waste material). *International Nano Letters*, 2, pp.29-33.

Rahdar, S., Taghavi, M., Khaksefidi, R. & Ahmadi, S., 2019 Adsorption of arsenic (v) from aqueous solution using modified saxaul ash: Isotherm and thermodynamic study. *Applied Water Science*, 9, pp.87-95.

Sahu, O. & Singh, N., 2019 13 - significance of bioadsorption process on textile industry wastewater. In: Shahid Ul, I. & Butola, B.S. (eds.). *The impact and prospects of green chemistry for textile technology*: Woodhead Publishing.

Sawyer, S., 2009 Analysis of variance: The fundamental concepts. *Journal of Manual & Manipulative Therapy*, 17, pp.27E-38E.

Segurolo, J., Allen, N.S., Edge, M. & Mc Mahon, A., 1999 Design of eutectic photoinitiator blends for uv/visible curable acrylated printing inks and coatings. *Progress in Organic Coatings*, 37, pp.23-37.

Shoba, B., Jeyanthi, J. & Vairam, S., 2018 Synthesis, characterization of cellulose acetate membrane and application for the treatment of oily wastewater. *Environ Technol*, 10.1080/09593330.2018.1543353, pp.1-16.

Syed, S., Alhazzaa, M. & Asif, M., 2011 Treatment of oily water using hydrophobic nanosilica. *Chemical Engineering Journal*, 167, pp.99-103.

Syuhada, N., Mohd Ghazi, R. & Ismail, N., 2017 Response surface methodology optimization of oil removal using banana peel as biosorbent. *Malaysian Journal of Analytical Sciences*, 21, pp.1101-1110.

Todkar, B.S., Deorukhkar, O.A. & Deshmukh, S.M., 2016 Extraction of silica from rice husk. *Int. J. Eng. Res. Dev.*, 12, pp.69-74.

Vocciante, M., Finocchi, A., D Auris, A.D.F., Conte, A., Tonziello, J., Pola, A. & Reverberi, A.P., 2019 Enhanced oil spill remediation by adsorption with interlinked multilayered graphene. *Materials (Basel, Switzerland)*, 12, pp.2231.



Wang, J., Zheng, Y. & Wang, A., 2012 Effect of kapok fiber treated with various solvents on oil absorbency. *Industrial Crops and Products*, 40, pp.178-184.

Zahed, M.A., Aziz, H.A., Isa, M.H., Mohajeri, L. & Mohajeri, S., 2010 Optimal conditions for bioremediation of oily seawater. *Bioresource Technology*, 101, pp.9455-9460.

Zhang, L., Lin, Y., Wu, H., Cheng, L., Sun, Y., Yasui, T., Yang, Z., Wang, S., Yoshioka, T. & Matsuyama, H., 2019 An ultrathin in situ silicification layer developed by an electrostatic attraction force strategy for ultrahigh-performance oil–water emulsion separation. *Journal of Materials Chemistry A*, 7, pp.24569-24582.

Chapter Six: Response Surface Optimization of Oil Removal Using Synthesized Polypyrrole- Silica Polymer Composite

Abstract

Oily wastewater ranks high on the environmental issues list. The severity of pollution, brought about by improper management, arising from oily wastewater increases daily with an increase in the exploration and usage of oil especially with an increase in industrialization. Conventional oil treatment methods are either expensive or time consuming, hence the need for new technologies. This study reports the synthesis of polypyrrole modified silica by the copolymerization of pyrrole and silica in the presence of ferric chloride hexahydrate for oil removal in oil impacted wastewater. A central composite model was developed in the design expert software to describe the efficiency of oil removal using the polypyrrole modified silica under the influence of initial oil concentration, adsorbent dosage and contact time. The synthesized adsorbent had FTIR bands at 3000–3500 cm^{-1} (due to the N-H), 1034 cm^{-1} (attributed to the Si-O of silica), 1607 cm^{-1} and 1615 cm^{-1} due to the stretching vibration of C=C of pyrrole ring. The adsorption capacity values predicted by the central composite model were in good agreement with the actual experimental values, indicating that the model can be used to optimize the removal of oil from oily wastewater in the presence of polypyrrole modified silica. The adsorbent showed excellent oil uptake when compared with similar materials. The optimum conditions for oil removal were 7091 mg/L oil concentration, 0.004 g adsorbent dosage and contact time of 16 h. Under these conditions, the percentage oil adsorption was 99.3% and adsorption capacity was 8451 mg/g. As a result of the low optimum dosage and the lack of agitation, the material was found to be applicable in the remediation of field wastewater

Keywords: polypyrrole; silica; synthetic oily wastewater; central composite design; adsorption.

6.1. Introduction

Generally, oils in wastewaters are classified as either dissolved or dispersed. Dissolved oils are either aromatics, acids or phenols while dispersed oils are either aromatics, acids or aliphatics. These group of compounds are stable to light and heat as a result, they do not biodegrade easily and thus have a high pollution potential (Obuekwe et al., 2009). They are released into the environment during mining and transportation thereby earning a top spot on the environmental issues list (Xue et al., 2011; Kwon et al., 2012; Hu et al., 2014; Yang et al., 2014; Wang et al.,

2015). Methods that have been previously used in the removal of organic pollutants from water and in the treatment of oily wastewater are coagulation, filtration with coagulation, precipitation, ozonation, adsorption, ion exchange, reverse osmosis, biological methods and advanced oxidation processes. These methods, with the exception of adsorption, are expensive to run, cannot be used without proper training, and in the case of biological methods, takes up too much time (Rashed, 2013).

Adsorption has proven to be one of the best methods in the remediation of oily wastewater especially when the right adsorbent is employed (Wang et al., 2014). An ideal adsorbent should have high adsorption capacity, high lipophilicity and low hydrophobicity, should be recyclable and should be environmentally friendly (Dong et al., 2012).

It has been challenging to fabricate the ideal adsorbent for oil removal so far (Khosravi and Azizian, 2015). Several natural adsorbents have been used for oil sorption. These include rice husk ash (Angelova et al., 2011), carbonized peat bagasse (Asadpour et al., 2013), saw dust (Ismail, 2015) vegetable fibres (Annunciado et al., 2005) and sugarcane bagasse (Samsuir et al., 2016). One drawback of using natural adsorbents is that they are in short supply in some regions. Chemically modified natural adsorbents have also been used with some degree of success. For example, acetylated corncobs have been used in the remediation of oily water with a sorption capacity of 2500 mg/g (Nwadiogbu et al., 2018). Oleic acid modified sawdust has also been used and were found to have relatively high sorption capacity. Inorganic materials have been applied to adsorb oil and these materials include fly ash, activated carbon, zeolite and vermiculite (Korhonen et al., 2011; Sun et al., 2013; Xue et al., 2013; Gao et al., 2014; Xue et al., 2014; Ma et al., 2018). One drawback of the use of these materials, however, is the low adsorption ability. Other materials like carbon nanotubes, filter papers, metal meshes, superhydrophilic and underwater superoleophobic metal meshes, and diesel exhaust emission soot coated polyurethane foams have been applied in remediation of oily waters but these too have limitations like high cost and complex fabrication (Lee and Baik, 2010; Yu et al., 2018; Singh et al., 2019). Synthetic adsorbents, like poly dimethyl siloxane coated polyurethane (PU) sponge, perfluorooctyltriethoxysilane – polypyrrole sponge, and polypyrrole – palmitic acid polyurethane sponge have also been used with adsorption capacities reportedly higher than those of inorganic and natural adsorbents (Khosravi and Azizian, 2015).

Composites that have been used in oil sorption include polyurethane hybrid composite (Góes et al., 2020), nano porous carbon – silica composite (Fu et al., 2020) and natural

rubber/reduced-graphene oxide composite materials (Songsaeng et al., 2019) with adsorption capacities of 12.2 g/g, 0.4 g/g and 21 g/g respectively.

Silica precursor, diatomaceous earth, has been used in the raw and calcined form to adsorb different groups of oil like benzene, toluene, ethylbenzenes, p-xylenes and o-xylenes with adsorption capacities of 0.05 - 0.8 mg/g (Bandura et al., 2017).

One common denominator of the adsorbents that have been used in oil sorption studies is the fact that they have low adsorption capacities and that it takes a long time to remove oil. Given the relatively low adsorption capacities, and the problems associated with the use of some of these sorbents, it is important to find relatively cheap and reusable adsorbents. Also, most studies focus on the ability of adsorbents to take up oil but do not look at the quality of water after adsorption. This study reports, for the first time, the modification of silica extracted from the abundant diatomaceous earth with polypyrrole which introduces a π electron system suitable for adsorption and its application in the remediation of synthetic oily wastewater.

6.2. Materials and Methods

6.2.1 Materials

Silica aerogel previously extracted from diatomaceous earth was used after drying to constant weight (Izevbekhai et al., 2019), pyrrole, sodium dodecylsulphate, Iron (III) Chloride were of analytical grade and obtained from Sigma – Aldrich (St Louis, USA). Vacuum pump oil was obtained from Telstar technologies (Barcelona, Spain). Milli-Q water from Millipore S.A.S (Molsheim, France) ($18.2 \mu\text{S}/\text{cm}$ at 25°C) was also used in all dilutions. Tea bags were obtained from retail outlets in Thohoyandou, South Africa. Telstar Lyoquest-55 freeze dryer (Shanghai, China) was used to freeze dry all samples and spectroquant UV spectrophotometer from Merk Group (Germiston, South Africa) was used for total organic carbon testing and Stuart reciprocating shaker (Staffordshire, UK) was used for shaking. Ultrasonic processor (UP 4005) Hielscher ultrasound technology, with amplitude of 20 to 100% and cycle of 0.1 – 1 (Berlin, Germany) was used in wastewater preparation and ALPHA FT-IR spectrophotometer from Bruker Pty (Sandton, South Africa) was used in functional group analysis.

6.2.2. Preparation of polypyrrole modified silica

The polypyrrole modified silica was prepared by modifying the method used by Zhao et al. (2016). Typically, two solutions were prepared. Solution A was prepared by adding 0.3 g silica to 0.7 mL pyrrole and solution B was prepared by adding 2.7 g of ferric chloride hexahydrate to 23 mL of deionized water while stirring. Solution B was added dropwise to solution A with

stirring at room temperature. Stirring was continued for 24 h after which, the solution was filtered, the solute was washed with deionized water and dried in an oven at 60°C for 12 h.

6.2.3. Characterization of synthesized silica composite

The chemical composition of pyrrole, silica and polypyrrole functionalized silica were determined using an ALPHA FT-IR spectrophotometer. The morphology of the composite (size and shape at the surface) was investigated by sprinkling a small amount of the sample onto a scanning electron microscope (SEM) stub covered with carbon glue. The stubs were then coated with carbon in an evaporation coater. The SEM is a NanoSEM 230 (FEI Nova, Czechoslovakia Republic) with a field emission gun (FEG). The elemental analysis was carried out using an X-Max detector (Oxford, Abingdon, UK) equipped with Inca software, at 20 kV.

6.2.4. Preparation of synthetic oily wastewater

Synthetic oily wastewater (SOWW) was prepared using the method described by Shoba et al. (2018). Vacuum pump oil was mixed with sodium dodecyl sulphate (90:1, v/w) in 1 litre of water, sonicated for 5 min at an amplitude of 75% and cycle of 0.5 to obtain a homogenous solution. This was used in the optimization experiments.

6.2.5. Response surface optimization of oil removal

The procedure for optimization was carried out using the central composite design of the design expert software by placing variable amount of the prepared adsorbent in an empty tea bag whose content had been emptied out prior to the experiments (Figure 6.1b). To account for the effect of the tea bags and sealing of the tea bags, empty tea bags were also sealed and used in similar experiments (Figure 6.1a). The tea bags were then placed in the SOWW (prepared in section 6.2.4 and was allowed to stand ‘undisturbed’ for some time. After this, the solution was filtered, and the total organic carbon was measured for the initial SOWW and adsorbent treated SOWW and silica treated SOWW using a spectroquant UV spectrophotometer. The equilibrium adsorption was calculated using equation (6.1) and percentage removal using equation (6.2).



Figure 6. 1. (a) sealed empty tea bag (b) sealed tea bag containing adsorbents.

$$Q_e = \left(\frac{C_i - C_f}{m} \right) V \quad (6.1)$$

$$\% \text{ Removal} = \left(\frac{C_i - C_f}{C_i} \right) 100 \quad (6.2)$$

where C_i and C_f are the oil concentrations (mg/L) before and after treatment with adsorbent respectively; V (L) is the volume of the solution, m (g) is the mass of the adsorbent and Q_e is the equilibrium *adsorption* capacity per milligram dry weight of the adsorbent.

6.2.6. Experimental design

Experiments for optimization of oil removal were done by varying the weight of the adsorbent, oil concentration and contact time using the central composite design in the response surface methodology (RSM) software, using the procedure outlined in section 4.5. The range of optimized parameters are listed in Table 6.1.

Table 6. 1. Range of optimized parameters.

Parameter	Minimum	Maximum
Oil concentration (mg/L)	192	9250
sorbent dosage (g)	0.0011	0.004
contact time (h)	16	60.45

6.3. Results

6.3.1. Characterization of polypyrrole - silica composite

The polypyrrole-silica composite was scanned in the range between 4000 and 500 cm^{-1} so as to ascertain the success of the composite preparation. The FTIR spectrum of the synthesized polypyrrole-silica composite (Figure 6.2), shows a broadband at about 3000–3500 cm^{-1} due to the N-H stretching vibration of pyrrole in the polymer. This band is broader than what is found in pyrrole which shows a sharp band at 3390 cm^{-1} . This is probably as a result of intermolecular hydrogen bonding. This is consistent with findings by Zhao et al. (2016) and Yussuf et al. (2018) who studied the synthesis of polypyrrole. The double peak at 1607 cm^{-1} and 1615 cm^{-1} can be said to be due to the stretching vibration of C=C of pyrrole ring. This band shifted from 1530 cm^{-1} in pyrrole to these positions in polypyrrole possibly as a result of increased conjugation. The transmission band due to C-N shifted from 1417 cm^{-1} in pyrrole to 1407 cm^{-1} in polypyrrole probably as a result of increased conjugation and intermolecular hydrogen

bonding. The transmission band at about 1034 cm^{-1} (dwarfed by the other peaks) is attributed to the Si-O of silica which corresponds to the peak found in the spectra for silica.

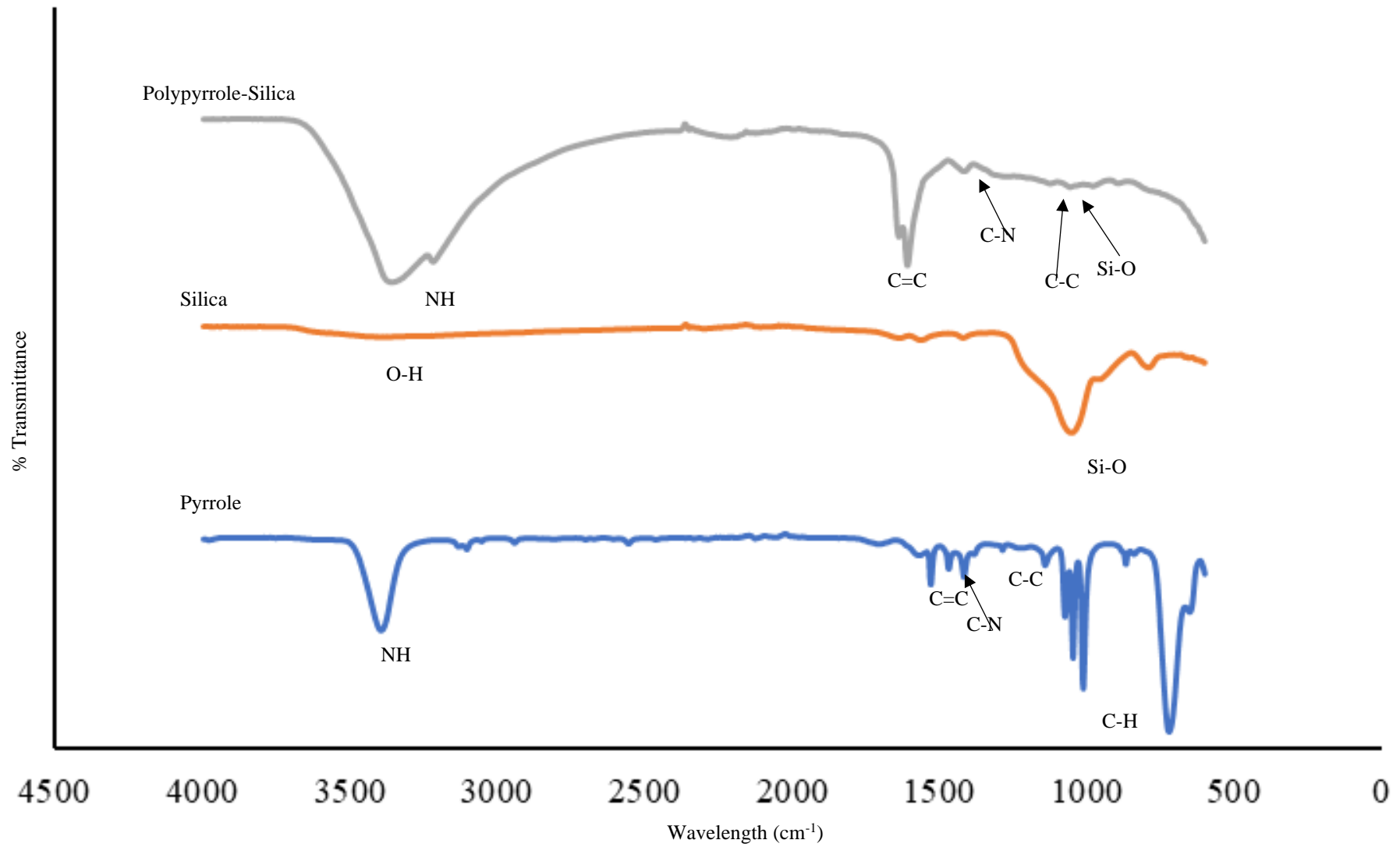


Figure 6. 2. FTIR plots of pyrrole, silica and polypyrrole-silica composite.

Figure 6.3 shows the SEM image of the unmodified silica and the as prepared polypyrrole -Si complex (a) and (c). The unmodified silica (a) was seen to have razor-like crystals with well defined external pores. This appearance changed to a one-dimensional morphology intertwined together in the polypyrrole modified silica (c). The rough surface suggests that the material will be a good adsorbent. The EDX of the unmodified silica (b) showed silica and oxygen as the major elements while the polypyrrole-silica composite (d) showed the presence of silica and elements like nitrogen and oxygen which make up the pyrrole ring indicating successful functionalization. This is consistent with findings by Zhao et al. (2016).

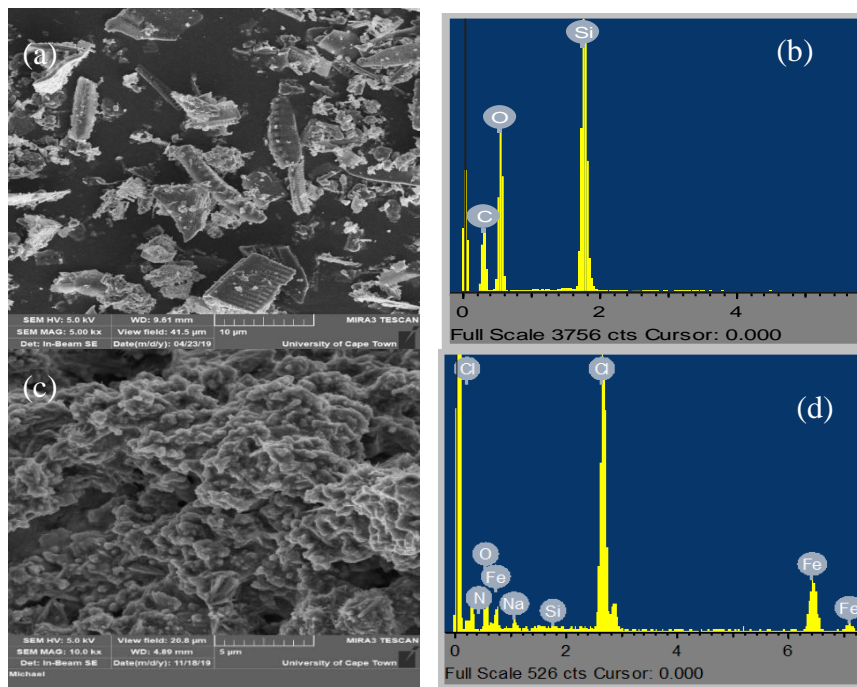


Figure 6.3. (a), (c) SEM of unmodified and polypyrrole-silica composite respectively and (b), (d) the corresponding EDX.

6.3.2. Optimization of oil removal

6.3.2.1. RSM Experiments and model fitting

Modelling of percentage removal of oil from SOWW was done using the quadratic model of the central composite design of the RSM software employing three reaction parameters, namely initial oil concentration (mg/L), adsorbent dosage (g) and contact time (h). The actual percentage removal as calculated using Equation 6.2 are presented in Table 6.2 and some pictures of the optimization experiments are shown in Figure 6.4.

Table 6. 2. RSM Design and the actual values of responses.

Run	Initial oil concentration (mg/L)	Sorbent dosage(g)	Contact time (h)	Final oil concentration (mg/L)	Experimental Percentage adsorption
1	6650	0.004	16.0	131	98.0
2	9250	0.003	38.2	226	97.6
3	704	0.001	60.5	144	79.5
4	9250	0.003	0.85	138	98.5
5	704	0.004	60.5	166	76.4
6	9250	0.003	38.2	220	97.6
7	704	0.004	16.0	218	69.0
8	6650	0.001	60.5	156	97.6
9	192	0.003	38.2	194	-1.04
10	9250	0.003	38.2	228	97.5
11	704	0.001	16.0	313	55.5
12	9250	0.005	38.2	245	97.3
13	7250	0.003	38.2	48	99.3
14	6650	0.001	16.0	262	96.0
15	6650	0.004	60.5	212	96.8
16	9250	0.0001	38.2	467	95.0
17	9250	0.003	38.2	222	97.6
18	9250	0.003	38.2	218	97.6
19	9250	0.003	75.6	142	98.5
20	9250	0.003	38.2	220	97.6

From the pictures in Figure 6.4, the colour of the adsorbent treated water had an inverse relationship with the percentage oil adsorption. The more intense the colour, the lower the percentage removal and vice versa. The trends observed in the table are as described in the response surface plots in section 6.3.2.



Figure 6. 4. Pictures of adsorbent treated synthetic oily wastewater (Experimental conditions are as presented in columns 1 to 3 of Table 6.3).

The model predictions for percentage removal of oil from SOWW and total organic carbon of the adsorbent treated SOWW were compared with the values obtained from experiments and plotted in Figure 6.5 (a) and (b) to obtain a coefficient of determination R^2 of 0.98 and 0.87 for percentage removal and TOC respectively indicating that predicted and actual values were in good agreement and that the quadratic polynomial model chosen was sufficient to explain the relationship between the responses and significant variables (Olawale et al., 2012; Adebisi et al., 2017; Syuhada et al., 2017).

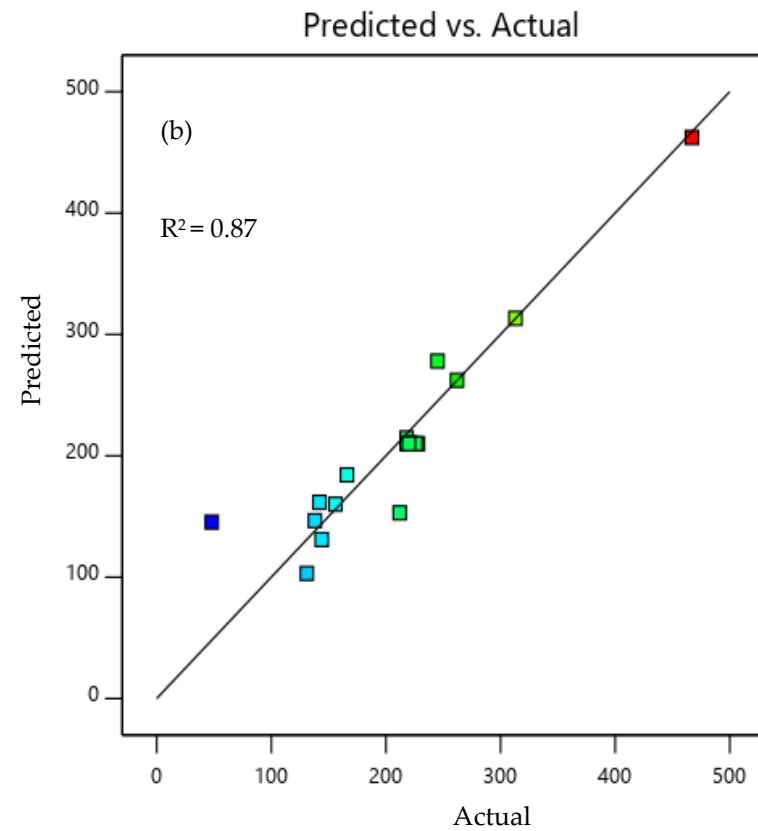
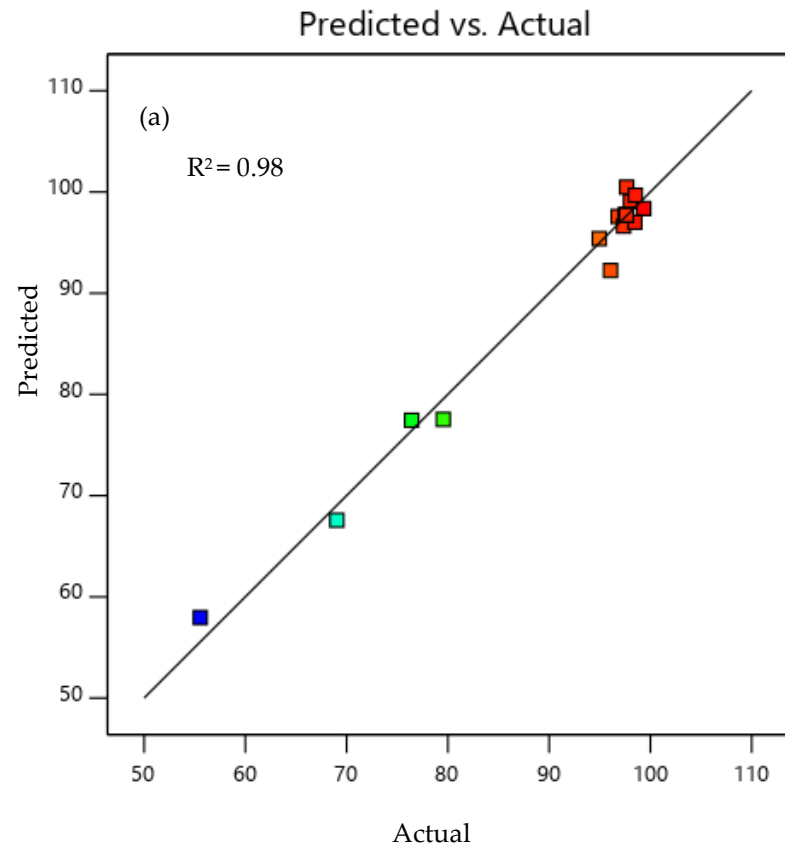


Figure 6. 5. Comparison between values predicted by response surface methodology (RSM) model and experimentally determined values for (a) percentage adsorption and (b) TOC.

6.3.2.2. Regression Model and Analysis of Variance (ANOVA)

In order to test the significance of the model and the model terms, analysis of variance (ANOVA) was done (Table 6.3). It was observed that the quadratic polynomial model used to represent both TOC and percentage adsorption were significant (at p – value less than 0.05 and high F – value). Model terms like initial oil concentration, adsorbent dosage, interaction between adsorbent dosage and contact time and the quadratic function of oil concentration and contact time had an effect on the total organic carbon while changes in initial oil concentration, adsorbent dosage, contact time, the interaction between these and their quadratic function had an effect on the percentage oil removed.

Table 6. 3. ANOVA for applied model and model terms.

Source	TOC		% Removal	
	F-value	p-value	F-value	p-value
Model	6.90	0.0041	63.15	< 0.0001
A-Oil concentration	0.3955	0.5450	457.32	< 0.0001
B-sorbent dosage	6.53	0.0309	5.29	0.0470
C-contact time	4.40	0.0653	32.00	0.0003
AB	2.40	0.1558	2.04	0.1874
AC	4.23	0.0698	33.54	0.0003
BC	6.17	0.0347	10.00	0.0115
A ²	8.07	0.0194	49.96	< 0.0001
B ²	22.38	0.0011	1.01	0.3410
C ²	2.72	0.1335	0.1358	0.7210

6.3.2.3. Effect of oil concentration and sorbent dosage

Figure 6.6 shows the response surface plot for oil concentration and sorbent dosage and their interaction on the TOC of the adsorbent treated SOWW and percentage removal of oil by the polypyrrole- silica composite. As observed, percentage oil removal increased steadily up to 99%, which was the maximum with an increase in initial oil concentration and then decreased

to 55% with a further increase in initial oil concentration. When initial oil concentration is increased, the oil droplets increased and passed into the pores of the adsorbent easily, hence the initial increase in percentage adsorption (Gomez et al., 2002; Ishak and Ayoub, 2019; Sahu and Singh, 2019). Also, as adsorbent dosage was increased, percentage adsorption increased slightly. This was likely as a result of the introduction of new binding sites on the adsorbents. Generally, as initial oil concentration increases, the net ability of adsorbents to remove oil decreases because the binding sites on the adsorbents eventually becomes saturated and the total organic carbon decreases (Hassan et al., 2019). This could also be as a result of a decrease in the surface area of the adsorbent brought about by an increase in the amount of oil adsorbed per unit weight of adsorbent (Hassan et al., 2019; Rahdar et al., 2019) but as the adsorbent dose is increased, more active sites are introduced leading to a decrease in TOC.

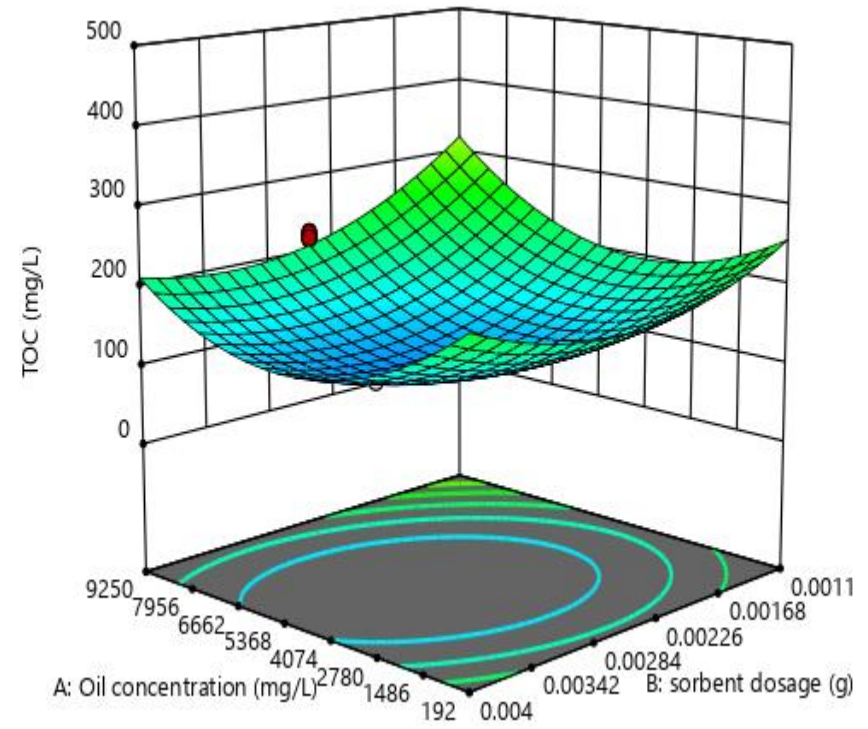
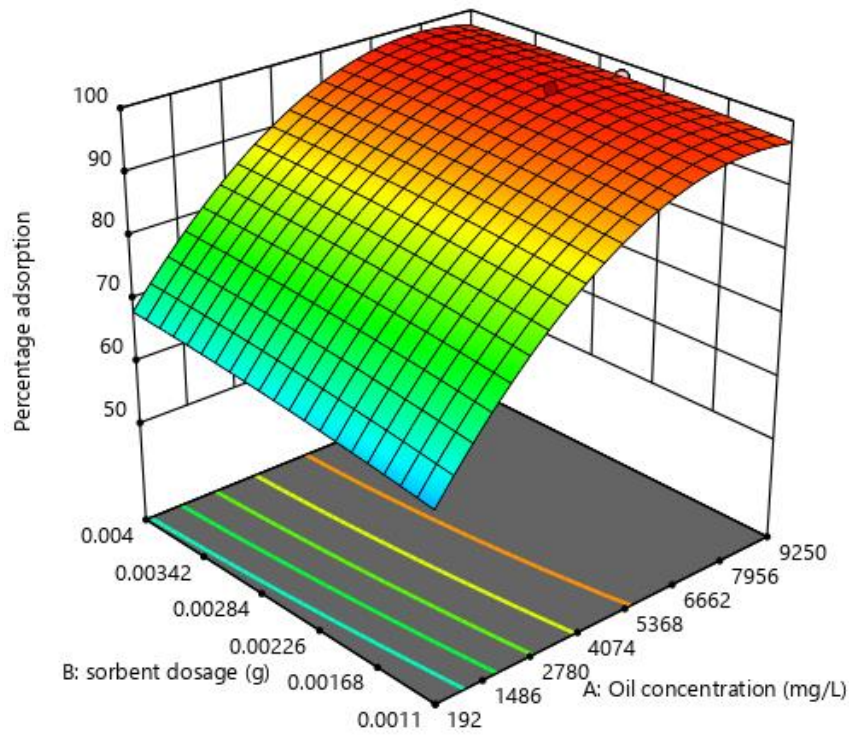


Figure 6. 6. Response surface plots for ‘effect of oil concentration and adsorbent dose.

6.3.2.4. Effect of oil concentration and time

As can be seen from the response surface plots in Figure 6.7, percentage oil removal increased with time, this is because there is an increased chance of positive interaction between the adsorbent and oil as the adsorbent stayed longer in contact with the solution. The opposite is true of TOC (Hassan et al., 2019).

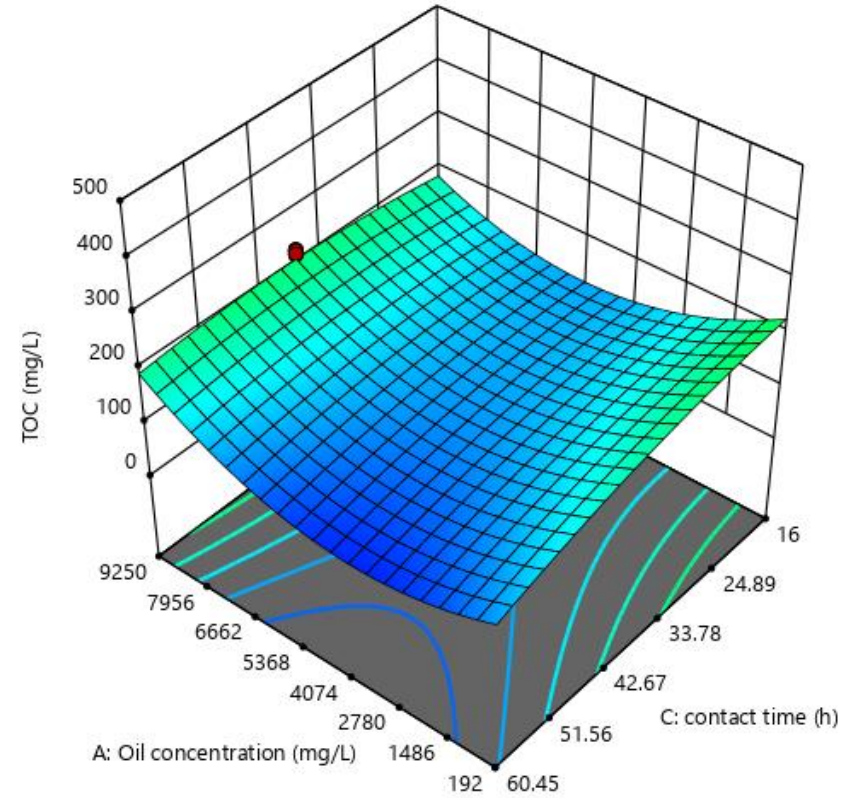
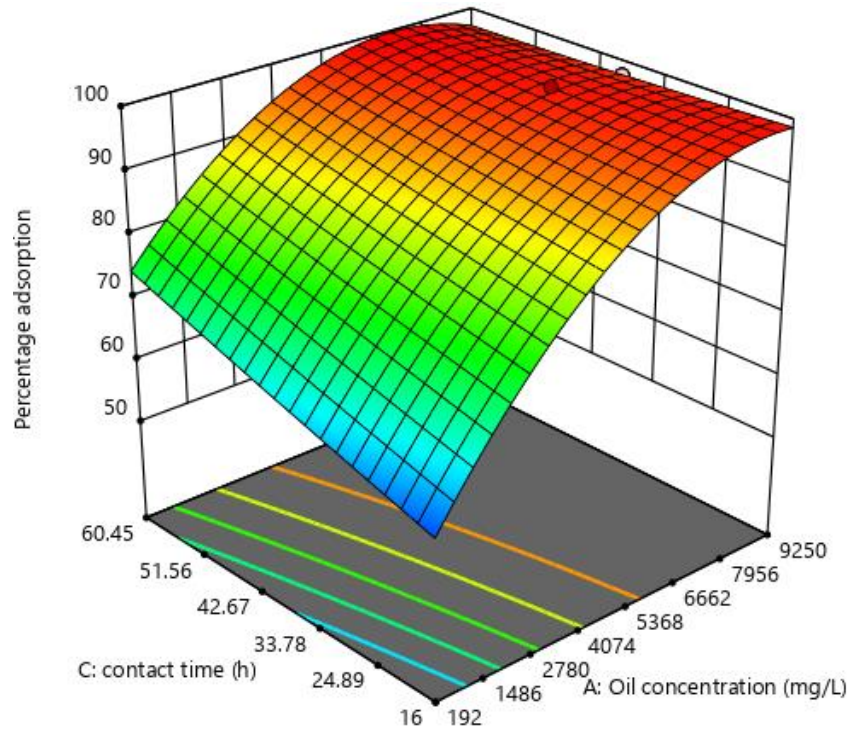


Figure 6. 7. Response surface plots for effect of oil concentration and time.

6.3.2.5. Effect of adsorbent dosage and time

Figure 6.8 illustrates the response surface plot for adsorbent dose and time and the interaction on TOC and percentage oil removal. Percentage adsorption was found to increase with both time and adsorbent dosage. The opposite was true of TOC but with adsorbent dosage, a minimum was reached, and percentage adsorption increased. As the dosage was increased, more binding sites are made available and as time was increased, there was more time for the oil molecules to interact with the binding sites. Therefore, at higher dosages, more oil is adsorbed since there are more empty binding sites leading to lower TOC values (Rahdar et al., 2019).

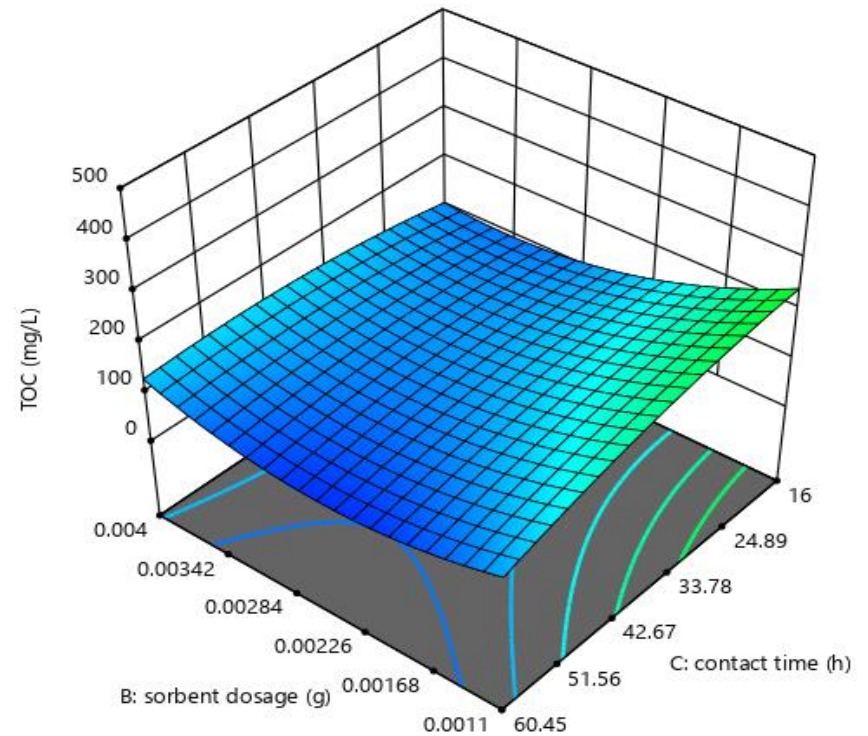
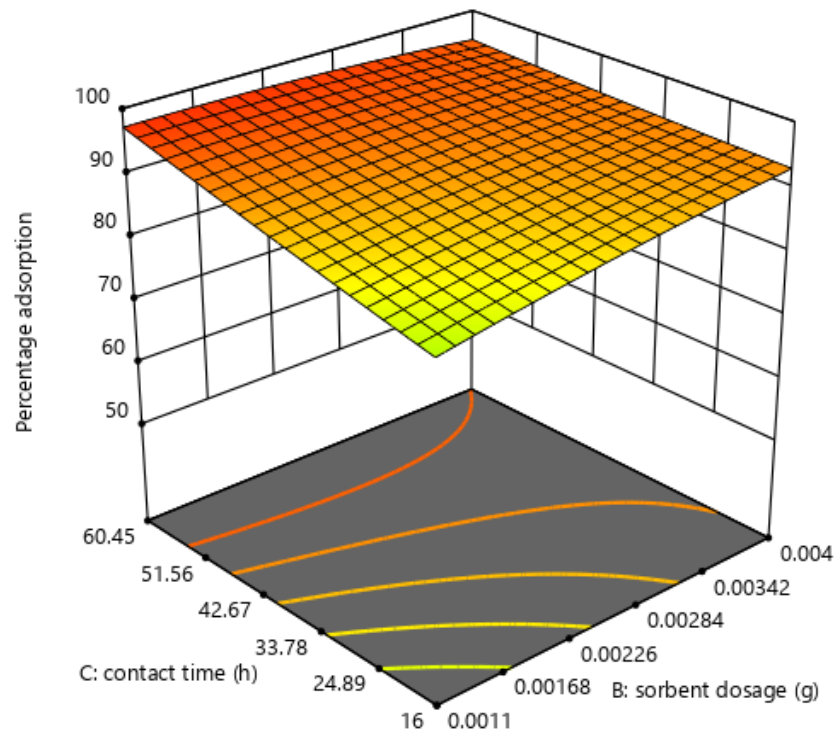


Figure 6. 8. Response surface plots for effect of contact time and adsorbent dosage.

6.3.3. Comparison to other adsorbents

Table 6.4 compares the adsorption capacity of the polypyrrole silica complex synthesized in this study with other reported adsorbents. It is noted that the adsorption capacity of the synthesized polypyrrole adsorbent is higher than most similar adsorbents but lower than the polypyrrole coated cigarette filters. However, it is common knowledge that the adsorption capacity is dependent on the type and concentration of adsorbent used. Zhang et al. (2020) used 2 mol/L pyrrole while 0.004 mol/L was used in this study. Also, all the literature studies reported here and almost all studies available in literature were only concerned about how much oil the adsorbents were able to take up (Filipovic et al., 2010; Zhao et al., 2016; Ma et al., 2018; Nwadiogbu et al., 2018; Shoba et al., 2018; Ishak and Ayoub, 2019; Zhang et al., 2020;), but this study looked mostly at the quality of the adsorbent treated water. Considering this, polypyrrole silica composite is a promising adsorbent for oily wastewater treatment.

Table 6. 4. Comparison of adsorption capacity for different adsorbents.

Adsorbent	Type of oil studied	Sorption capacity (mg/g)	Reference
Acetylated corncobs	Oily water	2500	Nwadiogbu et al. (2018)
Silica aerogels	Oil adsorption	3500	Filipovic et al. (2010)
Polypyrrole coated cigarette filters	Engine oil	13600	Zhang et al. (2020)
Polypyrrole – Si complex	SOWW	8451	This study

6.3.4. Effect of empty tea bags

The effect of empty tea bags was studied by placing sealed tea bags of similar shape and size in SOWW of same concentrations as used in Table 1. It was observed visually, as seen in Figure 6.9, that oil removal with sealed tea bags alone was not very effective and that the contribution of the sealed tea bags alone was negligible. The adsorbent treated SOWW in Figure 6.9a is clear as a

result of the action of the adsorbents on the oil in the water while the Figure 6.9b is ‘milky’ because the functional groups necessary for effective oil sorption are absent on the empty tea bags.

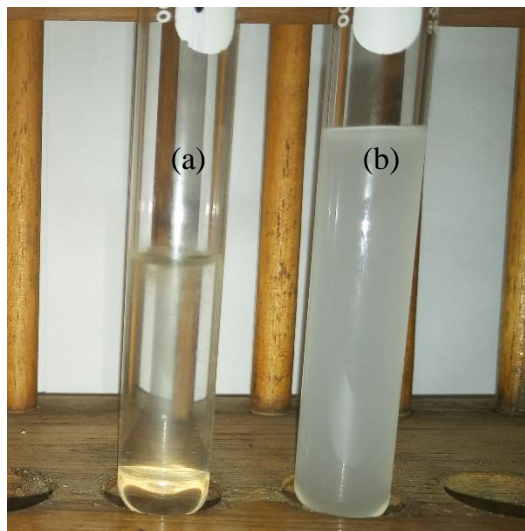


Figure 6. 9. (a) Adsorbent treated SOWW (b) Empty tea bag treated SOWW (Initial oil concentration – 6650mg/L; duration – 16 h.

6.4. Conclusions

Polypyrrole modified silica has been designed by the co-polymerization of pyrrole and silica in the presence of ferric chloride hexahydrate. The response surface model used revealed that initial oil concentration, adsorbent dosage and contact time, their interaction and the quadratic function of initial oil concentration determined the uptake of oil. The optimum conditions for the removal of oil from SOWW were 7091 mg/L oil concentration, 0.004 g adsorbent dosage and contact time of 16 h with a desirability of 0.95. The percentage oil adsorption was found to be 99.3% and the adsorption capacity under these conditions was found to be 8451 mg/g. Experiments were done without any form of agitation, and the adsorption capacity of the adsorbent in the removal of oil from SOWW was comparable to other adsorbents reported in literature. Given this, the synthesized adsorbent would be applicable in field wastewater.

6.5. References

Adebisi, J.A., Agunsoye, J.O., Bello, S.A., Kolawole, F.O., Ramakokovhu, M.M., Daramola, M.O. & Hassan, S.B., 2017 Extraction of silica from sugarcane bagasse, cassava periderm and maize stalk: Proximate analysis and physico-chemical properties of wastes. *Waste Biomass Valor*, pp.1-14.

Angelova, D., Uzunov, I., Uzunova, S., Gigova, A. & Minchev, L., 2011 Kinetics of oil and oil products adsorption by carbonized rice husks. *Chemical Engineering Journal*, 172, pp.306-311.

Annunciado, T., Sydenstricker, T. & Amico, S., 2005 Experimental investigation of various vegetable fibers as sorbent materials for oil spills. *Marine pollution bulletin*, 50, pp.1340-1346.

Asadpour, R., Sapari, N.B., Tuan, Z.Z., Jusoh, H., Riahi, A. & Uka, O.K., 2013 Application of sorbent materials in oil spill management: A review. *Caspian Journal of Applied Sciences Research*, 2, pp.46-58.

Bandura, L., Wozuk, A., Kołodyńska, D. & Franus, W., 2017 Application of mineral sorbents for removal of petroleum substances: A review. *Minerals*, 7.

Dong, X., Chen, J., Ma, Y., Wang, J., Chan-Park, M.B., Liu, X., Wang, L., Huang, W. & Chen, P., 2012 Superhydrophobic and superoleophilic hybrid foam of graphene and carbon nanotube for selective removal of oils or organic solvents from the surface of water. *Chem. Commun.*, 48, pp.10660.

Filipovic, R., Lazić, D., Perusic, M. & Stijepović, I., 2010 Oil absorption in mesoporous silica particles. *Processing and Application of Ceramics*, 4.

Fu, L., Zhu, J., Huang, W., Fang, J., Sun, X., Wang, X. & Liao, K., 2020 Preparation of nanoporous carbon-silica composites and its adsorption capacity to volatile organic compounds. *Processes*, 8, pp.372.

Gao, Y., Zhou, Y.S., Xiong, W., Wang, M., Fan, L., Rabiee-Golgir, H., Jiang, L., Hou, W., Huang, X., Jiang, L., Silvain, J.-F. & Lu, Y.F., 2014 Highly efficient and recyclable carbon soot sponge for oil cleanup. *ACS Applied Materials & Interfaces*, 6, pp.5924-5929.

Góes, M.M., Garcia, J.C., Rosa, S.L.F., Maurício, M.R. & Carvalho, G.M.d., 2020 New magnetic polyurethane hybrid composite for oil sorption. *Plastics, Rubber and Composites*, 49, pp.10-17.

Gomez, C., Caldentey, J., Wang, S., Gomez, L., Mohan, R. & Shoham, O., 2002 Oil/water separation in liquid/liquid hydrocyclones (llhc): Part 1 - experimental investigation. *SPE Journal*, 7, pp.353-372.

Hassan, A.A., Naeem, H.T. & Hadi, R.T., 2019 A comparative study of chemical material additives on polyacrylamide to treatment of waste water in refineries. *IOP Conference Series: Materials Science and Engineering*, 518, pp.062003.

Hu, H., Zhao, Z., Gogotsi, Y. & Qiu, J., 2014 Compressible carbon nanotube–graphene hybrid aerogels with superhydrophobicity and superoleophilicity for oil sorption. *Environ. Sci. Technol. Lett.*, 1, pp.214.

Ishak, K.E.H.K. & Ayoub, M.A., 2019 Predicting the efficiency of the oil removal from surfactant and polymer produced water by using liquid–liquid hydrocyclone: Comparison of prediction abilities between response surface methodology and adaptive neuro-fuzzy inference system. *IEEE Access*, 7, pp.179605-179619.

Ismail, A.S., 2015 Preparation and evaluation of fatty-sawdust as a natural biopolymer for oil spill sorption. *Chemistry Journal*, 5, pp.80-85.

Izevbekhai, O.U., Gitari, W.M. & Tavengwa, N.T., 2019 *Optimization of silica extraction from diatomaceous earth using response surface methodology*. Paper presented at 20th WaterNet/WARFSA/GWPSA Symposium, Indaba Hotel, Spa & Conference Centre Fourways, Johannesburg, South Africa:1-10.

Khosravi, M. & Azizian, S., 2015 Synthesis of a novel highly oleophilic and highly hydrophobic sponge for rapid oil spill cleanup. *ACS Applied Materials & Interfaces*, 7, pp.25326-25333.

Korhonen, J.T., Kettunen, M., Ras, R.H.A. & Ikkala, O., 2011 Hydrophobic nanocellulose aerogels as floating, sustainable, reusable, and recyclable oil absorbents. *ACS Applied Materials & Interfaces*, 3, pp.1813-1816.

Kwon, G., Kota, A.K., Li, Y., Sohani, A., Mabry, J.M. & Tuteja, A., 2012 On-demand separation of oil-water mixtures. *Adv. Mater.*, 24, pp.3666.

Lee, C. & Baik, S., 2010 Vertically-aligned carbon nano-tube membrane filters with superhydrophobicity and superoleophilicity. *Carbon*, 48, pp.2192-2197.

Ma, Q., Li, G., Liu, X., Wang, Z., Song, Z. & Wang, H., 2018 Zeolitic imidazolate framework-8 film coated stainless steel meshes for highly efficient oil/water separation. *Chem Commun (Camb)*, 54, pp.5530-5533.

Nwadiogbu, J.O., Ajiwe, V.I.E. & Okoye, P.A.C., 2018 Removal of crude oil from aqueous medium by sorption on hydrophobic corncobs: Equilibrium and kinetic studies. *Journal of Taibah University for Science*, 10, pp.56-63.

Obuekwe, C.O., Al-Jadi, Z.K. & Al-Saleh, E.S., 2009 Hydrocarbon degradation in relation to cell-surface hydrophobicity among bacterial hydrocarbon degraders from petroleum-contaminated kuwait desert environment. *International Biodeterioration & Biodegradation*, 63, pp.273-279.

Olawale, O., Akinmoladun, A., I, Oyawale, F.A. & Baba, A.O., 2012 Application of response surface methodology for optimisation of amorphous silica extracted from rice husk. *International journal of scientific & engineering research*, 3, pp.2229-5518.

Rahdar, S., Taghavi, M., Khaksefidi, R. & Ahmadi, S., 2019 Adsorption of arsenic (v) from aqueous solution using modified saxaul ash: Isotherm and thermodynamic study. *Applied Water Science*, 9, pp.87-95.

Rashed, M.N., 2013 Adsorption technique for the removal of organic pollutants from water and wastewater. In: Rashed, M.N. (ed.). *Organic pollutants-monitoring, risk and treatment*. Rijeka, Croatia: InTech Publisher.

Sahu, O. & Singh, N., 2019 13 - significance of bioadsorption process on textile industry wastewater. In: Shahid Ul, I. & Butola, B.S. (eds.). *The impact and prospects of green chemistry for textile technology*: Woodhead Publishing.

Samsuir, A.A., Ismail, N. & Ghazi, R.M., 2016 Optimization of oil removal by sugarcane bagasse using response surface methodology. *J. Trop. Resour. Sustain. Sci.*, 4, pp.82-87.

Shoba, B., Jeyanthi, J. & Vairam, S., 2018 Synthesis, characterization of cellulose acetate membrane and application for the treatment of oily wastewater. *Environ Technol*, 10.1080/09593330.2018.1543353, pp.1-16.

Singh, V.P., Sharma, M. & Vaish, R., 2019 Separation of dyes/oils from water by diesel exhaust emission soot coated polyurethane foam: A kinetic and equilibrium isotherm study. *Engineering Research Express*, 1, pp.015010.

Songsaeng, S., Thamyongkit, P. & Poompradub, S., 2019 Natural rubber/reduced-graphene oxide composite materials: Morphological and oil adsorption properties for treatment of oil spills. *Journal of Advanced Research*, 20, pp.79-89.

Sun, H., Li, A., Zhu, Z., Liang, W., Zhao, X., La, P. & Deng, W., 2013 Superhydrophobic activated carbon-coated sponges for separation and absorption. *ChemSusChem*, 6, pp.1057-1062.

Syuhada, N., Mohd Ghazi, R. & Ismail, N., 2017 Response surface methodology optimization of oil removal using banana peel as biosorbent. *Malaysian Journal of Analytical Sciences*, 21, pp.1101-1110.

Wang, F., Lei, S., Xue, M., Ou, J. & Li, W., 2014 In situ separation and collection of oil from water surface via a novel superoleophilic and superhydrophobic oil containment boom. *Langmuir*, 30, pp.1281.

Wang, Z., Wang, D., Qian, Z., Guo, J., Dong, H., Zhao, N. & Xu, J., 2015 Robust superhydrophobic bridged silsesquioxane aerogels with tunable performances and their applications. *ACS Appl. Mater. Interfaces*, 7, pp.2016.

Xue, C.-H., Ji, P.-T., Zhang, P., Li, Y.-R. & Jia, S.-T., 2013 Fabrication of superhydrophobic and superoleophilic textiles for oil–water separation. *Applied Surface Science*, 284, pp.464-471.

Xue, Z., Wang, S., Lin, L., Chen, L., Liu, M., Feng, L. & Jiang, L., 2011 A novel superhydrophilic and underwater superoleophobic hydrogel-coated mesh for oil/water separation. *Adv Mater*, 23, pp.4270-4273.

Xue, Z., Cao, Y., Liu, N., Feng, L. & Jiang, L., 2014 Special wettable materials for oil/water separation. *J. Mater. Chem. A*, 2, pp.2445-2460.

Yang, Y., Deng, Y., Tong, Z. & Wang, C., 2014 Renewable lignin-based xerogels with self-cleaning properties and superhydrophobicity. *ACS Sustainable Chem. Eng.*, 2, pp.1729.

Yu, P., Lian, Z., Xu, J., Yu, Z., Ren, W. & Yu, H., 2018 Fabrication of superhydrophilic and underwater superoleophobic metal mesh by laser treatment and its application. *Materials Research Express*, 5, pp.045013.

Yussuf, A., Al-Saleh, M., Al-Enezi, S. & Abraham, G., 2018 Synthesis and characterization of conductive polypyrrole: The influence of the oxidants and monomer on the electrical, thermal, and morphological properties. *International Journal of Polymer Science*, 2018, pp.1-8.

Zhang, J., Xu, H., Guo, J., Chen, T. & Liu, H., 2020 Superhydrophobic polypyrrole-coated cigarette filters for effective oil/water separation. *Applied Sciences*, 10, pp.1985.

Zhao, J.H., Wu, J.P., Li, B., Du, W.M., Huang, Q.L., Zheng, M.B., Xue, H.G. & Pang, H., 2016 Facile synthesis of polypyrrole nanowires for high-performance supercapacitor electrode materials. *Progress in Natural Science-Materials International*, 26, pp.237-242.

Chapter Seven: Conclusions, recommendations, and future work

7.1. Conclusions and recommendations

All the set objectives of this work were successfully achieved and the following conclusions were made from each specific objective:

Response surface methodology was found to be a good experimental design method in the extraction of silica from diatomaceous earth (DE). It was also found that the conventional solvent extraction and ultrasound assisted extraction (using alkali) methods which were used were not sufficient for the extraction of silica from DE. In addition, it was concluded that the use of ultrasound and initial acid leaching before alkali extraction were very important steps in the extraction of silica from DE making the ultrasound assisted extraction (using acids) (acid UAE) the preferred method. The optimum parameters for the acid UAE were found to be 1.99 h for sonication time, 2.82 M for concentration of HCl, 220 mL for volume, 0.524 for cycle and 72.6% amplitude with a desirability of 1.00.

The second objective focused on the synthesis and characterization of 3-bromo-benzimidazolone polymer by the copolymerization of 3-bromo-benzimidazolone and silica extracted in the first objective for use as oil sorbent material. Response surface methodology was used to optimize the adsorption of oil from synthetic oily wastewater (SOWW) on to the prepared adsorbent. The optimum conditions were found to be 6650 mg/L oil concentration, adsorbent dosage of 0.004 g and adsorption time of 16 h. The percentage oil adsorption using these optimum conditions was found to be 97.9%.

Objective three achieved the modification of silica gel extracted in the first objective with acetyl groups using acetic anhydride. Response surface methodology was again employed in the optimization of oil removal from SOWW using acetylated silica and it was revealed that initial oil concentration, adsorbent dosage and contact time were the main factors that determined oil adsorption using this material. The optimum conditions oil removal using this material were 7867 mg/L oil concentration, with adsorbent dosage of 0.001 g and a duration of 21.6 h with a desirability of 1.00. The percentage oil adsorption was found to be 99.3%.

In the final objective, polypyrrole modified silica was designed by the co-polymerization of pyrrole and silica in the presence of ferric chloride hexahydrate. The response surface model was also used to optimize oil adsorption and the optimum conditions for the removal were 7091 mg/L oil concentration, 0.004 g adsorbent dosage and contact time of 16 h with a desirability of 0.95. with percentage adsorption capacity of 99.3%.

In summary in this study, three different silica-based adsorbents were developed and tested for oil take-up. The oil removal ability of these adsorbents were optimized with the aid of an ‘adsorbent-in-tea-bag’ method using the response surface methodology software, and it was found that all three adsorbents had oil removal capacity of over 90% with all three behaving in a similar way during optimization. Response surface methodology was shown to be a very useful tool in optimization and is recommended for use in optimization studies.

Although oil recovery and adsorbent regeneration studies were not carried out, preliminary studies done shows that the adsorbed oil can be recovered by applying pressure on the tea bags and drying at 60°C in an oven overnight.

7.2. Future Work

Based on the conclusions and recommendations, the following are recommended for future:

1. Optimization of synthesis of the adsorbents
2. Introduction of pore formers in synthesis procedures
3. Regeneration and oil recovery studies on the adsorbents
4. Application of adsorbents to field water